

Response from authors

Re: Review of WRF-GC: online coupling of WRF and GEOS-Chem for regional atmospheric chemistry modeling, Part 1: description of the one-way model (v1.0)

April 24, 2020

We thank the two Reviewers and the Executive Editor for their helpful comments. In response, we have carefully revised the manuscript to (1) better focus the scope of this work, (2) supplement technical details of the WRF-GC coupled model, (3) expand the comparison of the PM_{2.5} concentrations simulated by the WRF-GC and GEOS-Chem models, and (4) improve logic and clarity. We also revised the title of the paper to indicate the version numbers of the two parent models.

We respond to each specific comment in detail below. The referee comments are shown in red italics. Our replies are shown in black and modified text is shown in blue. The annotated page and line numbers refer to the revised copy of the manuscript.

1 Reviewer #1

The manuscript ‘WRF-GC: online coupling of WRF and GEOS-Chem for regional atmospheric chemistry modeling, Part 1: description of the one-way model (v1.0)’ written by Haipeng Liu and group team presented the development of regional chemical transport model coupled with global chemistry model of GEOS-Chem. The authors described the method of coupling of GEOS-Chem to WRF, and further conducted the test case over China, and compared model performances and computational time. Although I would like to consider the publication of

this attractive research to develop the sophisticated regional chemical transport models, I hope the manuscript is fully revised to address following comments.

Major comments:

R1.1 Introduction: As the introduction in this study, the authors well summarized CTMs in terms of off-line and on-line models, and also picked up some models such as CMAQ and WRF-Chem to discuss. Because the application of WRF-GC to show the performance improvements was just conducted in comparison with GEOS-Chem Classic, and without the direct comparison with other CTMs summarized in Table 1 (especially WRF-Chem as well stated in the manuscript), it is not appropriate to emphasize the superiority of WRF-GC model. I would like to suggest to focus only on GEOS-Chem Classic model in introduction section. For example, it seems to be one of the significant point in terms of the necessity of fine-scale simulation beyond the Classic nested version. In addition, I am not GEOS-Chem user, but the statement posed me some biases in GEOS-Chem. Especially, some criticism on WRF-Chem model can be avoided as much as possible without appropriate evidences.

Thank you for the criticism and suggestion. We removed Table 1 to better focus the scope of this work. We also revised large portions of the Introduction and other parts of the text to more objectively describe the advantages of WRF-GC and its comparison with GEOS-Chem Classic. For example:

P3-4, L80-87, Introduction:

WRF-GC offers users of WRF-Chem or other regional models the option to use the latest GEOS-Chem chemical module, which is actively developed by a large international user base, well-documented, traceable, benchmarked, and centrally-managed. Through WRF-GC, regional modellers also gain access to the specialty simulations in GEOS-Chem, such as the simulations of mercury (Horowitz et al., 2017; Soerensen et al., 2010) and persistent organic pollutants (Friedman et al., 2013). WRF-GC drives GEOS-Chem with online meteorological fields simulated by WRF, which in turn can be driven by initial and boundary meteorological conditions from many different assimilated

datasets or climate model outputs (Skamarock et al., 2008, 2019). As such, WRF-GC allows GEOS-Chem users to perform high-resolution simulations in both forecast and hindcast modes at any location and time of interest.

P18, L543-547, Section 6:

The WRF-GC coupling structure, including the GEOS-Chem column interface and the state conversion module, are extensible and can be adapted to models other than WRF. This opens up possibilities of coupling GEOS-Chem to other weather and Earth System models in an online, modular manner. Using native, out-of-the-box copies of parent models in coupled models reduces maintenance and avoids branching of the parent model code. It also enables the community to more easily transfer developments in the parent models to the coupled model, and vice versa.

R1.2 Application: Related above mentioned comment, without the evaluation to other models, this study should keep focus on the comparison between GEOS-Chem Classic and developed WRF-GC in terms of the model superiority. In addition, the application is just one case over China and only six days, it should be noted and soften the conclusion derived in this study. In this application, I have following two comments.

1. Sections 4.1 and 4.2:

GEOS-Chem Classic nested version includes 47 layers with 7 levels in the bottom of 1 km, whereas WRF-GC had 50 layers with 7 levels in the bottom of 1 km. Are these 7 levels (or surface level) identical? Even a few meters differences could cause the modeling performance difference, and I am suspicious the conclusion attributed to the behavior of planetary boundary layer. If the configuration of boundary layer is identical, the height of planetary boundary layer could be one reason as model difference; however, what are other basic meteorological parameters such as wind speed and its direction, temperature, relative humidity, and precipitation (related to wet scavenging)? More investigations on meteorological fields are required in this part.

Thank you for pointing this out. We revised the text to more objectively describe the comparison between WRF-

GC and GEOS-Chem Classic nested-China simulations of Chinese PM_{2.5}. We also expanded the validation of WRF-GC-simulated meteorological variables. We found that the meteorological variables simulated by WRF-GC (with nudging) better represented the spatiotemporal variability of the observed surface temperature, relative humidity, winds, and PBLH, relative to those in the GEOS-FP dataset. We revised the text as follows:

P12, L369-372, Section 4:

Our goal was to compare the performance of the two models in simulating Chinese surface PM_{2.5} under their normal mode of operation. To this end, the two simulations were configured as similarly as possible, but there are important innate differences between the two models, as described below.

P14-15, L438-459, Section 4.2:

Our analyses above show that the hourly and daily surface PM_{2.5} concentrations simulated by the WRF-GC model were in better agreement with observations than those simulated by the GEOS-Chem Classic nested-China model over Eastern China during January 22 to 27, 2015. We found that this was partially because the WRF-GC model, nudged with surface and upper-air meteorological observations, better represented the pollution meteorology, compared to the GEOS-FP dataset that was used to drive the GEOS-Chem Classic nested-China simulation. Figure S1 shows the average surface air temperature, relative humidity, and 10-m wind speed as simulated by the WRF-GC model and as provided by the GEOS-FP dataset against the observations during January 22 and 27, 2015 at 367 sites over China. The surface air temperature simulated by WRF-GC and those in the GEOS-FP dataset were both in good agreement with the observations over China. However, the relative humidity and wind speeds simulated by WRF-GC were more consistent with the observations, compared to those in the GEOS-FP dataset. Figure S2 assesses the hourly surface air temperature, relative humidity, and near-surface winds simulated by the WRF-GC model and those in the GEOS-FP assimilated meteorological dataset, against hourly surface measurements over China during January 22-27, 2015. For the 34 sites with publicly-available hourly measurements, the meteorological fields simulated by

the WRF-GC were generally more consistent with the measurements.

Figure 5 shows the mean planetary boundary layer height (PBLH) at 08:00 local time (00:00 UTC) and 20:00 local time (12:00 UTC) during January 22 to 27, 2015 in the GEOS-Chem Classic nested-China and the WRF-GC simulations, respectively, and compares them with the rawinsonde observations during this period (Guo et al., 2016). The PBLH in the GEOS-Chem Classic model was taken from the GEOS-FP dataset, whereas the boundary layer height was simulated by WRF in WRF-GC. Compared to the observations, the PBLH in the GEOS-FP dataset were generally biased-low over Eastern China and biased-high over over the mountainous areas in Southwestern China and Western China. This likely was a major reason for the severe overestimation of surface $PM_{2.5}$ concentrations in the GEOS-Chem Classic nested-China simulation over Eastern China. In comparison, the WRF-GC model correctly represented the PBLH over most regions in China, which was critical to its more accurate simulation of surface $PM_{2.5}$ concentrations.

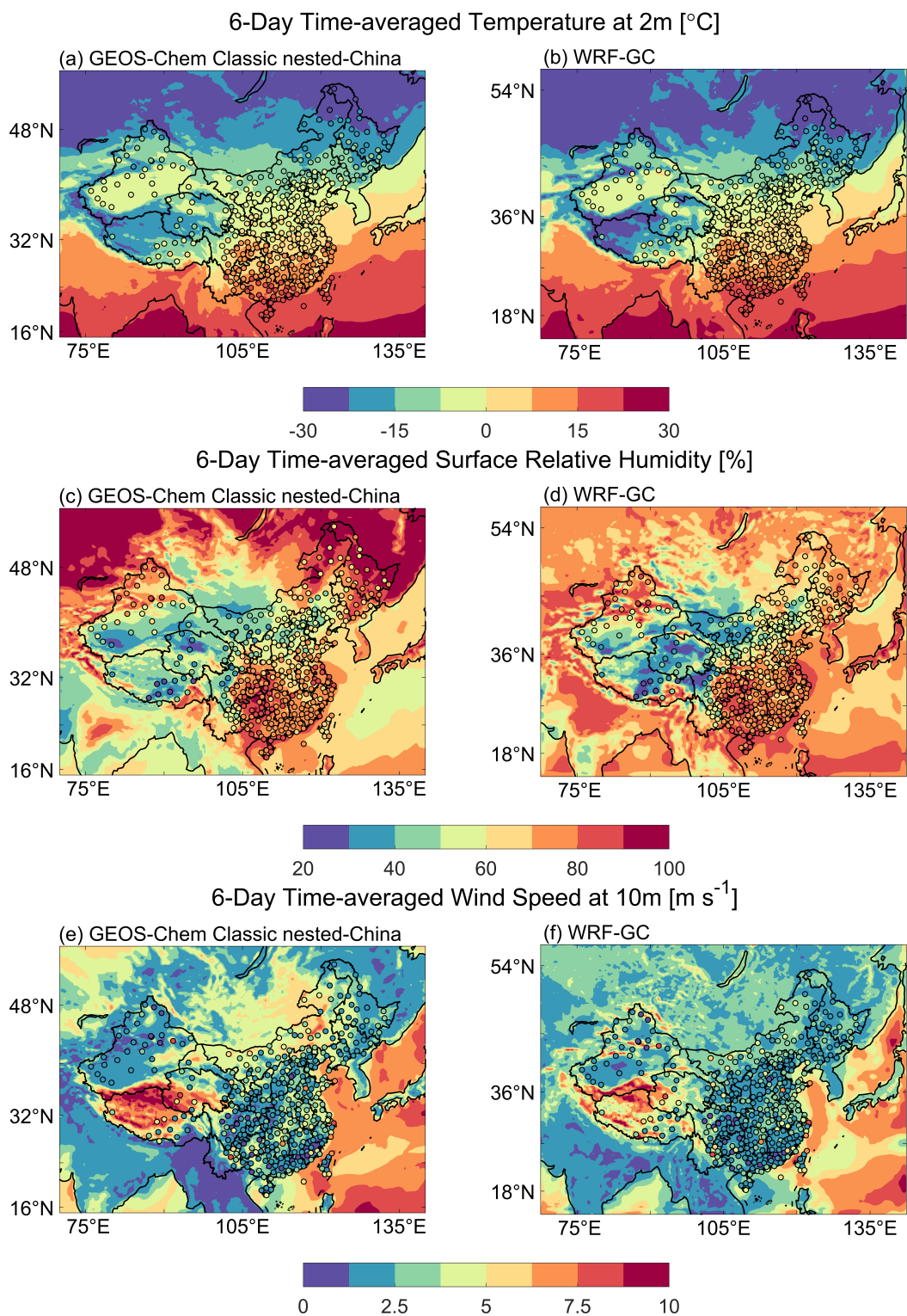


Figure S1. Six-day average values of simulated (filled contours) and observed (symbols) 2-m air temperature (upper panel), surface relative humidity (middle panel), and 10-m wind speed (bottom panel) during January 22-27, 2015: (a,c,e) meteorological variables used to drive the GEOS-Chem Classic nested-China simulation (i.e., the GEOS-FP dataset); (b,d,f) meteorological variables simulated by the WRF-GC model. Surface meteorological measurements at 367 sites were obtained from the U.S. National Climate Data Center (<https://gis.ncdc.noaa.gov/maps/ncei/cdo/hourly>).

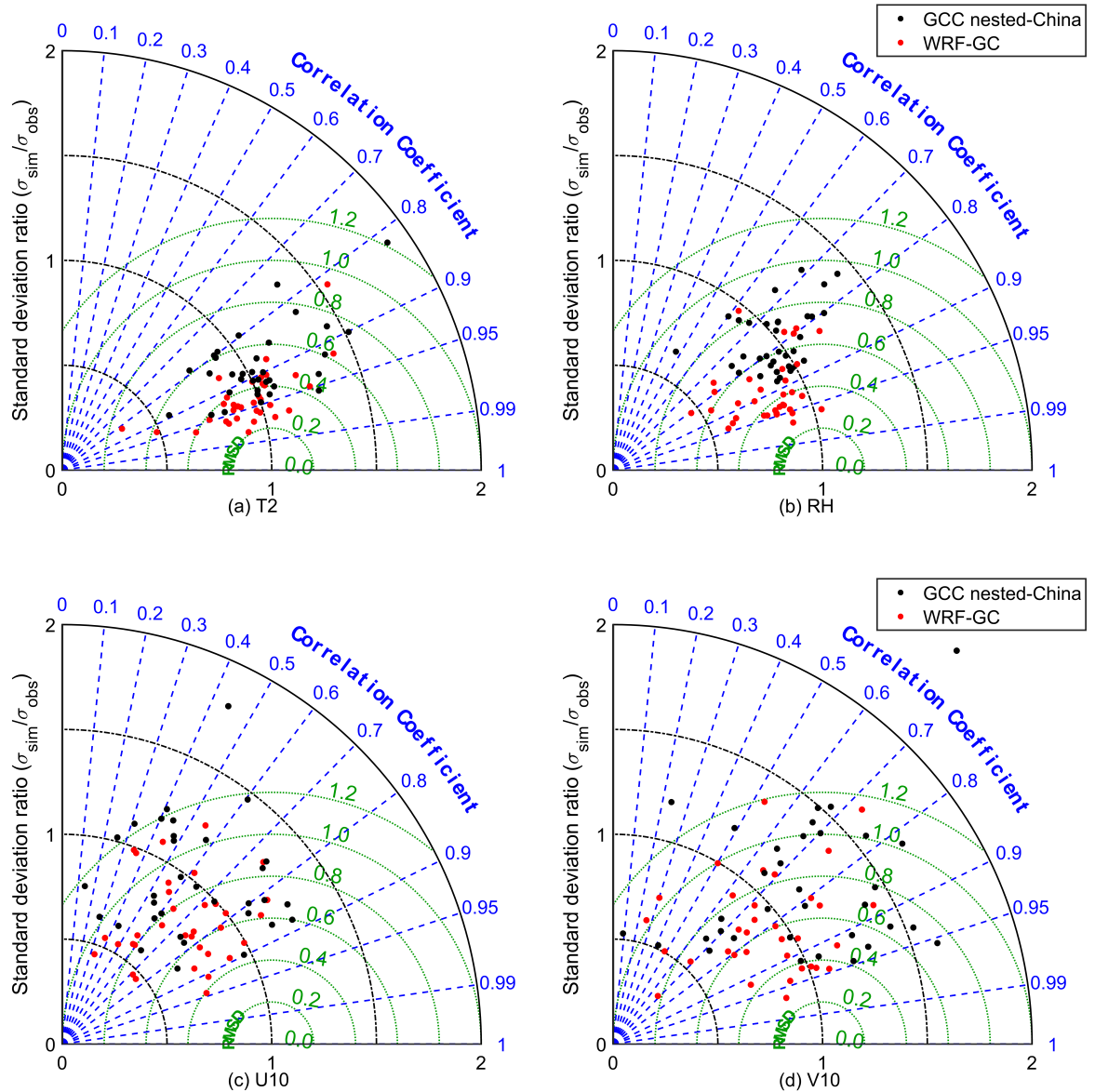


Figure S2. Assessments of the hourly meteorological variables simulated by the WRF-GC model (red dots) and those used to drive the GEOS-Chem Classic nested-China simulation (i.e., the GEOS-FP dataset, black dots) against hourly measurements at 34 surface sites during January 22-27, 2015: (a) 2-m air temperature, (b) surface relative humidity, (c) 10-m U-wind, and (d) 10-m V-wind. Green, black, and blue dashed lines indicate contours of the normalized centered root-mean-square differences (RMSD), the ratios of simulated versus observed standard deviations, and the Pearson correlation coefficients, respectively. Surface meteorological measurements were obtained from the U.S. National Climate Data Center (<https://gis.ncdc.noaa.gov/maps/ncei/cdo/hourly>). The 34 sites were selected (out of a total 367 sites) because hourly measurements were publicly-available at these sites.

R1.3 2. Section 5.1:

Again, what is the configuration of vertical layer in this WRF-GC? Without the identical setting of it, the comparison in computational performance is not appropriate. Under the same configuration of both models, the performance differences can be attributed to the importance of online and offline simulation. In addition to the behavior of meteorological fields, how about the importance of online and offline model?

Thank you for pointing out this lack of clarity. Our intention in Section 5.1 was to compare the computational efficiencies of the two models when they are applied to a similar simulation problem, under their respective typical configuration. We agree that the difference in computational efficiency is influenced by WRF-GC being an online model and GEOS-Chem Classic being an offline model. We revised the manuscript to make the purpose of Section 5.1 more clear, as well as include more details about the model configurations.

P15, L462-466, Section 5.1:

We evaluated the computational performance of a WRF-GC simulation and compared it with that of the GEOS-Chem Classic nested-grid simulation of a similar configuration. We configured the WRF-GC and GEOS-Chem Classic nested-grid simulations for the exact same domain (as shown in Figure 2(a)), with the exact same projection and horizontal resolution (0.25° latitude \times 0.3125° longitude resolution, 225×161 atmospheric columns). The GEOS-Chem Classic nested-grid simulation had 47 vertical levels, and the WRF-GC simulation comparably had 50 levels.

P16, L475-483, Section 5.1:

We found that the difference in computational efficiency was mainly due to the much faster dynamic and transport calculations in the WRF-GC model relative to the transport calculation in the GEOS-Chem Classic nested-grid model. In WRF-GC, the wall time taken up by the entire WRF (including transport, physics, I/O, and model initia-

tion) was 2462.5 seconds. In the GEOS-Chem Classic nested-grid simulation, 50% (8192 seconds) of the total wall time was used for the transport of tracers, including large-scale advection (6355.7 seconds), convective transport (694.2 seconds), and boundary-layer mixing (1142.5 seconds). As a CTM, the GEOS-Chem Classic read archived meteorological data for the entire domain at 3-model-hour intervals from hard drives using a single computational core, which becomes increasingly burdensome for simulations with more grid boxes. In comparison, WRF-GC calculated meteorology online in node memory and updated the model boundary conditions from hard drives every 6 model-hours.

Minor comments:

R1.4 P6, L175-L179: Does WRF-GC cover both yield model and VBS model for SOA? It is not explicitly stated which is available.

Thank you for pointing out the omission. Yes, GEOS-Chem has two SOA production options. By default, GEOS-Chem simulates SOA production from volatile organic precursors using simple yields. A more complex scheme that includes the VBS model and additional aqueous productions is also available. WRF-GC supports both options. We revised the text to address this point.

P6, L166-171, Section 2.2:

GEOS-Chem has two options to describe the production of SOA, and both options are supported in WRF-GC. By default, SOA is produced irreversibly using simple yields from anthropogenic and biogenic volatile organic precursors (Kim et al., 2015). Alternatively, GEOS-Chem can simulate SOA production via the aging of semi-volatile and intermediate volatility POA using a volatility basis set (VBS) scheme (Robinson et al., 2007; Pye et al., 2010), as well as via the aqueous reactions of oxidation products from isoprene (Marais et al., 2016).

R1.5 P6, L179-180: What is size bins for sulfate, nitrate, ammonium, black carbon, and POA and SOA? Only dust and sea salt is described here.

Thank you for pointing out the lack of clarity. We revised the manuscript to more precisely describe the treatment of aerosols.

P6, L158-166, Section 2.2:

Aerosol species in GEOS-Chem includes secondary inorganic aerosols (sulfate, nitrate, ammonium), elemental carbon aerosol (EC), primary organic carbon (POC), secondary organic aerosol (SOA), dust, and sea salt. By default, secondary inorganic aerosols, EC, POC, and SOA are simulated as speciated bulk masses. Dust aerosols are represented in 4 size bins (0.1-1.0, 1.0-1.8, 1.8-3.0, and 3.0-6.0 μm) (Fairlie et al., 2007), while sea salt aerosols are represented in 2 size bins (0.1-0.5 and 0.5-4.0 μm) (Jaeglé et al., 2011). The thermodynamics of secondary inorganic aerosol are coupled to gas-phase chemistry and computed by the ISORROPIA II module (Park et al., 2004; Fountoukis and Nenes, 2007; Pye et al., 2009). EC and POC are represented in GEOS-Chem as partially hydrophobic and partially hydrophilic, with a conversion timescale from hydrophobic to hydrophilic of 1.2 days (Wang et al., 2014). The organic matter to organic carbon (OM/OC) mass ratio is assumed to be 2.1 for POC by default, with an option to use seasonally and spatially varying OM/OC ratios (Philip et al., 2014).

R1.6 P7, L203: How can we prepare the initial and boundary conditions for chemical variables? It is not well stated in the current document.

Thank you for pointing out the issue. Initial and boundary concentrations of chemical species are taken from the GEOS-Chem global model output and interpolated to the horizontal and vertical grids of the WRF-GC model using a modified version of the WRF-Chem preprocessor tool mozbc. The initial and boundary conditions are read by WRF

in netCDF format. We have revised the manuscript to clarify.

P7-8, L213-217, Section 3.1:

IC/BC for meteorological and chemical variables are prepared by the user in netCDF format and read by WRF. Meteorological IC/BC can be prepared using the WRF pre-processor system (WPS) from datasets available from NCAR's Research Data Archive (<https://rda.ucar.edu>). IC/BC of chemical species concentrations are taken from GEOS-Chem Classic global model outputs and interpolated to the WRF-GC models grids using a modified version of the WRF-Chem preprocessor tool mozbc (available along with the WRF-GC code).

R1.7 P7, L206: What is the “choice of chemical species”? In P6, L163-164, it is only stated “241 chemical species and 981 reactions”. Do we need to set chemical species in model simulation?

P7, L206: What is the “chemical mechanisms”? In P6, L160-161, we can see “the standard chemical mechanism in GEOS-Chem”, but what is other options in GEOSChem?

Thank you for pointing out the issue. This was an oversight in the wording of the paragraph and we have revised the text to clarify.

P6, L146-149, Section 2.2:

Chemical calculations in WRF-GC v1.0 use GEOS-Chem version 12.2.1 (doi:10.5281/zenodo.2580198). The standard chemical mechanism in GEOS-Chem v12.2.1, used by default in WRF-GC, includes detailed O_x-NO_x-VOC-ozone-halogen-aerosol in the troposphere, as well as the Unified tropospheric-stratospheric chemistry extension (UCX) (Eastham et al., 2014) for stratospheric chemistry and stratosphere-troposphere exchange.

P6, L151-155, Section 2.2:

In addition, GEOS-Chem uses the FlexChem pre-processor (a wrapper for the Kinetic PreProcessor, KPP, Damian

et al. (2002); Sandu and Sander (2006)) to configure chemical kinetics (Long et al., 2015). This allows users to add or modify gaseous species and reactions to develop custom mechanisms and diagnostic quantities in GEOS-Chem. GEOS-Chem also supports the optional "Tropchem" (troposphere-only chemistry) mechanism, where UCX is disabled and replaced by a parameterized linear chemistry in the stratosphere (McLinden et al., 2000).

P7-8, L211-213, Section 3.1:

Chemical options within GEOS-Chem, including the choice of standard or custom chemical mechanisms, emission inventories in HEMCO, and diagnostic quantities to be output, are defined by users in the GEOS-Chem configuration files (`input.geos`, `HEMCO_Config.rc`, and `HISTORY.rc`).

R1.8 P7, L206: What is the meaning of diagnostics? This wording is ambiguous.

Thank you for pointing out the lack of clarity. GEOS-Chem refers to all output quantities, including for example chemical concentrations, and production and loss rates, from GEOS-Chem as "diagnostics". We replaced the word with "diagnostic quantities" throughout the text. For example:

P7-8, L211-213, Section 3.1:

Chemical options within GEOS-Chem, including the choice of standard or custom chemical mechanisms, emission inventories in HEMCO, and diagnostic quantities to be output, are defined by users in the GEOS-Chem configuration files (`input.geos`, `HEMCO_Config.rc`, and `HISTORY.rc`).

P8, L225-226, Section 3.1: At the end of the WRF-GC simulation, WRF outputs all meteorological and chemical diagnostic quantities in WRF's standard format.

R1.9 P8, L230: This means that WRF-GC only supports the newly established WRF vertical grids, and does

not have the choice to old terrain-following grids?

Thank you for pointing this out. Yes, WRF-GC can only use the hybrid sigma-eta grids, which has become the default option in WRF for versions 4 and higher. We revised the text and the new Table 4 to note this.

P4, L95-97, Section 2.1:

WRF uses the Advanced Research WRF (ARW) dynamical solver, which solves fully compressible, Eulerian non-hydrostatic equations on either hybrid sigma-eta (default) or terrain-following vertical coordinates defined by the user.

P4, L105-106, Section 2.1:

Table 3 lists the configuration and physical options supported by WRF-GC v1.0. In particular, only the hybrid sigma-eta vertical coordinate is currently supported in WRF-GC.

R1.10 P10, L310-311: So what is the available lightning NO_x emissions in current WRF-GC? It is not available, or using climatological value?

Thank you for pointing out this issue. There are currently no Lightning NO_x emissions in WRF-GC. We revised the text to note this.

P7, L185-186, Section 2.2:

With the exception of lightning NO_x, these meteorology-dependent emissions are supported in WRF-GC v1.0.

P11, L327-328, Section 3.3.1:

Lightning NO_x emissions is not yet supported in WRF-GC v1.0 but will be added in a future version.

R1.11 P11, L317-319 and P11, L328-335: From these paragraphs, I understand that the WRF-GC simulation have the limitations in the selection of various WRF options. This information is necessary to understand the limitation of applicability of WRF-GC model.

Therefore, I would like to strongly suggest to put table for the summary of available options in WRF for WRF-GC.

Thank you for the important suggestion. We added Table 3 to the main text to summarize the WRF options supported in WRF-GC v1.0:

Table 3: List of WRF configuration and physical options supported in WRF-GC v1.0

Namelist option	Description	Supported value
WRF Preprocessing System (WPS)		
max_dom	Maximum number of domains	1
map_proj	Map projection	lat-lon; mercator
geog_data_res	Static geographical data source	usgs_*
WRF dynamics		
hybrid_opt	Use hybrid sigma-pressure grid?	2 (Yes)
WRF physics		
bl_pbl_physics	Planetary boundary layer	All
cu_physics	Cumulus parameterization	7 (Zhang-McFarlane scheme), 16 (New Tiedtke scheme)
mp_physics	Microphysics option	6 (WRF single-moment 6-class scheme), 8 (New Thompson scheme), 10 (Morrison double-moment scheme)
ra_lw_physics	Longwave radiation	3 (CAM3 scheme), 4 (RRTMG), 5 (New Goddard scheme)
ra_sw_physics	Shortwave radiation	4 (RRTMG shortwave)
sf_sfclay_physics	Surface layer	All
sf_surface_physics	Land surface	All
sf_lake_physics	Lake physics	All
sf_urban_physics	Urban surface	All

R1.12 P11, L327: For WRF model itself, the land cover can be obtained by both USGS and MODIS, but WRF-GC can be available both datasets? Please explicitly stated for the available land cover information.

Thank you for pointing out this omission. Only the USGS land cover classification is supported in WRF-GC v1.0. Routines to map the MODIS land cover classification to work with WRF-GC have been reserved in the code and can be implemented in a future WRF-GC version. We have included this information in Table 4, and have revised the text as follows:

P12, L352-357, Section 3.3.3:

Dry deposition is calculated in GEOS-Chem using a resistance-in-series scheme (Wesely, 1989; Wang et al., 1998). The land cover data for the simulated domain is read by and used in WRF, but for now WRF-GC only supports the use of the U.S. Geological Survey (USGS) classification. The land cover information is passed to GEOS-Chem, where it is mapped to the land cover classifications of Olson et al. (2001) to assign values of surface roughness and canopy resistance (Wang et al., 1998). The dry deposition velocities are calculated locally using WRF-simulated surface air momentum, sensible heat fluxes, temperature, and solar radiation.

R1.13 P13, L391 and P25, L460: I understand that this is one test case, but the comparison should not be “preliminary”.

Thank you for your suggestion. We expanded on the analysis of the hourly PM_{2.5} concentrations simulated by the WRF-GC and GEOS-Chem Classic model, as well as the analysis of the meteorological fields in the two models.

P14-15, L411-459, Section 4.2:

Figure 2 compares the 6-day average surface PM_{2.5} concentrations during January 22 to 27, 2015 as simulated by WRF-GC and GEOS-Chem Classic, respectively. Also shown are the PM_{2.5} concentrations measured at 578 surface sites, managed by the Ministry of Ecology and Environment of China (www.cnemc.cn). We removed invalid hourly

surface PM_{2.5} observations following the protocol in Jiang et al. (2020). The 578 sites were selected by (1) removing surface sites with less than 80% valid hourly measurements during our simulation period, and (2) sampling the site closest to the model grid center, if that model grid contained multiple surface sites. Both models reproduced the general spatial distributions of the observed PM_{2.5} concentrations, including the higher concentrations over Eastern China relative to Western China, as well as the hotspots over the North China Plain, Central China, and the Sichuan Basin. However, both models overestimated the PM_{2.5} concentrations over Eastern China. The mean 6-day PM_{2.5} concentrations averaged for the 578 sites as simulated by WRF-GC and by GEOS-Chem Classic were $117 \pm 68 \mu\text{g m}^{-3}$ and $120 \pm 76 \mu\text{g m}^{-3}$, respectively. In comparison, the observed mean 6-day PM_{2.5} concentration averaged for the 578 sites was $98 \pm 43 \mu\text{g m}^{-3}$.

Figure 3 shows the scatter plots of the simulated and observed daily average PM_{2.5} concentrations over Eastern China (eastward of 103°E, 507 sites) during January 22 to 27, 2015. We focused on Eastern China, because the spatiotemporal variability of PM_{2.5} concentrations was higher over this region. Again, both models overestimated the daily PM_{2.5} concentrations over Eastern China. The daily PM_{2.5} concentrations simulated by WRF-GC were 29% higher than the observations (quantified by the reduced major-axis regression slope between the simulated and observed daily PM_{2.5} concentration), with a correlation coefficient of $r = 0.68$. The daily PM_{2.5} concentrations simulated by the GEOS-Chem Classic were 55% higher than the observations, with a correlation coefficient of $r = 0.72$.

Figure 4 shows the Taylor diagrams of the hourly PM_{2.5} concentrations simulated by the two models at 48 major eastern Chinese cities, including 13 cities in the Beijing-Tianjin-Hebei (BTH) area, 22 cities in the Yangtze River Delta (YRD) area, and 13 other major cities. The Taylor diagram (Taylor, 2001) evaluates the simulated time series of PM_{2.5} against the observations, using the Pearson correlation coefficients, the ratio between the simulated and observed standard deviations ($\frac{\sigma_{sim}}{\sigma_{obs}}$), and the normalized root-mean-square differences (RMSDs) as metrics. Proximity to the point "1" on the X-axis in Figure 4 indicates that the simulation accurately reproduced both the mean concentration and the temporal variability of the observations. For most cities in the BTH area and for most of the

other 13 major cities, the hourly $PM_{2.5}$ concentrations simulated by WRF-GC showed smaller RMSDs and higher correlation coefficients against observations, compared to those simulated by the GEOS-Chem Classic model. In the YRD area, the performances of the two models were similar.

Our analyses above show that the hourly and daily surface $PM_{2.5}$ concentrations simulated by the WRF-GC model were in better agreement with observations than those simulated by the GEOS-Chem Classic nested-grid model over Eastern China during January 22 to 27, 2015. We found that this was partially because the WRF-GC model, nudged with meteorological observations, better represented the pollution meteorology, compared to the GEOS-FP dataset that was used to drive the GEOS-Chem Classic model. Figure S1 shows the average surface air temperature, relative humidity, and 10-m wind speed as simulated by the WRF-GC model and as provided by the GEOS-FP dataset against the observations during January 22 and 27, 2015 at 367 sites over China. The surface air temperature simulated by WRF-GC and those provided by the GEOS-FP dataset were both in good agreement with the observations over China. However, the relative humidity and wind speeds simulated by WRF-GC were most consistent with the observations, compared to those provided in the GEOS-FP dataset. Figure S2 assesses the hourly surface air temperature, relative humidity, and near-surface winds simulated by the WRF-GC model and those in the GEOS-FP assimilated meteorological dataset, against hourly surface measurements over China during January 22-27, 2015. For the 34 sites with publicly-available hourly measurements, the meteorological fields simulated by the WRF-GC were generally more consistent with the measurements, compared to the GEOS-FP dataset.

Figure 5 shows the mean planetary boundary layer height (PBLH) at 08:00 local time (00:00 UTC) and 20:00 local time (12:00 UTC) during January 22 to 27, 2015 in the GEOS-Chem Classic model and in the WRF-GC model, respectively, and compares them with the rawinsonde observations during this period (Guo et al., 2016). The PBLH in the GEOS-Chem Classic model was taken from the GEOS-FP dataset, whereas the boundary layer height was simulated by WRF in WRF-GC. Compared to the observations, the PBLH in the GEOS-FP dataset were generally biased-low over Eastern China and biased-high over over the mountainous areas in Southwestern China and Western China. This likely was a major reason for the severe overestimation of surface $PM_{2.5}$ concentrations in the GEOS-

Chem Classic nested-grid simulation over Eastern China. In comparison, the WRF-GC model correctly represented the PBLH over most regions in China, which was critical to the accurate simulation of surface PM_{2.5} concentrations.

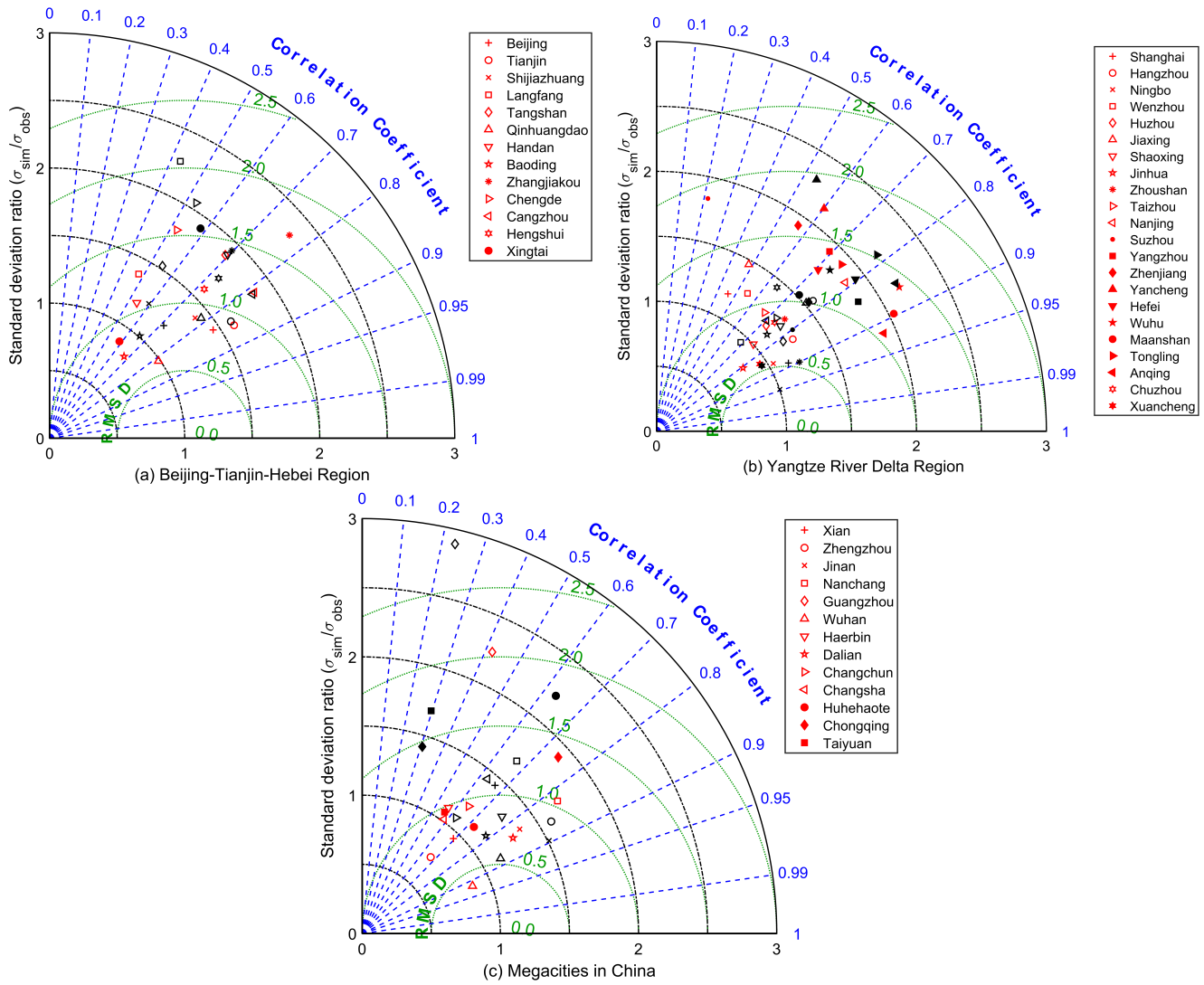


Figure 4: Taylor diagrams of PM_{2.5} concentrations during Jan 22 to 27, 2015 from the GEOS-Chem Classic nested-China simulation (black) and WRF-GC nudged simulation (red) in (a) the Beijing-Tianjin-Hebei Region (BTH), (b) the Yangtze River Delta Region (YRD) and (c) major megacities in China.

R1.14 L13, L391-L402 and Figure 4: This paragraph needs amendments in its expression. There is two expressions of “GEOS-FP dataset” and “GEOS-Chem Classic nested China”. I understand that GEOS-Chem model uses GEOS-FP; however, it seems to be better to unify its expression for readability.

Thank you for pointing out this issue. We have carefully revised the wording throughout the text to improve clarity and consistency. For example:

P14-15, L440-442, Section 4.2:

We found that this was partially because the WRF-GC model, nudged with meteorological observations, better represented the pollution meteorology, compared to the GEOS-FP dataset that was used to drive the GEOS-Chem Classic nested-China simulation.

Figure 5 (previously Figure 4) caption:

Comparison of the simulated (fill contours) and observed (fill symbols) planetary boundary layer heights (PBLH) at 08:00 local time (upper panel) and 20:00 local time (bottom panel) averaged between January 22 and 27, 2015. (a,c) PBLH from the GEOS-FP dataset, which was used to drive the GEOS-Chem Classic nested-China simulation, and (b,d) PBLH simulated by the WRF-GC model.

R1.15 P14, L424-431: I guess that this WRF-GC model for the discussion of scalability is same model in Section 5.1. If so, this paragraph contains some redundant information. Please clarify and repetition should be avoided.

Thank you for pointing out this issue. We revised the manuscript for greater clarity and avoided repetition.

P16, L500, Section 5.2:

We analyzed the scalability of the WRF-GC model using timing tests of the 48-hour simulation described in

Section 5.1.

R1.16 Figure 1: In left corner of “WRF-GC input”, there is the statement on “emissions”. What is the difference of this emissions and HEMCO?

Thank you for pointing out this issue. We revised Figure 1 to clarify that the ”emission” refers to the emissions input files. HEMCO is the GEOS-Chem module that performs the emission calculation.

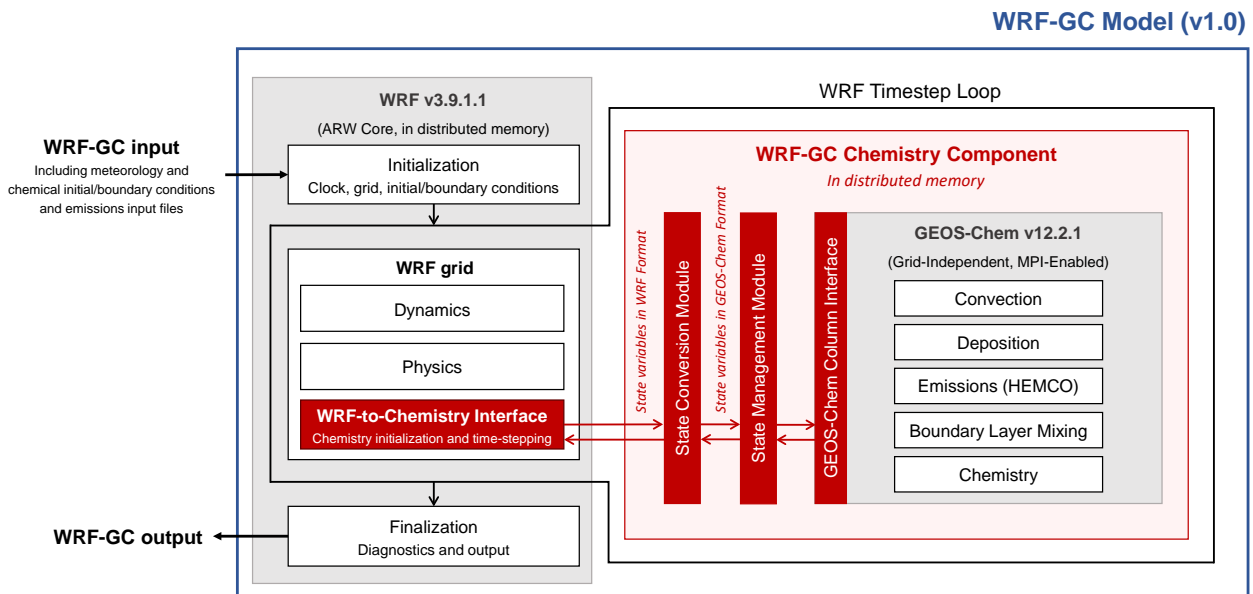


Figure 1: Architectural overview of the WRF-GC model (v1.0). The WRF-GC Coupler (all parts shown in red) includes interfaces to the two parent models, as well as the state conversion and state management modules. The parent models (shown in grey) are standard codes downloaded from their sources, without any modifications.

R1.17 Figures 2 and 4: The map line is thinner, so please enhance the map line for readability.

Thank you for pointing out the issue. We redrew Figures 2 and 4 to improve readability.

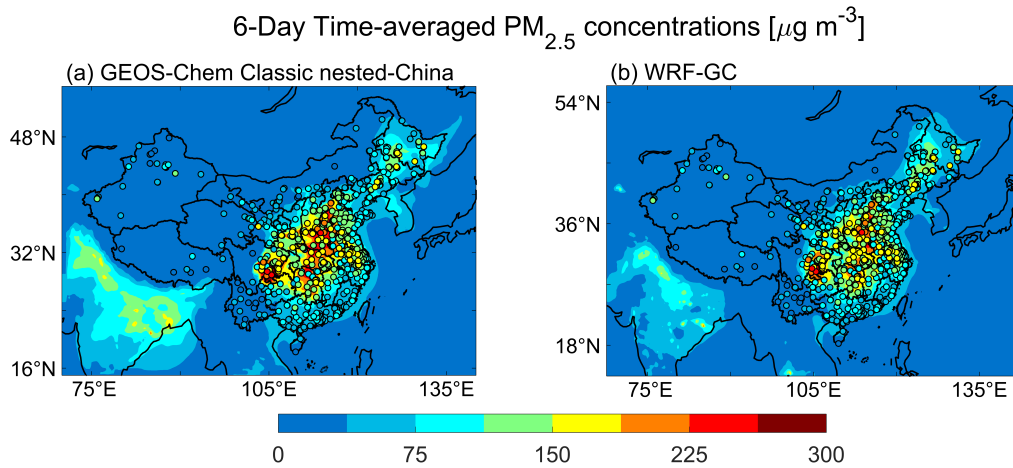


Figure 2: Comparison of the simulated (filled contours) 6-day average PM_{2.5} concentrations during Jan 22 to 27, 2015 from (a) the GEOS-Chem Classic nested-China simulation and (b) the WRF-GC nudged simulation. Also shown are the observed 6-day average PM_{2.5} concentrations during this period at 578 surface sites managed by the Ministry of Ecology and Environment of China.

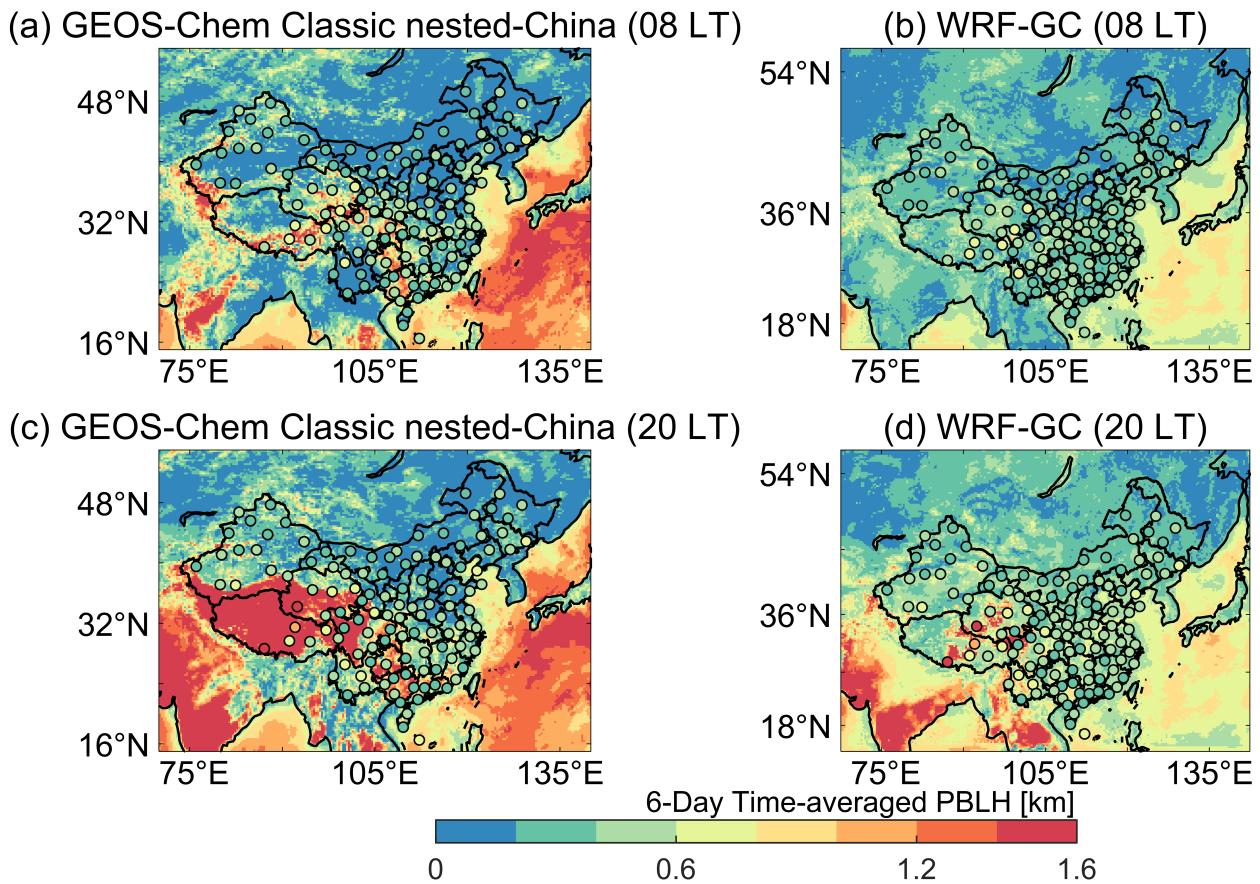


Figure 5: Comparison of the simulated (fill contours) and observed (fill symbols) planetary boundary layer heights (PBLH) at 08:00 local time (upper panel) and 20:00 local time (bottom panel) averaged between Jan 22 and 27, 2015. (a,c) GEOS-Chem Classic nested-China simulation (read from the GEOS-FP dataset), (b,d) WRF-GC simulation.

R1.18 Figure 6: Gray lines is hard to see. Please change the thickness of lines, or change into black color for readability.

Thank you for pointing out this issue. We revised the y-axis scale, the color, and the line thickness in Figure 7 to improve readability.

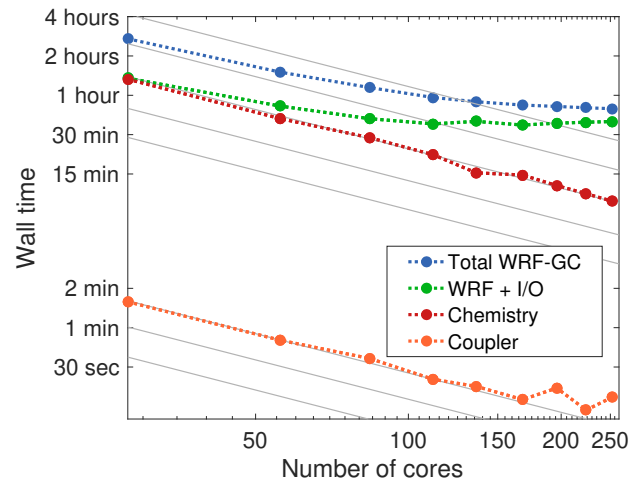


Figure 7: WRF-GC model scalability by processes. Gray lines indicate perfect scalability, i.e. halved computational time for each doubling of processor cores.

R1.19 Technical comments: L2 in the caption of Figure 3: Need space (“theGEOS-Chem”).

Corrected. Thank you.

2 Reviewer #2

This paper describes how GEOS-Chem has been implemented in the WRF model. The topic and the description of its implementation is appropriate for the GMD audience. There are certain details that need elaboration for future users of the code and I have made several suggestions. In addition, some the statements are clearly biased that overstate the capabilities of the model without actual proof. At times, the text sounds more salesmanship than scientific. Both of these concerns should be relatively easy to address.

Major Comments:

R2.1 Boundary layer mixing is handled separately by GEOS-Chem. I am a concerned about this approach which is glossed over. Most, but not, all of the meteorology from WRF is used and that point is passed over in other parts of the text. WRF-Chem uses parameters from the WRF boundary layer parameterizations so that the vertical mixing is treated in as similar as possible. In this way, mixing of chemical species occurs within the same boundary layer depth as the meteorology. It is not clear whether vertical mixing in GEOS-Chem and WRF are consistent. If not, it may be possible for GEOSChem to have a deeper or shallower boundary layer than in WRF. If deeper, than more chemistry variables will be transported by free tropospheric air and boundary layer air. The authors should delve into this in more detail to let users know what the approach for vertical mixing actually is and the potential consequences. This applies to the results shown in Figure 4.

Thank you for pointing this out. In WRF-GC, GEOS-Chem does use the meteorological variables (including boundary layer height and thermodynamic variables) from WRF to calculate boundary-layer mixing. We have revised the text to make this clear.

P12, L347-350, Section 3.3.2:

Boundary layer mixing is calculated in GEOS-Chem using a non-local scheme (Holtslag and Boville, 1993; Lin and McElroy, 2010). The boundary layer height, thermodynamic variables, and the vertical level and pressure

information are calculated by WRF and passed to GEOS-Chem through the state conversion module. Again, this methodology is the same as that in the WRF-Chem model.

P7, L187-191, Section 2.2: Other physical calculations in GEOS-Chem are coupled to WRF meteorological fields in WRF-GC; we describe the coupling in detail in Section 3.3. Convective transport of chemical species is calculated using a single-plume parameterization (Allen et al., 1996; Wu et al., 2007), which is in turn driven by the cumulus parameterization in WRF. Boundary layer mixing is calculated using a non-local scheme, driven by the WRF-simulated atmospheric instability and boundary layer height (Lin and McElroy, 2010).

R2.2 At several places in the manuscript, the authors point out the reasons for the advantages of coupling GEOS-Chem within WRF. For the GEOS-Chem community the advantages are obvious. But it is not as clear what the WRF-Chem community gains. The WRF-Chem community would have another chemistry option, but this paper does not explore the types of chemical processes that might be missing (perhaps halogen chemistry) already in the model. The current aerosol treatment is rather simple (is it even “state-of the science”?) and similar in many respects to existing simple aerosol options in WRF-Chem. Users choose particular treatments in a community model, such as WRF, for various reasons such as overall performance (i.e. how well the model represents reality), physics complexity, and computational considerations. The authors have failed to articulate what the advantages are to the WRF community. The future developments beyond v1.0 may change this picture and make that argument more apparent. But if the authors want to frame their arguments in this paper, then a few more concrete points of the advantages to the WRF community are needed.

Thank you for pointing out this important issue. In our view, the biggest advantage of the WRF-GC code is that it couples native copies of WRF and GEOS-Chem, such that the very active developments in the two parent models by their respective community can be quickly incorporated into WRF-GC. The use of unmodified copies of the

parent models also allow WRF-GC users to more easily contribute their developments back to the parent models.

We modified the text to reflect these points:

P3-4, L69-87, Introduction:

In this work, we developed a new online regional atmospheric chemistry model, WRF-GC, by coupling the WRF meteorology model with the GEOS-Chem chemistry model. Both WRF and GEOS-Chem are open-source and actively developed by the community. We constructed WRF-GC with the following guidelines, in order to best take advantage of new developments in the two parent models and to enhance usability:

1. The coupling structure of WRF-GC should be abstracted from the parent models, and both parent models remain unmodified from their respective sources. In this way, future updates of the parent models can be quickly incorporated into WRF-GC with ease, such that WRF-GC can stay cutting-edge. It also enables WRF-GC users to more easily contribute their developments back to the parent models.
2. The WRF-GC coupled model should scale from conventional computation hardware to massively parallel computation architectures.
3. The WRF-GC coupled model should be easy to install and use, open-source, version-controlled, and well-documented.

WRF-GC offers users of WRF-Chem or other regional models the option to use the latest GEOS-Chem chemical module, which is actively developed by a large international user base, well-documented, traceable, benchmarked, and centrally-managed. Through WRF-GC, regional modellers also gain access to the specialty simulations in GEOS-Chem, such as the simulations of mercury (Horowitz et al., 2017; Soerensen et al., 2010) and persistent organic pollutants (Friedman et al., 2013). WRF-GC drives GEOS-Chem with online meteorological fields simulated by WRF, which in turn can be driven by initial and boundary meteorological conditions from many different assimilated datasets or climate model outputs (Skamarock et al., 2008, 2019). As such, WRF-GC allows GEOS-Chem users to perform high-resolution simulations in both forecast and hindcast modes at any location and time of interest.

P18, L545-547, Section 6:

Using native, out-of-the-box copies of parent models in coupled models reduces maintenance and avoids branching of the parent model code. It also enables the community to more easily transfer developments in the parent models to the coupled model, and vice versa.

R2.3 Specific Comments: Lines 7-8: “is designed to be easy to use, ... extendable, and easy to update” are relative terms and depends on an individual’s point of view. This is something I’m struggling with here. “is designed” is probably the key phrase. It is hard for a reviewer to verify the last part of the sentence without using the code itself. WRF itself is a rather complex model, although users with “sufficient” expertise in atmospheric models and computational hardware can learn how to run the model in a short period (i.e. days) of time. Those without “sufficient” expertise, might not describe it as easy to use. Nor am I sure what “extendable” means here. All computational models by their very nature are extendable by modifying code.

Thank you for your suggestion. We deleted this sentence but added descriptive details to the related statements in the abstract.

Abstract, L6-10

WRF-GC uses unmodified copies of WRF and GEOS-Chem from their respective sources; the coupling structure allows future versions of either one of the two parent models to be integrated into WRF-GC with relative ease. Within WRF-GC, the physical and chemical state variables are managed in distributed memory and translated between WRF and GEOS-Chem by the WRF-GC Coupler at runtime.

Abstract, L15-19

The WRF-GC model is parallelized across computational cores and scales well on massively parallel architec-

tures. In our tests where the two models were similarly configured, the WRF-GC simulation was three times more efficient than the GEOS-Chem Classic nested-grid simulation, owing to the efficient transport algorithm and the MPI-based parallelization provided by the WRF software framework.

R2.4 Lines 15-17. I have some concerns regarding the statement on PBL heights, in which I will comment on later in the appropriate section.

Thank you for your comments. We revised the manuscript and added further analysis of the simulated meteorological fields. Please refer to responses to your comment R2.25.

R2.5 Lines 18-19: The sentence "Both parent models..." is redundant with an earlier statement. It probably can be deleted and the thought merged with the earlier statement.

The previous sentence with repeated information was deleted. This sentence was revised as follows.

Abstract, L15-16

The WRF-GC model is parallelized across computational cores and scales well on massively parallel architectures.

R2.6 Lines 27-28: "regional" is used twice in this sentence and is redundant and is self evident.

Thank you for your suggestion. We revised the text.

P2, L24-25, Introduction:

Regional models of atmospheric chemistry simulate the emission, transport, chemical evolution, and removal of

atmospheric constituents over a given domain.

R2.7 Lines 33-34: "to better serve the public, inform policy makers, and advance science" is a laudable goal. However, I think these types of models are used primarily to "advance science". WRF has been used to provide short-range operational forecasts (e.g. HRRR model), but NOAA is phasing out the use of WRF. WRF-CMAQ has been serving EPA regulatory interest in addition to advancing science, but I am not sure GEOS-Chem serves that purpose.

Thank you for pointing this out. GEOS-Chem has been used as part of the GEOS system to provide a near real-time forecast at NASA in the GEOS-CF (Composition Forecast) system (https://gmao.gsfc.nasa.gov/weather_prediction/GEOS-CF/). Here, we revised the text to better represent the potential applications of WRF-GC.

P2, L29-30, Introduction:

We present here the development of a new regional atmospheric chemistry model, WRF-GC, specifically designed to allow easy updates and be computationally efficient, for use in research and operation applications.

R2.8 Lines 73-86: The authors state that online models are more difficult to keep up to date than offline models. I disagree. There are many factors that contribute to how quickly and the frequency of updates made in models (some described by the authors) that have nothing to do with whether the model is online or offline. The authors first mention resources used to provide benchmarking, validating, and documentation, which is probably a good thing for both offline and online models. This process does take longer for more complex models, but offline models can be complex too. It is also not a good idea to translate research findings into publicly available without due diligence. Some times new scientific findings are proven to be incorrect and/or the findings are based on a limited case study; therefore, it is not wise or appropriate for use by a broad community. The authors second

point on expertise residing in different communities. I agree this is an issue, but this is largely governed by how the organization wishes to develop the code, and not whether the model is offline or online. In the case of WRF, it has always been a community model so that contributions originate from various organizations and universities. Nor has NCAR insisted that all physics schemes be compatible with each other, and sometimes there are good reasons why some physics schemes should not be made compatible. Had NCAR decided to be the sole developer, the code would no doubt be more streamlined but would probably lack scientific options many users want. It seems strange to me that the authors are arguing that bring communities together introduces problems, when the purpose of WRF-GC is yet another iteration of bringing very different communities together. The authors correctly point out that not everything in WRF-Chem (and WRF for that matter) is compatible, but it is not clear whether the same holds for the various treatments in GEOS-Chem.

Thank you for the very important comment. We modified the text to better frame the advantages of the WRF-GC model. In our view, the biggest advantage of the WRF-GC code is that it couples native copies of WRF and GEOS-Chem, such that the very active developments in the two parent models by their respective community can be quickly incorporated into WRF-GC. The use of unmodified copies of the parent models also allow WRF-GC users to more easily contribute their developments back to the parent models.

We modified the text to reflect these points:

P3, P63-68, Introduction:

However, keeping the representation of atmospheric processes up-to-date is potentially more challenging for on-line models than it is for offline models. One of the reasons for this is that the interactions between the chemical and meteorological modules are hard-wired in some online models, such that updating either module requires considerable effort. For the same reason, if users make improvements to the chemical or meteorological processes in the online model, those improvements may be relatively difficult to propagate to the broader community. This may lead to the model diverging into different branches, and users may be forced to work with stale, branched versions

of the code.

P3, L69-76, Introduction:

In this work, we developed a new online regional atmospheric chemistry model, WRF-GC, by coupling the WRF meteorology model with the GEOS-Chem chemistry model. Both WRF and GEOS-Chem are open-source and actively developed by the community. We constructed WRF-GC with the following guidelines, in order to best take advantage of new developments in the two parent models and to enhance usability:

1. The coupling structure of WRF-GC should be abstracted from the parent models, and both parent models remain unmodified from their respective sources. In this way, future updates of the parent models can be quickly incorporated into WRF-GC with ease, such that WRF-GC can stay cutting-edge. It also enables WRF-GC users to more easily contribute their developments back to the parent models.

P18, L545-547, Section 6:

Using native, out-of-the-box copies of parent models in coupled models reduces maintenance and avoids branching of the parent model code. It also enables the community to more easily transfer developments in the parent models to the coupled model, and vice versa.

R2.9 Lines 98-98. This sentence is kind of a put-down to WRF (in the context of this paragraph) and other models listed in Table 1. As with another statement in the introduction, this depends on one's point-of-view and difficult to prove. What is "state-of-the-science" anyway? This overused phrase is almost meaningless at this point. For examples, some chemistry and aerosol disciplines are changing very rapidly (weekly) and it is very difficult to argue which model has the most "up-to-date" science. I suggest the authors rephrase this sentence to be a bit more fair and unbiased.

Thank you for your suggestion. We have revised the manuscript according to your comments.

P3-4, L80-83, Introduction:

WRF-GC offers users of WRF-Chem or other regional models the option to use the latest GEOS-Chem chemical module, which is actively developed by a large international user base, well-documented, traceable, benchmarked, and centrally-managed. Through WRF-GC, regional modellers also gain access to the specialty simulations in GEOS-Chem, such as the simulations of mercury (Horowitz et al., 2017; Soerensen et al., 2010) and persistent organic pollutants (Friedman et al., 2013).

R2.10 Line 100: The authors state that that GEOS-Chem is driven by the meteorological fields simulated by WRF. But after reading material later in the paper, this may not be entirely true. It seems that GEOS-Chem still uses its own turbulent vertical mixing which could be different from WRF. I have some other comments on this point later in the paper.

Thank you for pointing this out. In WRF-GC, GEOS-Chem does calculate turbulent mixing in the PBL, but the calculation is driven by WRF-simulated meteorology. This methodology is same as the methodology in WRF-Chem. We have revised section 3.3.2 regarding vertical mixing.

P12, L347-350, Section 3.3.2:

Boundary layer mixing is calculated in GEOS-Chem using a non-local scheme (Holtslag and Boville, 1993; Lin and McElroy, 2010). The boundary layer height, thermodynamic variables, and the vertical level and pressure information are calculated by WRF and passed to GEOS-Chem through the state conversion module. Again, this methodology is the same as that in the WRF-Chem model.

P7, L187-191, Section 2.2: Other physical calculations in GEOS-Chem are coupled to WRF meteorological fields in WRF-GC; we describe the coupling in detail in Section 3.3. Convective transport of chemical species is calculated using a single-plume parameterization (Allen et al., 1996; Wu et al., 2007), which is in turn driven by

the cumulus parameterization in WRF. Boundary layer mixing is calculated using a non-local scheme, driven by the WRF-simulated atmospheric instability and boundary layer height (Lin and McElroy, 2010).

R2.11 Lines 168-169: Based on this sentence, it sounds like the bulk treatment is similar to GOCART. But the last sentence in the paragraph implies a modal treatment for dust and sea-salt. So is dust and sea-salt in bulk bins or actually prescribed using a size distribution? Just need to be consistent in the text here.

Thank you for pointing this out. We revised the text to include more detail:

P6, L158-161, Section 2.2:

Aerosol species in GEOS-Chem includes secondary inorganic aerosols (sulfate, nitrate, ammonium), elemental carbon aerosol (EC), primary organic carbon (POC), secondary organic aerosol (SOA), dust, and sea salt. By default, secondary inorganic aerosols, EC, POC, and SOA are simulated as speciated bulk masses. Dust aerosols are represented in 4 size bins (0.1-1.0, 1.0-1.8, 1.8-3.0, and 3.0-6.0 μm) (Fairlie et al., 2007), while sea salt aerosols are represented in 2 size bins (0.1-0.5 and 0.5-4.0 μm) (Jaeglé et al., 2011).

R2.12 Lines 169-172: These two sentences might be better at the end of the paragraph. It would be better to have all the discussion on the present aerosol model together, rather than broken up with what is not in the code in the middle.

Thank you for your suggestion. We revised the paragraph to improve clarity:

P6, L158-174, Section 2.2:

Aerosol species in GEOS-Chem includes secondary inorganic aerosols (sulfate, nitrate, ammonium), elemental carbon aerosol (EC), primary organic carbon (POC), secondary organic aerosol (SOA), dust, and sea salt. By default, secondary inorganic aerosols, EC, POC, and SOA are simulated as speciated bulk masses. Dust aerosols are

represented in 4 size bins (0.1-1.0, 1.0-1.8, 1.8-3.0, and 3.0-6.0 μm) (Fairlie et al., 2007), while sea salt aerosols are represented in 2 size bins (0.1-0.5 and 0.5-4.0 μm) (Jaeglé et al., 2011). The thermodynamics of secondary inorganic aerosol are coupled to gas-phase chemistry and computed by the ISORROPIA II module (Park et al., 2004; Fountoukis and Nenes, 2007; Pye et al., 2009). EC and POC are represented in GEOS-Chem as partially hydrophobic and partially hydrophilic, with a conversion timescale from hydrophobic to hydrophilic of 1.2 days (Wang et al., 2014). The organic matter to organic carbon (OM/OC) mass ratio is assumed to be 2.1 for POC by default, with an option to use seasonally and spatially varying OM/OC ratios (Philip et al., 2014). GEOS-Chem has two options to describe the production of SOA, and both options are supported in WRF-GC. By default, SOA is produced irreversibly using simple yields from anthropogenic and biogenic volatile organic precursors (Kim et al., 2015). Alternatively, GEOS-Chem can simulate SOA production via the aging of semi-volatile and intermediate volatility organic precursors using a volatility basis set (VBS) scheme (Robinson et al., 2007; Pye et al., 2010), as well as via the aqueous reactions of the oxidation products from isoprene (Marais et al., 2016). The GEOS-Chem model also has the option of simulating detailed, size-dependent aerosol microphysics using the Two-Moment Aerosol Sectional microphysics (TOMAS) module (Kodros and Pierce, 2017) or the Advanced Particle Microphysics (APM) module (Yu and Luo, 2009), but these two modules are not yet supported in WRF-GC.

R2.13 Lines 181-185: I think some discussion is needed regarding higher-resolution emission datasets. GEOS-Chem has been used traditionally at global scales and there are several global emission datasets available. But if the point of WRF-GC is to run at higher resolution, this would be defeated in part by an emission inventory that is much coarser than what could be simulated by the model. What is the strategy for that? Will other inventories used by EPA and the WRF-Chem community be used? Or are users expected to generate emissions on their own? Also, emissions are discussed in more detail later in Section 3.3.1. So I am wondering if it is even necessary to talk about emissions here. This material can be merged into Section 3.3.1.

Thank you for pointing out the lack of clarity. We revised the text to first describe how HEMCO calculates emissions in GEOS-Chem and the default inventories in Section 3.3.1. We then describe how WRF-GC can choose to use the existing inventories in HEMCO or prepare their own in Section 3.3.1.

P6-7, L175-186, Section 2.2:

Emissions of chemical species in WRF-GC are calculated using the HEMCO emissions component in GEOS-Chem (Keller et al., 2014). HEMCO allows users to select emission inventories from the HEMCO data directory or add their own inventories, and interpolate the emission fluxes to the model domain and resolution at runtime. The HEMCO data directory currently includes more than 20 global and regional emission inventories, mostly at their respective native resolutions (http://wiki.seas.harvard.edu/geos-chem/index.php/HEMCO_data_directories). By default, the Community Emissions Data System (CEDS) inventory (0.5×0.5 resolution, monthly) (Hoesly et al., 2018) is used for most of the world; over Asia and the U.S., the CEDS is superseded by the MIX inventory (0.25 × 0.25 native resolution, monthly, Li et al. (2017b)) and the 2011 National Emission Inventory (NEI 2011) (0.1 km × 0.1 km native resolution, hourly, U.S. Environmental Protection Agency (2014)), respectively. HEMCO also has extensions to compute emissions with meteorological dependencies, such as the emissions of biogenic species (Guenther et al., 2012), soil NO_x (Hudman et al., 2012), lightning NO_x, sea salt (Gong, 2003), and dust (Zender et al., 2003). With the exception of lightning NO_x, these meteorology-dependent emissions are supported in WRF-GC v1.0. Further details about the use of HEMCO in WRF-GC is given in Section 3.3.1.

P11, L318-328, section 3.3.1

Chemical emissions in WRF-GC are calculated online by the HEMCO module in GEOS-Chem (Keller et al., 2014) and configured in `HEMCO_Config.rc`. HEMCO and its data directory are updated as part of the GEOS-Chem model and remain unmodified in WRF-GC. Users can choose to use one or combine several of the emission inventories already in the HEMCO data directory (Section 2.2). Some of the inventories currently available in the HEMCO data directory may not be of sufficiently fine resolution to support the high-resolution WRF-GC simulations.

In that case, users can prepare their own emission input files in netCDF format at arbitrary spatiotemporal resolutions, and HEMCO will interpolate them to the WRF-GC model domain and resolution at runtime. HEMCO also allow users to specify scale factors and diurnal/weekly/monthly variation profiles in `HEMCO_Config.rc` to be applied to the emission fluxes at runtime. WRF-GC calls HEMCO to compute meteorology-dependent emissions online using WRF-simulated meteorology. These currently include the emissions of biogenic species (Guenther et al., 2012), soil NO_x (Hudman et al., 2012), sea salt (Gong, 2003), and dust (Zender et al., 2003). Lightning NO_x emissions is not yet supported in WRF-GC v1.0 but will be added in a future version.

R2.14 Line 198: I am not sure what “greater modularity” means here. WRF-Chem is structured in a way to have modularity for important chemistry and aerosol processes. For example, there are several option for online emissions, deposition, etc. The modularity also permits users to add their own treatments if they wish. In some cases, there are treatments that can be used for multiple chemistry or aerosol options. For example, wet scavenging can be handled similarly for MADE-SORGAM (modal aerosols) and MOSAIC (sectional aerosols). But I doubt if the modules in GEOS-Chem can be used or accessed by other treatments in the code, given the structure on how it was implemented. So, if the authors want to use the phrase “greater modularity” some description is need to know exactly what this means.

Thank you for pointing out this issue. This sentence has been deleted.

R2.15 Line 206: What is the “WRF-to-chemistry interface”. Is GEOS-Chem handled in the registry.chem file, much like the other chemistry options? Given Figure 1, I think this will be discussed later and it looks like the material is in Section 3.2.2. I just found this a bit vague at this point.

Thank you for your suggestion. We revised the text here and also in Sections 3.2.2 and 3.2.3 to improve clarity.

P7, L208-210, Section 3.1:

Users also "turn on" GEOS-Chem in WRF-GC by specifying `chem_opt = 233` in `namelist.input`, similar to the way that users specify the chemical mechanism in WRF-Chem. GEOS-Chem is initialized by the WRF model using the WRF-to-chemistry interface described in Section 3.2.3.

P9, L266-268, Section 3.2.2:

When the user sets the environment variable `WRF_CHEM` to 1 in the WRF compile script, WRF reads a registry file (`registry.chem`) containing the GEOS-Chem chemical species information (duplicated from `input.geos`) and builds these species into the WRF model framework.

P9, L275-279, Section 3.2.3:

In WRF-Chem, WRF calls its interface to chemistry, `chem_driver`, which then calls each individual chemical processes. We abstracted this `chem_driver` interface by removing direct calls to chemical processes. Instead, our `chem_driver` calls the WRF-GC state conversion module (`WRFGC_Convert_State_Mod`) and the GEOS-Chem column interface (`GIGC_Chunk_Run`) to perform chemical calculations. We also modified `chemics_init` to initialize GEOS-Chem through the column interface `GIGC_Chunk_Init`.

R2.16 Line 213: See the first major comment above.

Thank you for your suggestion. We clarified the treatment of boundary-layer mixing.

P12, L347-350, Section 3.3.2

Boundary layer mixing is calculated in GEOS-Chem using a non-local scheme (Holtslag and Boville, 1993; Lin and McElroy, 2010). The boundary layer height, thermodynamic variables, and the vertical level and pressure

information are calculated by WRF and passed to GEOS-Chem through the state conversion module. Again, this methodology is the same as that in the WRF-Chem model.

R2.17 Line 220: In Section 3.2, the text implies that GEOS-chem is compiled and run on top of the host WRF model. The text implies but does not explicitly state that the addition of GEOS-Chem has not impaired the use of WRF-Chem. One of the rules in the WRF community is that any new additions must be shown to not “break” other parts of the code. So have the authors performed tests with the new code to ensure that other chemistry options produce the same results went the code is compiled with GEOSchem?

Thank you for pointing this out. At the time WRF-GC started development, the workflow for installing WRF-Chem was that the user downloaded the WRF model in WRFV3/, and a separate WRF-Chem zip file which contained the subdirectory to be placed in WRFV3/chem/. So, at the time, the WRF-GC development did not “break” any part of the WRF model.

Two years later the landscape has changed, as the latest WRF version now bundles the chemistry routines with its distribution. Our implementation of WRF-GC still has not “broken” the “WRF” part of the latest WRF model, but at present the chemical routines of WRF-Chem cannot work alongside the GEOS-Chem chemical module in a single WRF-GC top directory.

We have revised the manuscript to clarify this point.

P9, L255-260, section 3.2.2

WRF-GC is installed by downloading the parent models, WRF and GEOS-Chem, and the WRF-GC Coupler, directly from their respective software repositories. The WRF model is installed in a top-level directory, while the WRF-GC Coupler and GEOS-Chem are installed under the chem/ sub-directory, where the chemistry routines for WRF-Chem originally reside. An unmodified copy of the GEOS-Chem code is installed in the chem/gc/ sub-directory, and a set of sample GEOS-Chem configuration files is in chem/config/. The WRF meteorology model

remains unmodified in WRF-GC, but at present the chemical routines of WRF-Chem cannot work alongside GEOS-Chem under a single WRF-GC top directory.

R2.18 Lines 312-335: As the authors imply, subgrid and removal processes, will depend on both “resolved” and “unresolved” clouds. In contrast with global models, simulations at fine enough resolutions may be best run with any “unresolved” cloud parameterizations. Ideally, a cumulus parameterization would have a progressively smaller and smaller impact at higher and higher resolutions. The subgrid and removal processes depend on the current behavior of what is in WRF. It would be useful to provide some discussion for users regarding the implications of these assumptions. Since this paper describes a new modeling framework, it would have been interesting to see some simulations at coarse and fine resolutions to demonstrate the differences on the vertical transport and wet scavenging. WRF-GC users will be able to run at smaller grid spacings, which is a good thing, but will they understand the subtleties of these assumptions that are not normally encountered at global scales?

Thank you for your suggestion. We added more detailed descriptions about the cumulus parameterization schemes currently implemented in WRF-GC, as well as recommendations for the choice of cumulus parameterization at different horizontal resolution.

P11, L338-346, Section 3.3.2:

In addition, the users should consider the horizontal resolution of the model when choosing which cumulus parameterization to use. The New Tiedtke scheme and the Zhang-McFarlane schemes are generally recommended for use in simulations at horizontal resolutions larger than 10 km (Skamarock et al., 2008; Arakawa and Jung, 2011). At horizontal resolutions between 2 to 10 km, the so-called “convective grey zone” (Jeworrek et al., 2019), the use of the Grell-Freitas scheme is recommended for the WRF model (Grell and Freitas, 2014), as it allows subsidence to spread to neighboring columns; this option will be implemented in a future WRF-GC version. At horizontal resolutions finer than 2 km, it is assumed that convections are resolved and cumulus parameterizations should not be

used (Grell and Freitas, 2014; Jeworrek et al., 2019). The scale-dependence of cumulus parameterizations and their impacts on convective mixing of chemical species is an active area of research, which we will explore in the future using WRF-GC.

R2.19 Lines 323-325: Same comment as before regarding vertical mixing. This is a different treatment than in WRF. So there could be mis-matches in how boundary layer mixing, and it impact the vertical extent of boundary layer mixing, between WRF (which is used to transport chemical species) and GEOS-Chem.

Thank you for pointing out the lack of clarity. In WRF-GC, GEOS-Chem calculate boundary-layer mixing using meteorological fields from WRF. We revised the manuscript to clarify.

P12, L347-350, Section 3.3.2

Boundary layer mixing is calculated in GEOS-Chem using a non-local scheme (Holtslag and Boville, 1993; Lin and McElroy, 2010). The boundary layer height, thermodynamic variables, and the vertical level and pressure information are calculated by WRF and passed to GEOS-Chem through the state conversion module. Again, this methodology is the same as that in the WRF-Chem model.

R2.20 Lines 350-359: The authors should include the meteorology simulation time step and chemical time step. What is not mentioned in the discussion of the model's implementation, but alluded to in the conclusion, is that a different chemical time step can be used (which is similar to WRFChem). In this way, transport of chemical species are done at the meteorological time step. Chemistry is usually simulated at a coarser time step to save computer time, but some care is needed since chemical time steps that are too large could introduce uncertainties in the predictions – especially at higher spatial resolutions. Since the paper is about WRF-GC and designed to work at higher spatial resolution, some discussion is needed in the best practice for the two types of time steps. Ideally, they should be the same for consistency.

Thank you for pointing out this omission. We specified the time steps in the two simulations as suggested.

P13, L380-381, 393, Section 4.1:

[For GEOS-Chem Classic nested-China simulation:] The dynamic time step and the external chemistry time step were 5 minutes and 10 minutes, respectively.

[For WRF-GC simulation:] The dynamic time step and the external chemistry time step were 2 minutes and 10 minutes, respectively.

We also added descriptions about the chemical time step in WRF-GC:

P11, L311-316, Section 3.3:

The dynamic and chemical time steps are specified by the user in the WRF configuration file `namelist.input`. The dynamic time step is constrained by the Courant-Friedrichs-Lewy stability criterion and should be short for high-resolution simulations. WRF-Chem recommends that the chemical time step be set the same as the dynamic time step as best practice (Peckham et al., 2017). Because GEOS-Chem uses a Rosenbrock solver, which adapts its internal chemical time step to the stiffness of the chemical mechanism, a larger chemical time step may be used. However, it is recommended that the results be compared to a control simulation with the chemical time step set to the dynamic time step (Peckham et al., 2017).

R2.21 Line 353: The authors use FNL for the meteorological initial and boundary conditions. To be more consistent with the nested GEOS-Chem, why not use the meteorological conditions from that model?

Thank you for pointing this out. The GEOS-Chem Classic nested model uses the GEOS-FP meteorological dataset (reanalysis data), but WRF currently does not support the use of GEOS-FP as meteorological initial and

boundary conditions. We choose FNL as a representative meteorological dataset, since it is what many WRF-GC users would choose to use, and nudged WRF with meteorological observations. We added this point in the text.

P13, L385-387, Section 4.1:

The WRF model does not have the option of using the GEOS-FP dataset for meteorological IC/BC. Instead, we used the NCEP FNL dataset (doi:10.5065/D6M043C6) at $1^\circ \times 1^\circ$ resolution as IC/BC for WRF-GC; the FNL dataset was interpolated to WRF vertical levels and updated every 6 hours.

R2.22 Lines 356-359: It sounds like the authors are using the obs-nudging capability in WRF. Would be useful to cite a reference on that. What is not clear in the previous paragraph, for readers not familiar with GEOS-Chem, that the meteorological fields are prescribed analyses. Thus nudging in WRF would be appropriate to make the meteorology in the two simulations more compatible. The authors should be more specific on these points.

Thanks for your suggestion. We added citations to the nudging algorithms in Section 2.1 where the functionalities of WRF is described. We also revised the text in Section 4.1 to describe the nudging and its effect on our test simulation.

P4, L100-102, Section 2.1:

WRF supports grid-, spectral-, and observational-nudging (Liu et al., 2005, 2006; Stauffer and Seaman, 1990, 1994). This allows the WRF model to produce meteorological outputs that mimic assimilated meteorological fields for use in air quality hindcasts.

P13, L387-391, Section 4.1:

In addition, we nudged the WRF-simulated meteorological fields with surface (every 3 hours) and upper air (every 6 hours) observations of temperature, specific humidity, and winds from the NCEP ADP Global Surface/Upper Air Observational Weather Database (doi:10.5065/39C5-Z211). This mimicked the effect of meteorological data

assimilation and allowed the WRF-simulated meteorology to stay close to the observed states of the atmosphere.

R2.23 Line 363-364: Do the anthropogenic emissions vary diurnally? This seems to be an important point in simulating diurnal and peak concentrations. Here the authors only show a 6-day average. Perhaps this is okay for demonstrate WRF-GC compared to GEOS-Chem, and this distinction should be made.

Thank you for your suggestion. We added description about the weekly/diurnal variation of the anthropogenic emissions. We also expanded the diagnosis of simulated hourly PM_{2.5} concentrations against observations.

P13, L397-400, Section 4.1:

Monthly mean anthropogenic emissions from China were from the Multi-resolution Emission Inventory for China (MEIC, Li et al. (2014)) at $0.25^\circ \times 0.25^\circ$ horizontal resolution. The MEIC inventory was updated for the year 2015 and included emissions from power generation, industry, transportation, and residential activities. Sector-specific weekly and diurnal variation from the MEIC inventory were applied (Li et al., 2017a).

P14, L429-437, Section 4.2:

Figure 4 shows the Taylor diagrams of the hourly PM_{2.5} concentrations simulated by the two models at 48 major eastern Chinese cities, including 13 cities in the Beijing-Tianjin-Hebei (BTH) area, 22 cities in the Yangtze River Delta (YRD) area, and 13 other major cities. The Taylor diagram (Taylor, 2001) evaluates the simulated time series of PM_{2.5} against the observations, using the Pearson correlation coefficients, the ratio between the simulated and observed standard deviations ($\frac{\sigma_{sim}}{\sigma_{obs}}$), and the normalized root-mean-square differences (RMSDs) as metrics. Proximity to the point "1" on the X-axis in Figure 4 indicates that the simulation accurately reproduced both the mean concentration and the temporal variability of the observations. For most cities in the BTH area and for most of the other 13 major cities, the hourly PM_{2.5} concentrations simulated by WRF-GC showed smaller RMSDs and higher

correlation coefficients against observations, compared to those in the GEOS-Chem Classic nested-china simulation.

In the YRD area, the performances of the two models were similar.

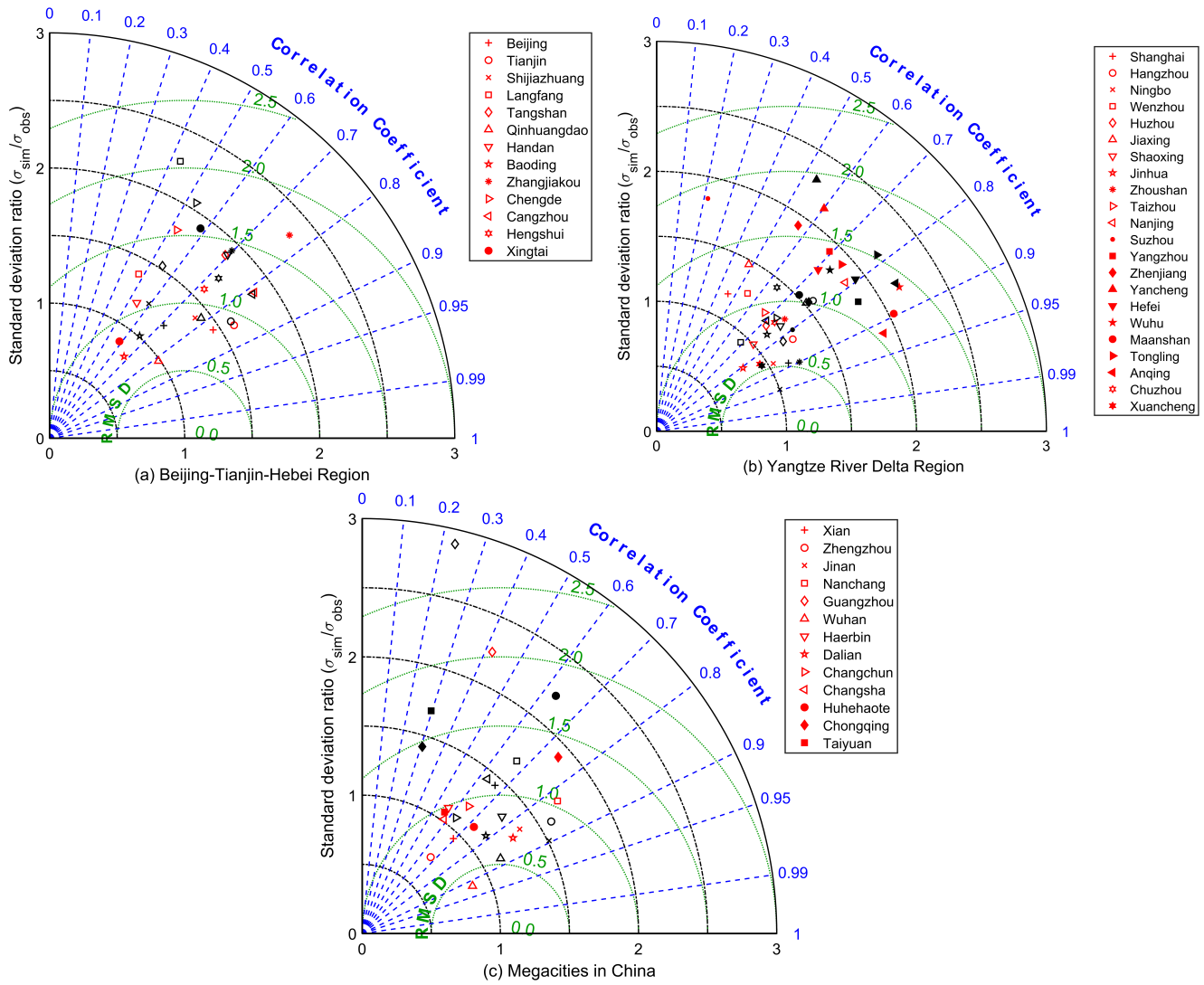


Figure 4: Taylor diagrams of $PM_{2.5}$ concentrations during Jan 22 to 27, 2015 from the GEOS-Chem Classic nested-China simulation (black) and WRF-GC nudged simulation (red) in (a) the Beijing-Tianjin-Hebei Region (BTH), (b) the Yangtze River Delta Region (YRD) and (c) major megacities in China.

R2.24 Lines 394: Are these boundary layer heights the same as predicted by WRF? Or different calculations in the GEOS-Chem modules?

Thank you for pointing this out. In WRF-GC, the boundary layer height is calculated by the WRF model and passed to GEOS-Chem. We have revised the manuscript to resolve this ambiguity.

P15, L451-455, Section 4.2:

Figure 5 shows the mean planetary boundary layer height (PBLH) at 08:00 local time (00:00 UTC) and 20:00 local time (12:00 UTC) during January 22 to 27, 2015 in the GEOS-Chem Classic model and in the WRF-GC model, respectively, and compares them with the rawinsonde observations during this period (Guo et al., 2016). The PBLH in the GEOS-Chem Classic model was taken from the GEOS-FP dataset, whereas the boundary layer height was simulated by WRF in WRF-GC.

R2.25 Lines 397-402: The 6-day averaging may be hiding some day-to-day variations when trying to assess the cause of the positive PM2.5 bias. While it is very likely that the boundary layer height issue is contributing to that, there are likely other differences in the meteorology that could also be attributing factors. The authors should at least acknowledge that if they do not wish to pursue a more detailed analysis of the simulations. I assume the same boundary layer scheme is being used in both models, but the differences arise in how that scheme is driven. I presume in GEOS-Chem the meteorology is from the large-scale analyses. Whereas, in WRF the prognostic land-surface model will be controlling the evolution of surface temperature and fluxes that will drive a boundary layer parameterization. So, some additional discussion as to why these differences in the boundary layer height would be useful.

Thanks for your suggestions. We expanded the validation of WRF-GC-simulated meteorological variables. We found that the meteorological variables simulated by WRF-GC (with nudging) better represented the spatiotemporal

variability of the observed surface temperature, relative humidity, winds, and PBLH, relative to those in the GEOS-FP dataset. We revised the text as follows:

P14-15, L438-459, Section 4.2:

Our analyses above show that the hourly and daily surface PM_{2.5} concentrations simulated by the WRF-GC model were in better agreement with observations than those simulated by the GEOS-Chem Classic nested-China model over Eastern China during January 22 to 27, 2015. We found that this was partially because the WRF-GC model, nudged with surface and upper-air meteorological observations, better represented the pollution meteorology, compared to the GEOS-FP dataset that was used to drive the GEOS-Chem Classic nested-China simulation. Figure S1 shows the average surface air temperature, relative humidity, and 10-m wind speed as simulated by the WRF-GC model and as provided by the GEOS-FP dataset against the observations during January 22 and 27, 2015 at 367 sites over China. The surface air temperature simulated by WRF-GC and those in the GEOS-FP dataset were both in good agreement with the observations over China. However, the relative humidity and wind speeds simulated by WRF-GC were more consistent with the observations, compared to those in the GEOS-FP dataset. Figure S2 assesses the hourly surface air temperature, relative humidity, and near-surface winds simulated by the WRF-GC model and those in the GEOS-FP assimilated meteorological dataset, against hourly surface measurements over China during January 22-27, 2015. For the 34 sites with publicly-available hourly measurements, the meteorological fields simulated by the WRF-GC were generally more consistent with the measurements.

Figure 5 shows the mean planetary boundary layer height (PBLH) at 08:00 local time (00:00 UTC) and 20:00 local time (12:00 UTC) during January 22 to 27, 2015 in the GEOS-Chem Classic nested-China and the WRF-GC simulations, respectively, and compares them with the rawinsonde observations during this period (Guo et al., 2016). The PBLH in the GEOS-Chem Classic model was taken from the GEOS-FP dataset, whereas the boundary layer height was simulated by WRF in WRF-GC. Compared to the observations, the PBLH in the GEOS-FP dataset were generally biased-low over Eastern China and biased-high over the mountainous areas in Southwestern China

and Western China. This likely was a major reason for the severe overestimation of surface $\text{PM}_{2.5}$ concentrations in the GEOS-Chem Classic nested-China simulation over Eastern China. In comparison, the WRF-GC model correctly represented the PBLH over most regions in China, which was critical to its more accurate simulation of surface $\text{PM}_{2.5}$ concentrations.

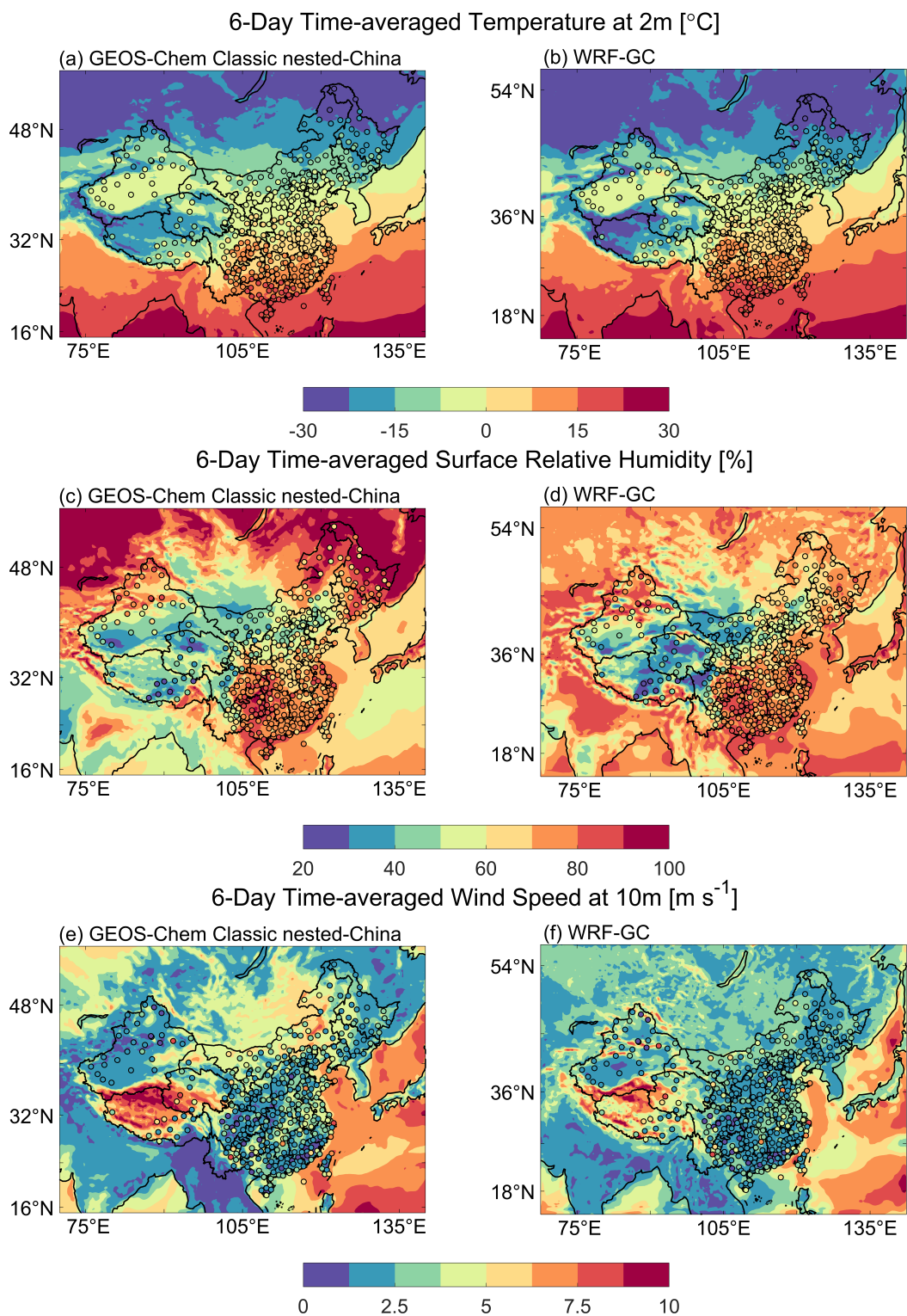


Figure S1. Six-day average values of simulated (filled contours) and observed (symbols) 2-m air temperature (upper panel), surface relative humidity (middle panel), and 10-m wind speed (bottom panel) during January 22-27, 2015: (a,c,e) meteorological variables used to drive the GEOS-Chem Classic nested-China simulation (i.e., the GEOS-FP dataset); (b,d,f) meteorological variables simulated by the WRF-GC model. Surface meteorological measurements at 367 sites were obtained from the U.S. National Climate Data Center (<https://gis.ncdc.noaa.gov/maps/ncei/cdo/hourly>). 48

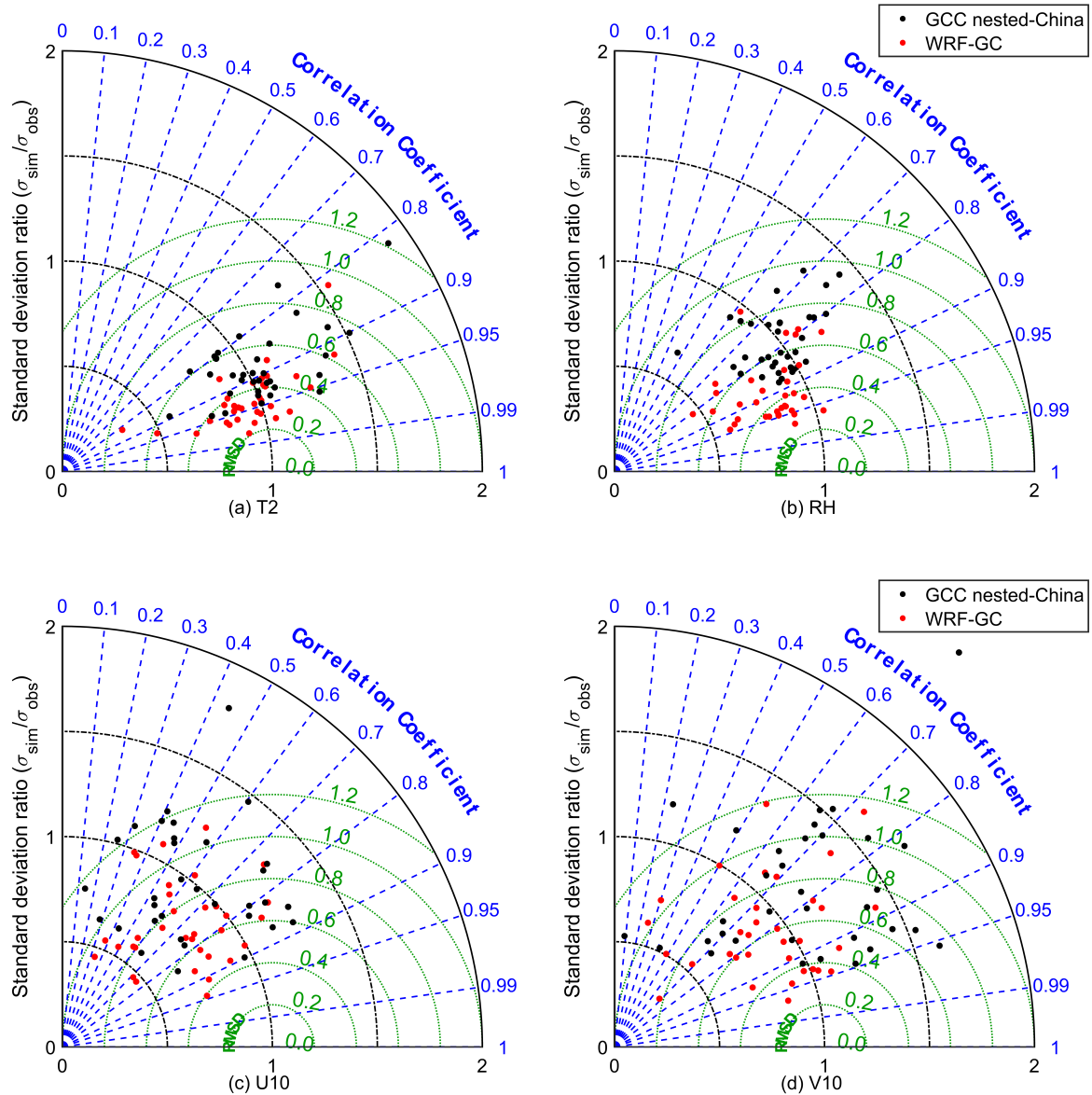


Figure S2. Assessments of the hourly meteorological variables simulated by the WRF-GC model (red dots) and those used to drive the GEOS-Chem Classic nested-China simulation (i.e., the GEOS-FP dataset, black dots) against hourly measurements at 34 surface sites during January 22-27, 2015: (a) 2-m air temperature, (b) surface relative humidity, (c) 10-m U-wind, and (d) 10-m V-wind. Green, black, and blue dashed lines indicate contours of the normalized centered root-mean-square differences (RMSD), the ratios of simulated versus observed standard deviations, and the Pearson correlation coefficients, respectively. Surface meteorological measurements were obtained from the U.S. National Climate Data Center (<https://gis.ncdc.noaa.gov/maps/ncei/cdo/hourly>). The 34 sites were selected (out of a total 367 sites) because hourly measurements were publicly-available at these sites.

R2.26 Line 417: Eliminating the need to read archived meteorology becomes even more important at high resolution offline approaches as more and more time is required for I/O.

Thank you for the suggestion. We have revised the text as follows.

P16, L480-482, Section 5.1:

As a CTM, the GEOS-Chem Classic read archived meteorological data for the entire domain at 3-model-hour intervals from hard drives using a single computational core, which becomes increasingly burdensome for simulations with more grid boxes.

R2.27 Line 418: I do not fully understand what reading from disks means. Do the authors mean the analyses are on some long-term storage device (tapes?) in which reading is slower than conventional hard-drives? Would a fairer timing test include having meteorological fields in a place with faster access?

Thank you for pointing this out. We meant that GEOS-Chem read meteorological data from hard drives. We used the exact same computational hardware with an Ethernet-connected file system for both WRF-GC and GEOS-Chem Classic for the computational performance assessment. We revise the manuscript to resolve this confusion.

P15, L471-472, section 5.1:

Both simulations were executed on the same single-node hardware with 32 Intel Broadwell physical cores and an Ethernet-connected hard disk array.

P16, L480-482, Section 5.1:

As a CTM, the GEOS-Chem Classic read archived meteorological data for the entire domain at 3-model-hour intervals from hard drives using a single computational core, which becomes increasingly burdensome for simulations with more grid boxes.

R2.28 Line 432: Figure 6 is difficult to interpret because of the scale on the y-axis. Ideally if one doubled the number of cores, one would want the wall clock time to be reduced by a factor of 2. It is hard to see this with the current scaling. To me it looks like the total performance does not improve much greater than 100 cores. In addition to “fragmentation” the authors mention, the most CPU time in WRF is due to the advection of species. The more chemical species there are the slower the code is. The authors mention 241 species on line 163 (presumably trace gas), but there would be aerosol species on top of that. This is more than other options in WRF-Chem, but less than others. In the conclusion the paper states that the WRF-chem community would benefit from GEOS-Chem, but it is not clear what the computational cost would be compared to other approaches. A large fraction of the users in the WRF community chose “simple” chemistry and aerosol schemes to save computational cost. While the authors may not wish to perform identical simulations with different chemical options to benchmark GEOS-Chem with others, the least they could do is compare the number of species to establish some sort of computational level of complexity.

Thank you for the excellent suggestion. We revised Figure 6 (now Figure 7) to a log-log plot and modified the discussion on the computational performance. In addition, we added a scalability test of WRF-GC on the cloud using the Amazon Web Services cloud.

P17, L518-522, Section 5.2:

The scalability test results are shown in Figure S3. In this massively parallel environment, WRF-GC scaled well up to 1728 cores, with the chemical module scaling well up to 2304 cores. The WRF-GC Coupler took less than 0.2% of the total computational time in this simulation and scaled perfectly up to 4608 cores. The deployability of WRF-GC on the cloud will enhance WRF-GC’s accessibility to new users by saving them the investment in hardware purchases and the effort in downloading and hosting large input datasets locally.

We also added a paragraph to compare the performance of WRF-Chem and WRF-GC, while specifying the dif-

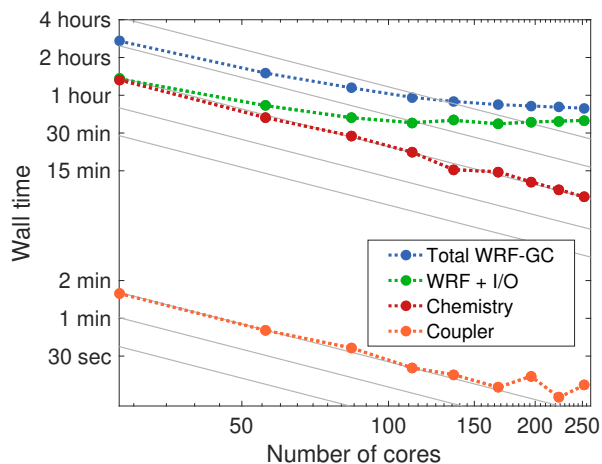


Figure 7. WRF-GC model scalability by processes. Gray lines indicate perfect scalability, i.e. halved computational time for each doubling of processor cores.

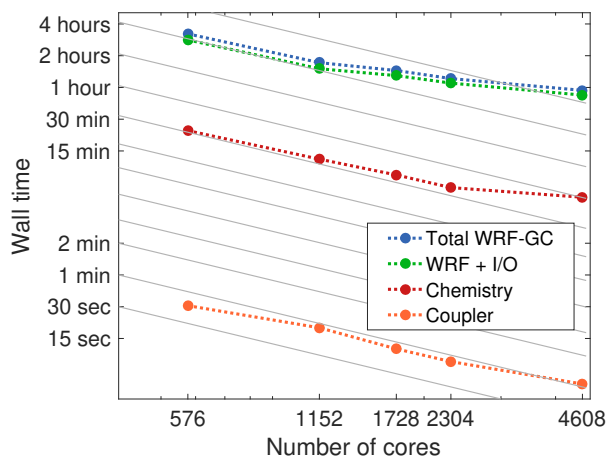


Figure S3. Scalability test of the WRF-GC model on the Amazon Web Services using up to 64 nodes and 4,608 cores. The simulation domain was over the continental U.S. at $5 \text{ km} \times 5 \text{ km}$ resolution (950×650 atmospheric columns), using 10-second dynamical time step and 5-minute external chemical time step.

ference in number of species advected.

P16, L489-498, Section 5.1:

A side-by-side wall time comparison between WRF-GC and WRF-Chem is difficult to do, because (1) the chemical routines in the two models are very different, and (2) the WRF-Chem has many possible configurations for chemistry. Nevertheless, we conducted one test simulation with WRF-Chem using a typical chemistry option (CBMZ-MOSAIC gas-phase chemistry, 4-bin aerosol microphysics and chemistry, and aqueous reactions; `chem_opt = 9` in `registry.chem`) with a total of 133 chemical species. This WRF-Chem simulation was configured for the same domain, at the same horizontal and vertical resolutions, and used the same physical and dynamical options as those in the WRF-GC simulation described above. The total wall time for the WRF-Chem simulation was 9985.8 seconds, which was almost twice as long as the wall time of WRF-GC (5127 seconds). Chemical routines in this WRF-Chem test simulation took up 61% of the total wall time (6134.3 seconds), despite the WRF-Chem having much fewer chemical species than the WRF-GC (241 chemical species). This may be partially due to the computationally inten-

sive bin-resolved aerosol microphysics calculation in the WRF-Chem simulation.

R2.29 Line 440: Change "light-weight" to "efficient".

Thank you for your suggestion. We have revised the text:

P17, L512-513, Section 5.2:

However, the degradation had negligible impact on the total WRF-GC wall time as the WRF-GC Coupler was computationally efficient.

R2.30 Line 449: The conclusion would benefit (perhaps at the end) about future directions. They are alluded to elsewhere in the text, but it would be good to briefly summarize them here. That would include things like more complex aerosol treatments and fully taking advantage of on-line coupling to include feedback effects (both of which are already in WRF-Chem). The conclusion would also be strengthened to foreshadow what would be discussed in part 2.

Thank you for your suggestion. We revised the last paragraph to describe future plans for WRF-GC development.

P18, L548-553, Section 6:

The WRF-GC model is free and open-source to all users. The one-way coupled version of WRF-GC (v1.0) is now publicly available at wrf.geos-chem.org. A two-way coupled version with chemical feedbacks from GEOS-Chem to WRF is under development and will be presented in a forthcoming paper. Further development of WRF-GC will aim to enable nested-domain simulations, support size-dependent aerosol microphysical calculations, as well as further improve the physical compatibility with WRF. We envision WRF-GC to become a powerful tool for research, forecast, and regulatory applications of regional atmospheric chemistry and air quality.

R2.31 Lines 460-463. As I mentioned earlier, the evaluation is rather simple. This paragraph should be rephrased to indicate this is only one case study (and thus not comprehensive) and other meteorological differences may be contributing to the PM2.5 predictions.

Thank you for your suggestion. We have revised the text following your comment. Please also refer to R2.25, where we have added validation of other simulated meteorological fields against the observations.

P17, L533-537

Our first application showed that the WRF-GC model was able to reproduce the spatiotemporal variation of surface PM_{2.5} concentrations over China in January 2015, with smaller biases compared to the results of the GEOS-Chem Classic nested-China simulation. This was partially because the WRF-GC model better represented the pollution meteorology, including the variability of the planetary boundary layer heights, over the region. In addition, the WRF-GC simulation was 3 times faster than a comparable GEOS-Chem Classic nested-grid simulation.

R2.32 Line 464: The first sentence is an overstatement and deceiving if a reader only looks at the conclusions. Yes, the chemistry part itself scales well but not the entire code.

Thank you for pointing this out. We have revised the text for accuracy. We also added a scalability analysis of the WRF-GC running on the Amazon Web Services.

P17, L516-521, Section 5.2:

We conducted a test simulation running WRF-GC on the Amazon Web Services (AWS) cloud with up to 128 nodes and 4608 cores. The simulation domain was over the continental U.S. at 5 km × 5 km resolution (950 × 650 atmospheric columns), with 10-second dynamical time step and 5-minute chemical time step. The scalability test results are shown in Figure S3. In this massively parallel environment, WRF-GC scaled well up to 1728 cores,

with the chemical module scaling well up to 2304 cores. The WRF-GC Coupler took less than 0.2% of the total computational time in this simulation and scaled perfectly up to 4608 cores.

P17-18, L538-542, Section 6:

WRF-GC demonstrated good scalability to massively parallel architectures, with near-perfect scalability of its chemistry component. This enables the WRF-GC model to be used on multiple-node systems or high-performance cloud computing platforms, which is not possible with the GEOS-Chem Classic. The GCHP model also scales to massively parallel architectures (Zhuang et al., 2020), but GCHP can only operate as a global model. The deployability of WRF-GC on the cloud will enhance WRF-GC's accessibility to new users.

3 Executive Editor

R3.1 In particular, please note that for your paper, the following requirement has not been met in the Discussions paper:

- "The main paper must give the model name and version number (or other unique identifier) in the title."

Please add a version number WRF and GEOS-CHEM in the title upon your revised submission to GMD (as named in the code availability section).

Thank you for your suggestion. We have revised the title of the paper:

WRF-GC (v1.0): online coupling of WRF (v3.9.1.1) and GEOS-Chem (v12.2.1) for regional atmospheric chemistry modeling, Part 1: description of the one-way model

References

- Allen, D. J., Rood, R. B., Thompson, A. M., and Hudson, R. D.: Three-dimensional radon 222 calculations using assimilated meteorological data and a convective mixing algorithm, *J. Geophys. Res. Atmos.*, 101, 6871–6881, <https://doi.org/10.1029/95JD03408>, 1996.
- Arakawa, A. and Jung, J. H.: Multiscale modeling of the moist-convective atmosphere - A review, *Atmos. Res.*, 102, 263–285, <https://doi.org/10.1016/j.atmosres.2011.08.009>, 2011.
- Damian, V., Sandu, A., Damian, M., Potra, F., and Carmichael, G. R.: The kinetic preprocessor KPP-a software environment for solving chemical kinetics, *Comput. Chem. Eng.*, 26, 1567–1579, [https://doi.org/10.1016/S0098-1354\(02\)00128-X](https://doi.org/10.1016/S0098-1354(02)00128-X), 2002.
- Eastham, S. D., Weisenstein, D. K., and Barrett, S. R.: Development and evaluation of the unified tropospheric–stratospheric chemistry extension (UCX) for the global chemistry-transport model GEOS-Chem, *Atmos. Environ.*, 89, 52–63, <https://doi.org/10.1016/j.atmosenv.2014.02.001>, 2014.
- Fairlie, T. D., Jacob, D. J., and Park, R. J.: The impact of transpacific transport of mineral dust in the United States, *Atmos. Environ.*, 41, 1251–1266, <https://doi.org/10.1016/j.atmosenv.2006.09.048>, 2007.
- Fountoukis, C. and Nenes, A.: ISORROPIA II: a computationally efficient thermodynamic equilibrium model for K^+ - Ca^{2+} - Mg^{2+} - NH_4^+ - Na^+ - SO_4^{2-} - NO_3^- - Cl^- - H_2O aerosols, *Atmos. Chem. Phys.*, 7, 4639–4659, <https://doi.org/10.5194/acp-7-4639-2007>, 2007.
- Friedman, C. L., Zhang, Y., and Selin, N. E.: Climate change and emissions impacts on atmospheric PAH transport to the Arctic, *Environ. Sci. Technol.*, 48, 429–437, <https://doi.org/10.1021/es403098w>, 2013.
- Gong, S. L.: A parameterization of sea-salt aerosol source function for sub-and super-micron particles, *Global Biogeochem. Cy.*, 17, <https://doi.org/10.1029/2003GB002079>, 2003.

- Grell, G. A. and Freitas, S. R.: A scale and aerosol aware stochastic convective parameterization for weather and air quality modeling, *Atmos. Chem. Phys.*, 14, 5233–5250, <https://doi.org/10.5194/acp-14-5233-2014>, 2014.
- Guenther, A. B., Jiang, X., Heald, C. L., Sakulyanontvittaya, T., Duhl, T., Emmons, L. K., and Wang, X.: The Model of Emissions of Gases and Aerosols from Nature version 2.1 (MEGAN2.1): an extended and updated framework for modeling biogenic emissions, *Geosci. Model. Dev.*, 5, 1471–1492, <https://doi.org/10.5194/gmd-5-1471-2012>, 2012.
- Guo, J., Miao, Y., Zhang, Y., Liu, H., Li, Z., Zhang, W., He, J., Lou, M., Yan, Y., Bian, L., and Zhai, P.: The climatology of planetary boundary layer height in China derived from radiosonde and reanalysis data, *Atmos. Chem. Phys.*, 16, 13 309–13 319, <https://doi.org/10.5194/acp-16-13309-2016>, 2016.
- Hoesly, R. M., Smith, S. J., Feng, L., Klimont, Z., Janssens-Maenhout, G., Pitkanen, T., Seibert, J. J., Vu, L., Andres, R. J., Bolt, R. M., Bond, T. C., Dawidowski, L., Kholod, N., Kurokawa, J.-I., Li, M., Liu, L., Lu, Z., Moura, M. C. P., O'Rourke, P. R., and Zhang, Q.: Historical (1750–2014) anthropogenic emissions of reactive gases and aerosols from the Community Emissions Data System (CEDS), *Geosci. Model. Dev.*, 11, 369–408, <https://doi.org/10.5194/gmd-11-369-2018>, 2018.
- Holtlag, A. and Boville, B.: Local Versus Nonlocal Boundary-Layer Diffusion in a Global Climate Model, *J. Climate*, 6, 1825–1842, [https://doi.org/10.1175/1520-0442\(1993\)006<1825:LVNBLD>2.0.CO;2](https://doi.org/10.1175/1520-0442(1993)006<1825:LVNBLD>2.0.CO;2), 1993.
- Horowitz, H. M., Jacob, D. J., Zhang, Y., Dibble, T. S., Slemr, F., Amos, H. M., Schmidt, J. A., Corbitt, E. S., Marais, E. A., and Sunderland, E. M.: A new mechanism for atmospheric mercury redox chemistry: implications for the global mercury budget, *Atmos. Chem. Phys.*, 17, 6353–6371, <https://doi.org/10.5194/acp-17-6353-2017>, 2017.
- Hudman, R. C., Moore, N. E., Mebust, A. K., Martin, R. V., Russell, A. R., Valin, L. C., and Cohen, R. C.: Steps towards a mechanistic model of global soil nitric oxide emissions: implementation and space based-constraints, *Atmos. Chem. Phys.*, 12, 7779–7795, <https://doi.org/10.5194/acp-12-7779-2012>, 2012.

- Jaeglé, L., Quinn, P. K., Bates, T. S., Alexander, B., and Lin, J.-T.: Global distribution of sea salt aerosols: new constraints from in situ and remote sensing observations, *Atmos. Chem. Phys.*, 11, 3137–3157, <https://doi.org/10.5194/acp-11-3137-2011>, 2011.
- Jeworrek, J., West, G., and Stull, R.: Evaluation of Cumulus and Microphysics Parameterizations in WRF across the Convective Gray Zone, *Weather. Forecast.*, 34, 1097–1115, <https://doi.org/10.1175/WAF-D-18-0178.1>, 2019.
- Jiang, Z., Jolleys, M. D., Fu, T.-M., Palmer, P. I., Ma, Y. P., Tian, H., Li, J., and Yang, X.: Spatiotemporal and probability variations of surface PM_{2.5} over China between 2013 and 2019 and the associated changes in health risks: An integrative observation and model analysis, *Sci. Total. Environ.*, 723, 137 896, <https://doi.org/10.1016/j.scitotenv.2020.137896>, 2020.
- Keller, C. A., Long, M. S., Yantosca, R. M., Da Silva, A. M., Pawson, S., and Jacob, D. J.: HEMCO v1.0: a versatile, ESMF-compliant component for calculating emissions in atmospheric models, *Geosci. Model Dev.*, 7, 1409–1417, <https://doi.org/10.5194/gmd-7-1409-2014>, 2014.
- Kim, P. S., Jacob, D. J., Fisher, J. A., Travis, K., Yu, K., Zhu, L., Yantosca, R. M., Sulprizio, M. P., Jimenez, J. L., Campuzano-Jost, P., Froyd, K. D., Liao, J., Hair, J. W., Fenn, M. A., Butler, C. F., Wagner, N. L., Gordon, T. D., Welti, A., Wennberg, P. O., Crouse, J. D., St. Clair, J. M., Teng, A. P., Millet, D. B., Schwarz, J. P., Markovic, M. Z., and Perring, A. E.: Sources, seasonality, and trends of southeast US aerosol: an integrated analysis of surface, aircraft, and satellite observations with the GEOS-Chem chemical transport model, *Atmos. Chem. Phys.*, 15, 10 411–10 433, <https://doi.org/10.5194/acp-15-10411-2015>, 2015.
- Kodros, J. and Pierce, J.: Important global and regional differences in aerosol cloud-albedo effect estimates between simulations with and without prognostic aerosol microphysics, *J. Geophys. Res. Atmos.*, 122, 4003–4018, <https://doi.org/10.1002/2016JD025886>, 2017.
- Li, M., Zhang, Q., Streets, D. G., He, K. B., Cheng, Y. F., Emmons, L. K., Huo, H., Kang, S. C., Lu, Z., Shao, M., Su,

- H., Yu, X., and Zhang, Y.: Mapping Asian anthropogenic emissions of non-methane volatile organic compounds to multiple chemical mechanisms, *Atmos. Chem. Phys.*, 14, 5617–5638, <https://doi.org/10.5194/acp-14-5617-2014>, 2014.
- Li, M., Liu, H., Geng, G., Hong, C., Liu, F., Song, Y., Tong, D., Zheng, B., Cui, H., Man, H., Zhang, Q., and He, K.: Anthropogenic emission inventories in China: a review, *Natl. Sci. Rev.*, 4, 834–866, <https://doi.org/10.1093/nsr/nwx150>, 2017a.
- Li, M., Zhang, Q., Kurokawa, J.-i., Woo, J.-H., He, K., Lu, Z., Ohara, T., Song, Y., Streets, D. G., Carmichael, G. R., Cheng, Y., Hong, C., Huo, H., Jiang, X., Kang, S., Liu, F., Su, H., and Zheng, B.: MIX: a mosaic Asian anthropogenic emission inventory under the international collaboration framework of the MICS-Asia and HTAP, *Atmos. Chem. Phys.*, 17, 935–963, <https://doi.org/10.5194/acp-17-935-2017>, 2017b.
- Lin, J.-T. and McElroy, M. B.: Impacts of boundary layer mixing on pollutant vertical profiles in the lower troposphere: Implications to satellite remote sensing, *Atmos. Environ.*, 44, 1726–1739, 2010.
- Liu, Y., Bourgeois, A., Warner, T., Swerdlin, S., and Hacker, J.: Implementation of Observation-Nudging Based FDDA into WRF for Supporting ATEC Test Operations, 2005 WRF user workshop, Boulder, CO, pp. 1–4, 2005.
- Liu, Y., Bourgeois, A., Warner, T., Swerdlin, S., and Yu, W.: An update on "observation nudging"-based FDDA for WRF-ARW: Verification using OSSE and performance of real-time forecasts, 2006 WRF user workshop, Boulder, CO, pp. 1–6, 2006.
- Long, M. S., Yantosca, R., Nielsen, J. E., Keller, C. A., da Silva, A., Sulprizio, M. P., Pawson, S., and Jacob, D. J.: Development of a grid-independent GEOS-Chem chemical transport model (v9-02) as an atmospheric chemistry module for Earth system models, *Geosci. Model Dev.*, 8, 595–602, <https://doi.org/10.5194/gmd-8-595-2015>, 2015.
- Marais, E. A., Jacob, D. J., Jimenez, J. L., Campuzano-Jost, P., Day, D. A., Hu, W., Krechmer, J., Zhu, L., Kim,

- P. S., Miller, C. C., Fisher, J. A., Travis, K., Yu, K., Hanisco, T. F., Wolfe, G. M., Arkinson, H. L., Pye, H. O. T., Froyd, K. D., Liao, J., and McNeill, V. F.: Aqueous-phase mechanism for secondary organic aerosol formation from isoprene: application to the southeast United States and co-benefit of SO₂ emission controls, *Atmos. Chem. Phys.*, 16, 1603–1618, <https://doi.org/10.5194/acp-16-1603-2016>, 2016.
- McLinden, C., Olsen, S., Hannegan, B., Wild, O., Prather, M., and Sundet, J.: Stratospheric ozone in 3-D models: A simple chemistry and the cross-tropopause flux, *J. Geophys. Res. Atmos.*, 105, 14 653–14 665, <https://doi.org/10.1029/2000JD900124>, 2000.
- Olson, D. M., Dinerstein, E., Wikramanayake, E. D., Burgess, N. D., Powell, G. V. N., Underwood, E. C., D'amico, J. A., Itoua, I., Strand, H. E., Morrison, J. C., Loucks, C. J., Allnutt, T. F., Ricketts, T. H., Kura, Y., Lamoreux, J. F., Wettengel, W. W., Hedao, P., and Kassem, K. R.: Terrestrial Ecoregions of the World: A New Map of Life on Earth: A new global map of terrestrial ecoregions provides an innovative tool for conserving biodiversity, *BioScience*, 51, 933–938, [https://doi.org/10.1641/0006-3568\(2001\)051\[0933:TEOTWA\]2.0.CO;2](https://doi.org/10.1641/0006-3568(2001)051[0933:TEOTWA]2.0.CO;2), 2001.
- Park, R. J., Jacob, D. J., Field, B. D., Yantosca, R. M., and Chin, M.: Natural and transboundary pollution influences on sulfate-nitrate-ammonium aerosols in the United States: Implications for policy, *J. Geophys. Res. Atmos.*, 109, <https://doi.org/10.1029/2003JD004473>, 2004.
- Peckham, S. E., Grell, G. A., McKeen, S. A., Ahmadov, R., Barth, M., Pfister, G., Wiedinmyer, C., Fast, J. D., Gustafson, W. I., Ghan, S. J., Zaveri, R., Easter, R. C., Barnard, J., Chapman, E., Hewson, M., Schmitz, R., Salzman, M., B. V., and Freitas, S. R.: WRF-Chem Version 3.9.1.1 User's Guide, 2017.
- Philip, S., Martin, R. V., Pierce, J. R., Jimenez, J. L., Zhang, Q., Canagaratna, M. R., Spracklen, D. V., Nowlan, C. R., Lamsal, L. N., Cooper, M. J., and Krotkov, N. A.: Spatially and seasonally resolved estimate of the ratio of organic mass to organic carbon, *Atmos. Environ.*, 87, 34–40, <https://doi.org/10.1016/j.atmosenv.2013.11.065>, 2014.

- Pye, H. O. T., Liao, H., Wu, S., Mickley, L. J., Jacob, D. J., Henze, D. K., and Seinfeld, J. H.: Effect of changes in climate and emissions on future sulfate-nitrate-ammonium aerosol levels in the United States, *J. Geophys. Res. Atmos.*, 114, <https://doi.org/10.1029/2008JD010701>, 2009.
- Pye, H. O. T., Chan, A. W. H., Barkley, M. P., and Seinfeld, J. H.: Global modeling of organic aerosol: the importance of reactive nitrogen (NO_x and NO_3), *Atmos. Chem. Phys.*, 10, 11 261–11 276, <https://doi.org/10.5194/acp-10-11261-2010>, 2010.
- Robinson, A. L., Donahue, N. M., Shrivastava, M. K., Weitkamp, E. A., Sage, A. M., Grieshop, A. P., Lane, T. E., Pierce, J. R., and Pandis, S. N.: Rethinking organic aerosols: Semivolatile emissions and photochemical aging, *Science*, 315, 1259–1262, <https://doi.org/10.1126/science.1133061>, 2007.
- Sandu, A. and Sander, R.: Technical note: Simulating chemical systems in Fortran90 and Matlab with the Kinetic PreProcessor KPP-2.1, *Atmos. Chem. Phys.*, 6, 187–195, <https://doi.org/10.5194/acp-6-187-2006>, 2006.
- Skamarock, W. C., Klemp, J. B., Dudhia, J., Gill, D. O., Liu, Z., Berner, J., and Huang, X.: NCAR Tech. Note NCAR/TN-556+STR: A Description of the Advanced Research WRF Model Version 4, <https://doi.org/10.5065/1dfh-6p97>, 2019.
- Skamarock, W. C. et al.: NCAR Tech. Note NCAR/TN-475+STR: A Description of the Advanced Research WRF Version 3, <https://doi.org/10.5065/D68S4MVH>, 2008.
- Soerensen, A. L., Sunderland, E. M., Holmes, C. D., Jacob, D. J., Yantosca, R. M., Skov, H., Christensen, J. H., Strode, S. A., and Mason, R. P.: An improved global model for air-sea exchange of mercury: High concentrations over the North Atlantic, *Environ. Sci. Technol.*, 44, 8574–8580, <https://doi.org/10.1021/es102032g>, 2010.
- Stauffer, D. R. and Seaman, N. L.: Use of Four-Dimensional Data Assimilation in a Limited-Area Mesoscale Model. Part I: Experiments with Synoptic-Scale Data, *Mon. Weather. Rev.*, 118, 1250–1277, [https://doi.org/10.1175/1520-0493\(1990\)118<1250:UOFDDA>2.0.CO;2](https://doi.org/10.1175/1520-0493(1990)118<1250:UOFDDA>2.0.CO;2), 1990.

- Stauffer, D. R. and Seaman, N. L.: Multiscale Four-Dimensional Data Assimilation, *J. Appl. Meteorol.*, 33, 416–434, [https://doi.org/10.1175/1520-0450\(1994\)033<0416:MFDDA>2.0.CO;2](https://doi.org/10.1175/1520-0450(1994)033<0416:MFDDA>2.0.CO;2), 1994.
- Taylor, K.: Summarizing multiple aspects of model performance in a single diagram., *J. Geophys. Res. Atmos.*, 106, 7183–7192, <https://doi.org/10.1029/2000JD900719>, 2001.
- U.S. Environmental Protection Agency: 2011 National Emissions Inventory, version 1 Technical Support Document, 2014.
- Wang, Q., Jacob, D. J., Spackman, J. R., Perring, A. E., Schwarz, J. P., Moteki, N., Marais, E. A., Ge, C., Wang, J., and Barrett, S. R. H.: Global budget and radiative forcing of black carbon aerosol: Constraints from pole-to-pole (HIPPO) observations across the Pacific, *J. Geophys. Res. Atmos.*, 119, 195–206, <https://doi.org/10.1002/2013JD020824>, 2014.
- Wang, Y., Jacob, D. J., and Logan, J. A.: Global simulation of tropospheric O₃-NO_x-hydrocarbon chemistry: 1. Model formulation, *J. Geophys. Res. Atmos.*, 103, 10 713–10 725, <https://doi.org/10.1029/98JD00158>, 1998.
- Wesely, M. L.: Parameterization of surface resistances to gaseous dry deposition in regional-scale numerical models, *Atmos. Environ.*, 23, 1293–1304, [https://doi.org/10.1016/0004-6981\(89\)90153-4](https://doi.org/10.1016/0004-6981(89)90153-4), 1989.
- Wu, S., Mickley, L. J., Jacob, D. J., Logan, J. A., Yantosca, R. M., and Rind, D.: Why are there large differences between models in global budgets of tropospheric ozone?, *J. Geophys. Res. Atmos.*, 112, <https://doi.org/10.1029/2006JD007801>, 2007.
- Yu, F. and Luo, G.: Simulation of particle size distribution with a global aerosol model: contribution of nucleation to aerosol and CCN number concentrations, *Atmos. Chem. Phys.*, 9, 7691–7710, <https://doi.org/10.5194/acp-9-7691-2009>, 2009.
- Zender, C. S., Bian, H., and Newman, D.: Mineral Dust Entrainment and Deposition (DEAD) model: Description and 1990s dust climatology, *J. Geophys. Res. Atmos.*, 108, <https://doi.org/10.1029/2002JD002775>, 2003.

Zhuang, J., Jacob, D. J., Lin, H., Lundgren, E. W., Yantosca, R. M., Gaya, J. F., Sulprizio, M. P., and Eastham, S. D.:
Enabling high-performance cloud computing for Earth science modeling on over a thousand cores: application to
the GEOS-Chem atmospheric chemistry model, *J. Adv. Model. Earth. Sy.*, n/a, e2020MS002 064, <https://doi.org/10.1029/2020MS002064>, 2020.

WRF-GC (v1.0): online coupling of WRF (v3.9.1.1) and GEOS-Chem (v12.2.1) for regional atmospheric chemistry modeling, Part 1: description of the one-way model(v1.0)

Haipeng Lin^{1,2}, Xu Feng¹, Tzung-May Fu^{3,4*}, Heng Tian¹, Yaping Ma¹, Lijuan Zhang¹, Daniel J. Jacob², Robert M. Yantosca², Melissa P. Sulprizio², Elizabeth W. Lundgren², Jiawei Zhuang², Qiang Zhang⁵, Xiao Lu^{1,2}, Lin Zhang¹, Lu Shen², Jianping Guo⁶, Sebastian D. Eastham⁷, and Christoph A. Keller⁸

¹Department of Atmospheric and Oceanic Sciences, School of Physics, Peking University, Beijing, China

²Harvard John A. Paulson School of Engineering and Applied Sciences, Harvard University, Cambridge, MA, USA

³State Environmental Protection Key Laboratory of Integrated Surface Water-Groundwater Pollution Control, School of Environmental Science and Engineering, Southern University of Science and Technology, Shenzhen, Guangdong, China

⁴Shenzhen Institute of Sustainable Development, Southern University of Science and Technology, Shenzhen, Guangdong, China

⁵Ministry of Education Key Laboratory for Earth System Modeling, Department of Earth System Science, Tsinghua University, Beijing, China

⁶State Key Laboratory of Severe Weather & Key Laboratory of Atmospheric Chemistry of CMA, Chinese Academy of Meteorological Sciences, Beijing, China

⁷Laboratory for Aviation and the Environment, Massachusetts Institute of Technology, Cambridge, MA, USA

⁸Universities Space Research Association, Columbia, Maryland, USA

Correspondence: Tzung-May Fu (fuzm@sustech.edu.cn)

Abstract. We developed the WRF-GC model, an online coupling of the Weather Research and Forecasting (WRF) mesoscale meteorological model and the GEOS-Chem atmospheric chemistry model, for regional atmospheric chemistry and air quality modeling. ~~Both~~ WRF and GEOS-Chem are ~~both~~ open-source ~~and community-supported~~ **community models**. WRF-GC ~~provides regional chemistry modellers easy~~ **offers regional modellers** access to the **latest** GEOS-Chem chemical module, which is ~~stably-configured~~, state-of-the-science, well-documented, traceable, benchmarked, actively developed by a large international user base, and centrally managed by a dedicated support team. At the same time, WRF-GC ~~gives~~ **enables** GEOS-Chem users ~~the ability~~ to perform high-resolution forecasts and hindcasts for any ~~location~~ **region** and time of interest. WRF-GC ~~is designed to be easy to use, massively parallel, extendable, and easy to update. The WRF-GC uses unmodified copies of WRF and GEOS-Chem from their respective sources; the~~ coupling structure allows future versions of either one of the ~~two parent models to be immediately~~ integrated into WRF-GC ~~. This enables with relative ease. Within WRF-GC to stay state-of-the-science with traceability to parent model versions. Physical~~, ~~the physical~~ and chemical state variables ~~in WRF and in GEOS-Chem~~ are managed in distributed memory and translated between ~~the two models~~ **WRF and GEOS-Chem** by the WRF-GC Coupler at runtime. We used the WRF-GC model to simulate surface PM_{2.5} concentrations over China during January 22 to 27, 2015 and compared the results to surface observations and the outcomes from a GEOS-Chem ~~nested-grid~~ **Classic** ~~nested-China~~ simulation. Both models were able to reproduce the observed spatiotemporal variations of regional PM_{2.5}, but the WRF-GC model (r = 0.68, bias = 29%) reproduced the observed daily PM_{2.5} concentrations over Eastern China better than the

GEOS-Chem ~~Classic~~ model did ($r = 0.72$, bias = 55%). This was ~~mainly because our~~ ~~because the~~ WRF-GC simulation, nudged with surface and upper-level meteorological observations, was able to better represent the ~~spatiotemporal variability of the planetary boundary layer heights over China during the simulation period. Both parent models and the pollution meteorology~~ ~~during the study period. The~~ WRF-GC ~~Coupler are~~ model is parallelized across computational cores and ~~can scale to scales well on~~ massively parallel architectures. ~~The~~ ~~In our tests where the two models were similarly configured, the~~ WRF-GC simulation was three times more efficient than the GEOS-Chem ~~Classic~~ nested-grid simulation ~~at similar resolutions and for the same number of computational cores~~, owing to the ~~more~~ efficient transport algorithm and the MPI-based parallelization provided by the WRF software framework. WRF-GC ~~scales nearly perfectly up to a few hundred cores on a variety of computational~~ ~~platforms. Version 1.0 of the WRF-GC model v1.0~~ supports one-way coupling only, using WRF-simulated meteorological fields to drive GEOS-Chem with no ~~feedbacks from GEOS-Chem~~ ~~chemical~~ ~~feedbacks~~. The development of two-way coupling capabilities, i.e., the ability to simulate radiative and microphysical feedbacks of chemistry to meteorology, is under-way. The WRF-GC model is open-source and freely available from <http://wrf.geos-chem.org>.

1 Introduction

30 Regional models of atmospheric chemistry simulate the emission, transport, chemical evolution, and removal of atmospheric constituents over a ~~regional~~ ~~given~~ domain. These models are widely useful for forecasts of air quality, for impact-assessment associated with polluting activities, and for theory-validation by comparisons against observations. It is thus crucial that regional models be frequently updated to reflect the latest scientific understandings of atmospheric processes. At the same time, the increasing demand for fine-resolution simulations requires models to adapt to massively parallel computation ~~structures ar-~~ ~~chitectures~~ with high scalability. We present here the development of a new regional atmospheric chemistry model, WRF-GC, specifically designed to ~~stay state-of-the-science~~ ~~allow~~ ~~easy~~ ~~updates~~ and be computationally efficient, ~~in order to better serve the public, inform policy makers, and advance science~~ ~~for use in research and operation applications~~.

Regional atmospheric chemistry models fall into two categories: offline models and online models. Offline models (also called chemical transport models, CTMs) use archived meteorological fields, either those simulated by models alone or those ~~40~~ assimilated with observations, to drive the transport and chemical evolution of atmospheric constituents (Baklanov et al., 2014). By eliminating the need to solve dynamical processes online, the developers of offline models can focus their efforts to solving more complex chemical processes. For example, one popular regional CTM is the GEOS-Chem model in its nested-grid configuration (Bey et al., 2001; Wang et al., 2004; Chen et al., 2009; Zhang et al., 2015), which is driven by high-resolution assimilated meteorological data from the Goddard Earth Observation System (GEOS) ~~model~~ of the NASA Global ~~45~~ Modeling and Assimilation Office (GMAO). GEOS-Chem has undergone three major chemical updates in the last year. Its latest standard chemical mechanism (~~version 12.6.0 as of the time of this submission~~) includes state-of-the-science O_x - NO_x -VOC-halogen-aerosol reactions. In addition, GEOS-Chem offers a number of specialty simulations to address a variety of scientific questions, such as simulations of CO_2 (Nassar et al., 2010), CO (Fisher et al., 2017), methane (Maasackers et al., 2019), mercury (Horowitz et al., 2017; Soerensen et al., 2010), persistent organic pollutants (Friedman et al., 2013), and

50 dicarbonyls (Fu et al., 2008, 2009; Cao et al., 2018). ~~Another widely-used regional CTM is the Community Multiscale Air Quality Modeling System (CMAQ) (Byun and Schere, 2006), which is driven by meteorology fields simulated by the Weather Research and Forecasting model (WRF) (Skamarock et al., 2008). CMAQ has undergone three major chemical updates in the last four years. The standard chemical mechanism of CMAQ (v5.3 as of the time of this submission) also includes updated options for O_x-NO_x-VOC-halogen-aerosol chemistry. Several other regional offline models in common use are summarized in~~
55 ~~Table ??.~~ ~~The chemical mechanisms in these offline models are generally updated at least once a year.~~

Despite their updated representation of chemical processes and relative ease of use, offline models have several key shortcomings. First, the applications of some offline models are limited by the time span and resolution of the available meteorological data. In the case of the GEOS-Chem nested-grid model, its application is currently limited to $0.5^\circ \times 0.625^\circ$ latitude \times 0.625° longitude or coarser resolution between 1979 and the present day when using the Modern-Era Retrospective analysis for Research and Applications, Version 2 (MERRA-2) dataset, or to $0.25^\circ \times 0.3125^\circ$ latitude \times 0.3125° longitude or coarser resolution between 2013 and the present day when using the GEOS-Forward Processing (GEOS-FP) dataset. The temporal interpolation of sparsely-archived meteorological data can also cause significant errors in the CTM simulations (Yu et al., 2018). Most importantly, offline models cannot simulate meteorology-chemistry interactions due to the lack of chemical feedback to meteorology.

65 In contrast, online regional atmospheric chemistry models perform integrated meteorological and chemical calculations, managed through operator splitting (Baklanov et al., 2014). In this way, online models can simulate regional atmospheric chemistry at any location and time of interest, without the need for temporal interpolation of the meteorological variables. Moreover, online models have the option to include "two-way coupling" processes, i.e., the response of meteorology to gases and aerosols via interactions with radiation and cloud processes. Many studies have demonstrated the importance of two-way
70 interactions in accurate air quality simulations (e.g., Li et al. (2011); Ding et al. (2013); Wang et al. (2014a)). One of the most ~~extensively used online models for regional atmospheric chemistry~~ widely used online regional models is the Weather Research and Forecasting model coupled with Chemistry (WRF-Chem), with options for either one-way or two-way coupling (Grell et al., 2005; Fast et al., 2006). The latest version of WRF-Chem (v4.1) includes many options for O_x-NO_x-VOC-aerosol chemistry. WRF-Chem simulates the two-way interactions between chemistry and meteorology by taking into account the
75 scattering and absorption of radiation by gases and aerosols, as well as the activation of aerosols as cloud condensation nuclei and ice nuclei (Fast et al., 2006; Gustafson et al., 2007; Chapman et al., 2009).

However, keeping the representation of atmospheric processes up-to-date is ~~considerably more difficult~~ potentially more challenging for online models than it is for offline models. ~~Table 1 summarizes some of the regional online models currently in use. These online models are updated annually at best, considerably less frequent than the chemical updates to offline models. The reasons for the relatively infrequent updates to online models are threefold. First, the resources available to the development teams of online models are spread thinner, such that updating, benchmarking, validating, and documenting the many more individual components of online models are difficult to do in a timely way. Second, the modelling expertise for atmospheric physical and chemical processes resides in different communities, such that each community would often develop its own model variations without communicating the changes back to the full model. As a result, model versions may~~

85 quickly diverge, and the integrity of the full model is difficult to maintain. This is currently an issue with the WRF-Chem
model, where the different optional schemes are developed by different communities and not always compatible with one
another. ~~Thirdly, the~~ ~~One of the reasons for this is that the~~ interactions between the chemical and meteorological modules
are ~~often~~ hard-wired in some online models, such that updating either module requires considerable effort. ~~An example of~~
90 ~~this last point is the online WRF-CMAQ model, which is a coupled implementation of the WRF model and the CMAQ~~
~~model(Wong et al., 2012; Yu et al., 2014). This implementation involved direct code modifications to WRF, which reduced the~~
~~immediate applicability to updates of either parent models~~ For the same reason, if users make improvements to the chemical
or meteorological processes in the online model, those improvements may be relatively difficult to propagate to the broader
community. This may lead to the model diverging into different branches, and users may be forced to work with stale, branched
versions of the code.

95 In this work, we developed a new online regional atmospheric chemistry model, WRF-GC, by coupling the WRF meteo-
rology model with the GEOS-Chem chemistry model. Both WRF and GEOS-Chem are open-source and ~~supported~~ actively
~~developed~~ by the community. We ~~developed~~ constructed WRF-GC with the following guidelines, in order to ~~facilitate usage,~~
~~maintenance, and extension of model capability in the future~~ best take advantage of new developments in the two parent models
and to enhance usability:

- 100 1. The coupling structure of WRF-GC should be abstracted from the parent models ~~and involve no hard-wired codes to~~
~~either parent model, such that~~, and both parent models remain unmodified from their respective sources. In this way,
future updates of the parent models can be ~~immediately~~ quickly incorporated into WRF-GC with ease-, ~~such that WRF-~~
GC can stay cutting-edge. It also enables WRF-GC users to more easily contribute their developments back to the parent
models.
- 105 2. The WRF-GC coupled model should scale from conventional computation hardware to massively parallel computation
architectures.
3. The WRF-GC coupled model should be easy to install and use, open-source, version-controlled, and well-documented.

WRF-GC ~~provides~~ offers users of WRF-Chem or other regional models ~~access to the option to use~~ the latest GEOS-Chem
chemical module. ~~The advantage of GEOS-Chem is that it is state-of-the-science, well-documented, traceable, benchmarked,~~
110 ~~, which is~~ actively developed by a large international user base, ~~and centrally managed by a dedicated support team. At the~~
~~same time,~~ well-documented, traceable, benchmarked, and centrally-managed. Through WRF-GC, regional modellers also
gain access to the specialty simulations in GEOS-Chem, such as the simulations of mercury (Horowitz et al., 2017; Soerensen
et al., 2010) and persistent organic pollutants (Friedman et al., 2013). WRF-GC drives ~~the~~ GEOS-Chem ~~chemical module~~
with online meteorological fields simulated by ~~the WRF~~ open-source meteorological model. ~~WRF~~ WRF, which in turn can be
115 driven by initial and boundary meteorological conditions from many different assimilated datasets or climate model outputs
(Skamarock et al., 2008, 2019). As such, WRF-GC allows GEOS-Chem users to perform high-resolution ~~regional chemistry~~
simulations in both forecast and hindcast modes at any location and time of interest.

In this Part 1 paper, we describe the development of the WRF-GC model (v1.0, doi:10.5281/zenodo.3550330) for simulation over a single domain with one-way coupling capability. The nested domain and two-way coupling capabilities are under development and will be described in a forthcoming paper.

2 The parent models: WRF and GEOS-Chem

2.1 The WRF model

Meteorological processes and advection of atmospheric constituents in the WRF-GC coupled model are simulated by the WRF model (version 3.9v3.9.1.1 or later versions). ~~WRF is an open-source community~~, a mesoscale numerical weather model designed for both for research and operational applications (Skamarock et al., 2008, 2019). WRF currently offers its users many options for model configurations and physical schemes. WRF uses the Advanced Research WRF (ARW) dynamical solver, which solves fully compressible, Eulerian non-hydrostatic equations on ~~terrain-following, hybrid vertical coordinates~~. Vertical levels in WRF can be either hybrid sigma-eta (default) or terrain-following vertical coordinates defined by the user. Horizontal grids in WRF are staggered Arakawa C-grids, which can be configured by the user using four map projections: latitude-longitude, Lambert conformal, Mercator, and polar stereographic. WRF supports the use of multiple nested domains to simulate the interactions between large-scale dynamics and meso-scale meteorology. WRF supports grid-, spectral-, and observational-nudging (Liu et al., 2005, 2006; Stauffer and Seaman, 1990, 1994). This allows the WRF model to produce meteorological outputs that mimic assimilated meteorological fields for use in air quality hindcasts. The WRF model offers many options for land surface physics, planetary boundary layer physics, radiative transfer, cloud microphysics, and cumulus parameterization, for use in meteorological studies, real-time numerical weather prediction, idealized simulations, and data assimilation on meso-to regional scales (Skamarock et al., 2008, 2019). Table 3 lists the configuration and physical options supported by WRF-GC v1.0. In particular, only the hybrid sigma-eta vertical coordinate is currently supported in WRF-GC.

The WRF model incorporates a highly modular software framework that is portable across a range of computing platforms. WRF supports two-level domain decomposition for distributed-memory (MPI) and shared-memory (OpenMP) parallel computation. Distributed parallelism is implemented through the Runtime System Library lite (RSL-lite) module, which supports irregular domain decomposition, automatic index translation, distributed input/output, and low-level interfacing with MPI libraries (Michalakes et al., 1999).

2.2 The GEOS-Chem model

Our development of WRF-GC is was made possible by a recent structural overhaul of GEOS-Chem (Long et al., 2015; Eastham et al., 2018), which enabled the use of GEOS-Chem as a self-contained chemical module within the WRF-GC model. The original GEOS-Chem CTM (before version 11.01 prior to v11.01) was structured specifically for several sets of static static sets of global or regional 3-D grids at pre-determined-prescribed horizontal and vertical resolutions (Bey et al., 2001). Parallelism for the original GEOS-Chem was implemented through OpenMP, which limited the deployment of the such that the original

GEOS-Chem ~~to~~ can only operate on single-node hardware with large shared memory. Long et al. (2015) restructured the
150 core processes in GEOS-Chem, including emission, chemistry, convective mixing, planetary boundary layer ~~transport~~mixing,
and deposition processes, to work in modular units of atmospheric vertical columns. Information about the horizontal grids,
formerly fixed at compile-time, are now passed to the GEOS-Chem chemical module at runtime. This development enabled
the use of the GEOS-Chem chemical module with any horizontal grid structure and horizontal resolution.

The new, modularized structure of the GEOS-Chem has been implemented in two types of configurations. The first type
155 of configuration uses GEOS-Chem as the core of offline CTMs. For example, in the GEOS-Chem "Classic" implementation
(GCC), the GEOS-Chem chemical module is driven by the GEOS ~~assimilated~~ meteorological data and is parallelized using
OpenMP. This implementation treats the ~~pre-defined~~prescribed global or regional model ~~domain as a contiguous set~~domains
~~as contiguous sets~~ of atmospheric columns ~~placed at regular latitude/longitude intervals~~, with vertical layers ~~pre-configured~~
~~pre-defined~~ to match those of the GEOS model. In essence, ~~this configuration~~the GCC implementation mimics the "original"
160 GEOS-Chem model before the structural overhaul by Long et al. (2015). Other grid systems can also be used with the GEOS-
Chem chemical module. For example, the GEOS-Chem High Performance implementation (GCHP) (Eastham et al., 2018) calls
the GEOS-Chem module on the native cubed-sphere coordinates of the NASA GEOS model via a column interface
in GEOS-Chem ~~-(GIGC_Chunk_Run)~~. This column interface was built on the Earth System Modeling Framework (ESMF)
(Eastham et al., 2018) and permits runtime specification of the horizontal grid parameters. The GCHP implementation uses
165 MPI to parallelize GEOS-Chem across nodes through the Model Analysis and Prediction Layer framework (MAPL) (Suarez
et al., 2007), which is a wrapper on top of ESMF specifically designed for the ~~GMAO-GEOS-NASA~~ GEOS model system.

Alternatively, GEOS-Chem can be used as a module coupled to weather models or Earth System models to perform online
chemical calculations. Using this capability, Hu et al. (2018) developed an online implementation of GEOS-Chem by coupling
it to the NASA GEOS-5 model to simulate global atmospheric chemistry. Lu et al. (2019) coupled GEOS-Chem to the Beijing
170 Climate Center Atmospheric General Circulation Model (BCC-AGCM). However, both the ~~NASA~~ GEOS-5 model and the
BCC-AGCM are proprietary.

WRF-GC is the first implementation that couples the GEOS-Chem chemical module to an open-access high-resolution
meteorological model. We developed a modular coupler between WRF and GEOS-Chem that draws from the technology of
GCHP but does not rely on ESMF (described in ~~section~~Section 3.2). We also made changes to GEOS-Chem to accept arbitrary
175 vertical discretization from WRF at runtime and to improve physical compatibility with WRF (described in ~~section~~Section
3.2.1). These changes have been incorporated into the mainline GEOS-Chem code. Our coupler and code modifications can be
adapted in the future to couple GEOS-Chem to other non-ESMF Earth System models.

Chemical calculations in WRF-GC v1.0 use ~~the~~GEOS-Chem version 12.2.1 (doi:10.5281/zenodo.2580198). The standard
chemical mechanism in GEOS-Chem ~~v12.2.1, used by default in WRF-GC~~, includes detailed O_x-NO_x-VOC-ozone-halogen-
180 aerosol in the troposphere, as well as the Unified tropospheric-stratospheric chemistry extension (UCX) (Eastham et al.,
2014) for stratospheric chemistry and stratosphere-troposphere exchange. The ~~standard~~ gas-phase mechanism ~~in GEOS-Chem~~
~~currently includes 241~~includes 208 chemical species and 981 reactions. Reactions and rates follow the latest recommendations
from the Jet Propulsion Laboratory and the International Union of Pure and Applied Chemistry. ~~In addition~~, GEOS-Chem uses

the FlexChem pre-processor (a wrapper for the Kinetic PreProcessor, KPP, Damian et al. (2002); Sandu and Sander (2006)) to configure chemical kinetics (Long et al., 2015). FlexChem also allows GEOS-Chem users to easily add chemical-
185 allows users to add or modify gaseous species and reactions, and to develop custom mechanisms and diagnostics. diagnostic quantities in GEOS-Chem. GEOS-Chem also supports the optional "Tropchem" (troposphere-only chemistry) mechanism, where UCX is disabled and replaced by a parameterized linear chemistry in the stratosphere (McLinden et al., 2000). GEOS-Chem uses the Rosenbrock rodas-3 solver (Sandu et al., 1997) for gas-phase chemistry by default, but users may choose other
190 solvers through KPP.

By default, aerosols in the Aerosol species in GEOS-Chem chemical module are simulated as speciated bulk masses, including includes secondary inorganic aerosols (sulfate, nitrate, ammonium), elemental carbon aerosol (EC), black carbon
primary organic aerosol (POA) carbon (POC), secondary organic aerosol (SOA), dust, and sea salt. Detailed, size-dependent aerosol microphysics are also available as options using the TwO-Moment Aerosol Sectional microphysics (TOMAS) module
195 (Kodros and Pierce, 2017) or the Advanced Particle Microphysics (APM) module (Yu and Luo, 2009). However, these two options are not yet supported by WRF-GC v1.0. By default, secondary inorganic aerosols, EC, POC, and SOA are simulated as speciated bulk masses. Dust aerosols are represented in 4 size bins (0.1-1.0, 1.0-1.8, 1.8-3.0, and 3.0-6.0 μm) (Fairlie et al., 2007), while sea salt aerosols are represented in 2 size bins (0.1-0.5 and 0.5-4.0 μm) (Jaeglé et al., 2011). The thermodynamics of secondary inorganic aerosol are coupled to gas-phase chemistry and computed with-by the ISORROPIA II
200 module (Park et al., 2004; Fountoukis and Nenes, 2007; Pye et al., 2009). Black carbon and POA EC and POC are represented in GEOS-Chem as partially hydrophobic and partially hydrophilic, with a conversion timescale from hydrophobic to hydrophilic of 1.2 days (Wang et al., 2014b). The organic matter to organic carbon (OM/OC) mass ratio is assumed to be 2.1 for POC by default, with an option to use seasonally and spatially varying OM/OC ratios (Philip et al., 2014). GEOS-Chem includes has two options to describe the production of SOA, and both options are supported in WRF-GC. By default, SOA are-is produced
205 irreversibly using simple yields from anthropogenic and biogenic volatile organic precursors (Kim et al., 2015). Alternatively, SOA can be complexly produced from the aqueous reactions of oxidation products from isoprene (Marais et al., 2016), as well as from the GEOS-Chem can simulate SOA production via the aging of semi-volatile and intermediate volatility POA-organic precursors using a volatility basis set (VBS) scheme (Robinson et al., 2007; Pye et al., 2010), as well as via the aqueous reactions of the oxidation products from isoprene (Marais et al., 2016). The GEOS-Chem model also has the option of simulat-
210 ing detailed, size-dependent aerosol microphysics using the TwO-Moment Aerosol Sectional microphysics (TOMAS) module (Kodros and Pierce, 2017) or the Advanced Particle Microphysics (APM) module (Yu and Luo, 2009), but these two modules are not yet supported in WRF-GC. Dust aerosols are represented in 4 size bins (Fairlie et al., 2007), while sea salt aerosols are represented in accumulation and coarse modes (Jaeglé et al., 2011).

All emissions in GEOS-Chem are configured at runtime using the Harvard-NASA Emissions Component (HEMCO) Emis-
215 sions of chemical species in WRF-GC are calculated using the HEMCO emissions component in GEOS-Chem (Keller et al., 2014). HEMCO allows users to select emission inventories from the GEOS-Chem library HEMCO data directory or add their own inventories, and interpolate the emission fluxes to the model domain and resolution at runtime. The HEMCO data directory currently includes more than 20 global and regional emission inventories, apply scaling factors, overlay and

~~mask inventories among other operations, without having to edit or compile the code.~~ mostly at their respective native resolu-
220 tions (http://wiki.seas.harvard.edu/geos-chem/index.php/HEMCO_data_directories). By default, the Community Emissions
Data System (CEDS) inventory ($0.5^\circ \times 0.5^\circ$ resolution, monthly) (Hoesly et al., 2018) is used for most of the world; over Asia
and the U.S., the CEDS is superseded by the MIX inventory ($0.25^\circ \times 0.25^\circ$ native resolution, monthly, Li et al. (2017b)) and
the 2011 National Emission Inventory (NEI 2011) ($0.1 \text{ km} \times 0.1 \text{ km}$ native resolution, hourly, U.S. Environmental Protection
Agency (2014)), respectively. HEMCO also has extensions to compute emissions with meteorological dependencies, such as
225 the emissions of biogenic species (Guenther et al., 2012), soil NO_x (Hudman et al., 2012), lightning NO_x , sea salt (Gong, 2003),
and dust (Zender et al., 2003). With the exception of lightning NO_x , these meteorology-dependent emissions are supported in
WRF-GC v1.0. Further details about the use of HEMCO in WRF-GC is given in Section 3.3.1.

Other physical calculations in GEOS-Chem ~~calculates the convective~~ are coupled to WRF meteorological fields in WRF-
GC; we describe the coupling in detail in Section 3.3. Convective transport of chemical species ~~using a simple~~ is calculated
230 ~~using a single-plume parameterization (Allen et al., 1996; Wu et al., 2007).~~ ~~Boundary layer~~, which is in turn driven by the
cumulus parameterization in WRF. Boundary layer mixing is calculated using a non-local scheme ~~that takes into account the~~
~~magnitude of the atmospheric instability~~, driven by the WRF-simulated atmospheric instability and boundary layer height
(Lin and McElroy, 2010). Dry deposition is based on a resistance-in-series scheme (Wesely, 1989; Wang et al., 1998). Aerosol
deposition is as described in Zhang et al. (2001), with updates to account for size-dependency for dust (Fairlie et al., 2007) and
235 sea salt (Alexander et al., 2005; Jaeglé et al., 2011). Wet scavenging of gases and water-soluble aerosols ~~in GEOS-Chem are~~ is
as described in Liu et al. (2001) and Amos et al. (2012) ~~and driven by WRF-simulated precipitation rates.~~

3 Description of the WRF-GC coupled model

3.1 Overview of the WRF-GC model architecture

Figure 1 gives an architectural overview of the WRF-GC coupled model. Our development of WRF-GC uses many of the
240 existing infrastructure in the WRF-Chem model that couples WRF to its chemistry module (Grell et al., 2005). The ~~interactions~~
~~subroutine calls~~ between WRF and the chemistry components are exactly the same in WRF-GC and in WRF-Chem. ~~Operator~~
~~splitting in WRF-GC is exactly as it is in the WRF-Chem model.~~ However, the chemistry components in the WRF-GC model
~~are organized with greater modularity.~~ Within WRF-GC, the WRF model and the GEOS-Chem model remain entirely intact.
The WRF-GC Coupler ~~interfacing the WRF and GEOS-Chem models~~ consists of ~~interfaces with the two parent models, as~~
245 ~~well as a state conversion module and a state management module.~~ The Coupler is separate from both parent models and is
written in a manner similar to an application programming interface. ~~The~~, ~~enabling independent updates of the parent models~~
~~within WRF-GC~~ Coupler consists of ~~interfaces with the two parent models~~, ~~as well as a state conversion module and a state~~
~~management module.~~

The WRF-GC model is initialized and driven by WRF, which sets up the simulation domain, establishes the global clock,
250 ~~handles the input and output of data~~, sets the initial and boundary conditions (IC/BC) for meteorological and chemical vari-
ables, ~~handles input and output, and~~ and manages cross-processor communication for parallelization. Users ~~define the configure~~

the WRF-GC model structure in the WRF configuration file (`namelist.input`), including the domain, projection, horizontal resolution, vertical coordinates, simulation time, ~~time steps, and~~ dynamic time step, external chemical time step, and other physical and dynamical options. Users also "turn on" GEOS-Chem in WRF-GC by specifying `chem_opt = 233` in ~~the WRF configuration file~~ (`namelist.input`), similar to the way that users specify the chemical mechanism in WRF-Chem. GEOS-Chem ~~initialization is also managed~~ is initialized by the WRF model ~~through using~~ the WRF-to-chemistry interface described in Section 3.2.3. Chemical options within GEOS-Chem, including the choice of ~~chemical species, chemical mechanisms, emissions, and diagnostics~~ standard or custom chemical mechanisms, emission inventories in HEMCO, and diagnostic quantities to be output, are defined by users in the GEOS-Chem configuration files (`input.geos`, `HEMCO_Config.rc`, and `HISTORY.rc`). IC/BC for meteorological and chemical variables are prepared by the user in netCDF format and read by WRF. Meteorological IC/BC can be prepared using the WRF pre-processor system (WPS) from datasets available from NCAR's Research Data Archive (<https://rda.ucar.edu>). IC/BC of chemical species concentrations are taken from GEOS-Chem Classic global model outputs and interpolated to the WRF-GC models grids using a modified version of the WRF-Chem preprocessor tool `mozbc` (available along with the WRF-GC code).

Dynamical and physical calculations are performed in WRF-GC exactly as they are in the WRF model. WRF also ~~performs~~ calculates the grid-scale advection of chemical species. At the beginning of each chemical time step, WRF calls the WRF-GC chemistry component through the WRF-to-Chemistry interface, `chem_driver`, which is a chemical driver similar to that in WRF-Chem. Spatial parameters and the internal state of WRF are translated at runtime to GEOS-Chem by the state conversion and management modules. The GEOS-Chem chemical module then performs convective transport, dry deposition, wet scavenging, emission calculations, boundary layer mixing, and chemistry calculations. This operator-splitting between WRF and GEOS-Chem is identical to that between WRF and the chemistry module in WRF-Chem. Then, the GEOS-Chem internal state is translated back to WRF, and the WRF time-stepping continues. At the end of the WRF-GC simulation, WRF outputs all meteorological and chemical ~~variables and diagnostics in its diagnostic quantities in WRF's~~ standard format.

~~By design,~~ WRF-GC ~~supports all v1.0~~ supports all the existing input and output functionality of the WRF model, including serial/parallel reading and writing of netCDF, HDF5, and GRIB2 datasets. ~~This allows current~~ WRF and WRF-Chem users ~~to~~ can use existing data pre- and post-processing tools to prepare input data and analyze ~~model results~~ results from WRF-GC.

3.2 Details about the WRF-GC Coupler technology

3.2.1 Further modularization of GEOS-Chem for WRF-GC coupling

Long et al. (2015) re-structured the GEOS-Chem model into modular units of atmospheric columns. However, there were limitations in that column structure and its interface which prohibit the coupling with WRF. First, the GEOS-Chem module developed by Long et al. (2015) was hard-coded to operate on ~~pre-defined~~ prescribed configurations of either 72 or 47 vertical levels. The former configuration was designed to match the native vertical levels of the GEOS model. The latter configuration was designed to match the lumped vertical levels often used by the GEOS-Chem "Classic" model. Second, the column interface

to the GEOS-Chem module as implemented in GCHP depends on the ESMF and MAPL frameworks, which WRF does not
285 support.

We modified the GEOS-Chem module and interface to facilitate more flexible coupling with WRF and other dynamical
models. We allowed GEOS-Chem to accept the A_p and B_p parameters for the hybrid sigma-eta vertical grids and the lo-
cal tropopause level from WRF at runtime. Stratospheric chemistry ~~will only be~~ **is only** calculated in GEOS-Chem above
the tropopause level passed from WRF. Also, 3-D emissions (such as the injection of biomass burning plumes into the free
290 troposphere) are interpolated in HEMCO to the WRF-GC vertical levels.

In addition, we modified the existing GCHP interface `GIGC_Chunk_Run` to remove its dependencies on ESMF and MAPL
when running in WRF-GC. We added a set of compatible error-handling and state management components to GEOS-Chem
that interacts with the ~~WRF-to-Chemistry interface, to~~ **WRF through the chemistry driver. These new components** replace the
functionalities originally provided by ESMF. This removes all dependency of the WRF-GC Coupler and the GEOS-Chem
295 column interface on external frameworks.

All of our changes adhere to the GEOS-Chem coding and documentation standards and have been fully merged into the
GEOS-Chem standard source code as of version 12.0.0 (doi: 10.5281/zenodo.1343547) and are controlled with the pre-
processor switch `MODEL_WRF` at compile time. In the future, these changes will be maintained as part of the standard GEOS-
Chem model.

300 **3.2.2 Runtime processes** **Installation and compilation process**

~~Similar to~~ From the user's standpoint, the installation and compilation of WRF-GC is very similar to the procedures for WRF-
Chem, ~~in~~. WRF-GC ~~all chemistry-related codes reside in the chem/ sub-directory under the WRF model directory. These~~
~~include~~ **is** installed by downloading the parent models, WRF and GEOS-Chem, and the WRF-GC Coupler, directly from their
respective software repositories. The WRF model is installed in a top-level directory, while the WRF-GC Coupler ~~code, an~~
305 ~~and~~ **and** GEOS-Chem are installed under the `chem/` sub-directory, where the chemistry routines for WRF-Chem originally reside.
An unmodified copy of the GEOS-Chem code **is installed** in the `chem/gc/` sub-directory, and a set of sample GEOS-Chem
configuration files **is in** `chem/config/`. **The WRF code remains unmodified in WRF-GC, but at present the chemical routines**
of WRF-Chem cannot work alongside GEOS-Chem under a single WRF-GC top directory.

The standard WRF model includes built-in compile routines for coupling with the WRF-Chem chemistry module. WRF-GC
310 uses these existing compile routines by substituting the parts pertinent to WRF-Chem with a generic chemistry interface. This
substitution process is self-contained in the WRF-GC Coupler and requires no manual changes to the WRF code. As such, the
installation and compilation of WRF-GC require no extra maintenance effort from the WRF developers, and WRF-GC operates
as a drop-in chemical module to WRF.

When the user sets the environment variable `WRF_CHEM` to 1 in the WRF compile script, WRF reads a registry file
315 (`registry.chem`) containing the GEOS-Chem chemical species information (duplicated from `input.geos`) and builds
these species into the WRF model framework. The WRF compile script then calls the `Makefile` in the `chem/` sub-directory
to compile an unmodified copy of GEOS-Chem (located in `chem/gc/`) with the pre-processor switch `MODEL_WRF`. This com-

piles GEOS-Chem into two libraries, which can be called by WRF. The first GEOS-Chem library (`libGeosCore.a`) contains all GEOS-Chem core routines. The second GEOS-Chem library (`libGIGC.a`) contains the GEOS-Chem column interface (GIGC_Chunk_Mod). The subsequent compilation process links these GEOS-Chem libraries and the WRF-to-Chemistry interface to the rest of the WRF code, creating a single WRF-GC executable (`wrf.exe`).

3.2.3 Runtime processes

In WRF-Chem, WRF calls its interface to chemistry, `chem_driver`, which then calls each individual chemical processes. We abstracted this `chem_driver` interface by removing direct calls to chemical processes. Instead, our `chem_driver` calls the WRF-GC state conversion module (`WRFGC_Convert_State_Mod`) and the GEOS-Chem column interface (`GIGC_Chunk_Run`) to perform chemical calculations. We also modified `chemics_init` to initialize GEOS-Chem through the column interface `GIGC_Chunk_Init`.

The WRF-GC state conversion module includes two subroutines. The `WRFGC_Get_WRF` subroutine receives meteorological data and spatial information from WRF and translates them into GEOS-Chem formats and units. Table 21 summarizes the WRF meteorological variables required to drive GEOS-Chem. Many meteorological variables in WRF only require a conversion of units before passing they are passed to GEOS-Chem. Some meteorological variables require physics-based diagnosis in the `WRFGC_Get_WRF` subroutine before passing being passed to GEOS-Chem. For example, GEOS-Chem uses the convective mass flux variable to drive convective transport. This variable is calculated in the cumulus parameterization schemes in WRF but not saved. We re-diagnose the convective mass flux variable in `WRFGC_Get_WRF` using the user-selected cumulus parameterization schemes in WRF and pass it to GEOS-Chem. Horizontal grid coordinates and resolutions are passed to GEOS-Chem in the form of latitudes and longitudes at the center and edges of each grid. Vertical coordinates are passed from WRF to GEOS-Chem at runtime as described in Section 3.2.1. A second subroutine, `WRFGC_Set_WRF`, receives chemical species concentrations from GEOS-Chem, converts the units, and saves them in the WRF chemistry variable array chemical variable array in WRF.

We developed the WRF-GC state management module (`GC_Stateful_Mod`) to manage manages the GEOS-Chem internal state in distributed memory, such that GEOS-Chem can run in the MPI parallel architecture provided by WRF MPI-parallel architecture. When running WRF-GC in the distributed-memory configuration, WRF decomposes the horizontal computational domain evenly across the available computational cores at the beginning of runtime. Each computational core has access only to its allocated subset of the full domain as a set of atmospheric columns, plus a halo of columns around that subset domain. The halo columns are used for inter-core communication of grid-aware processes, such as horizontal transport (Skamarock et al., 2008). The internal states of GEOS-Chem for each core are managed by the state management module; they are distributed at initialization and independent from each other. The WRF-GC state management module is also critical to the development of nested-grid simulations in the future.

3.2.3—Compilation processes

350 From the user's standpoint, the installation and configuration processes for WRF-GC and WRF-Chem are similar. WRF-GC is installed by downloading the parent models, WRF and GEOS-Chem, and the WRF-GC Coupler, directly from their respective software repositories. The WRF model is installed in a top-level directory, while the WRF-GC Coupler and GEOS-Chem are installed in the `chem/` sub-directory, where the original WRF-Chem chemistry routines reside.

355 The standard WRF model includes built-in compile routines for coupling with chemistry, which are used by the compilation of WRF-Chem. WRF-GC uses these existing compile routines by substituting the parts pertinent to WRF-Chem with a generic chemistry interface. This substitution process is self-contained in the WRF-GC Coupler and requires no manual changes to the WRF code. As such, the installation and compilation of WRF-GC require no extra maintenance effort from the WRF developers, and WRF-GC operates as a drop-in chemical module to WRF.

360 When the user sets a compile option `WRF_CHEM` to 1, WRF reads a registry file (`registry.chem`) containing chemical species information and builds these species into the WRF model framework. The WRF compile script then calls the `Makefile` in the `chem/` sub-directory to compile routines related to chemistry. We modified the `Makefile` in the `chem/` sub-directory to compile an unmodified copy of GEOS-Chem (located in `chem/ge/`) when the pre-processor switch `MODEL_WRF` is turned on. This compiles GEOS-Chem into two libraries, which can be called by WRF. The first GEOS-Chem library (`libGeosCore.a`) contains all GEOS-Chem core routines. The second GEOS-Chem library (`libGIGC.a`) contains the GEOS-Chem column interface (`GIGC_Chunk_Mod`). The subsequent compilation process links these GEOS-Chem libraries and the WRF-to-Chemistry interface to the rest of the WRF code, creating a single WRF-GC executable (`wrf.exe`).

3.3 Treatment of key processes in the WRF-GC coupled model

Below we describe the operator splitting between WRF and GEOS-Chem within WRF-GC, as well as the treatments of some of the key processes in the WRF-GC coupled model. The general Eulerian form of the coupled-continuity equation
370 for m chemical species with number density vector $\mathbf{n} = (n_1, \dots, n_m)^T$ is

$$\frac{\partial n_i}{\partial t} = -\nabla \cdot (n_i \mathbf{U}) + P_i(\mathbf{n}) + L_i(\mathbf{n}) \quad i \in [1, m] \quad (1)$$

\mathbf{U} is the wind vector, which is provided by the WRF model in WRF-GC. The first term on the right-hand-side of Eq. 1 indicate the transport of species i , which include includes grid-scale advection, as well as sub-grid turbulent mixing and convective transport. $P_i(\mathbf{n})$ and $L_i(\mathbf{n})$ are the local production and loss rates of species i , respectively (Long et al., 2015).

375 In the WRF-GC model, WRF simulates the meteorological variables using the dynamic equations and the initial and boundary conditions meteorological IC/BC. These meteorological variables are then passed to the GEOS-Chem chemical module (Table 1) to solve the local production and loss terms of the continuity equation. Large-scale (grid-scale) advection of chemical species is grid-aware and is calculated by the WRF dynamical core. Local (sub-grid) vertical transport processes, including turbulent mixing within the boundary layer and convective transport from the surface to the convective cloud top, are calculated
380 in GEOS-Chem using WRF-simulated meteorology. Dry deposition and wet scavenging of chemical species is also calculated in GEOS-Chem and driven by WRF. This operator-splitting arrangement is identical to that in the WRF-Chem model.

The dynamic and chemical time steps are specified by the user in the WRF configuration file `namelist.input`. The dynamic time step is constrained by the Courant-Friedrichs-Lewy stability criterion and should be short for high-resolution simulations. WRF recommends that the chemical time step be set the same as the dynamic time step as best practice (Skamarock et al., 2008). Because GEOS-Chem uses a Rosenbrock solver, which adapts its internal chemical time step to the stiffness of the chemical mechanism, a larger chemical time step may be used. However, it is recommended that the results be compared to a control simulation with the chemical time step set to the dynamic time step Skamarock et al. (2008).

3.3.1 Emission of chemical species

Chemical emissions in the WRF-GC model are calculated online using by the HEMCO module in GEOS-Chem (Keller et al., 2014). For each atmospheric column, HEMCO reads in emission inventories of arbitrary spatiotemporal resolutions at runtime. Input and configured in `HEMCO_Config.rc`. HEMCO and its data directory are updated as part of the GEOS-Chem model and remain unmodified in WRF-GC. Users can choose to use one or combine several of the emission data is parallelized through the domain decomposition process, which permits each CPU to read a subset of the data from the whole computational domain. HEMCO then regrids the emission fluxes to the user-defined inventories already in the HEMCO data directory (Section 2.2). Some of the inventories currently available in the HEMCO data directory may not be of sufficiently fine resolution to support the high-resolution WRF-GC simulations. In that case, users can prepare their own emission input files in netCDF format at arbitrary spatiotemporal resolutions, and HEMCO will interpolate them to the WRF-GC model domain and resolution at runtime. HEMCO also calculates allow users to specify scale factors and diurnal/weekly/monthly variation profiles in `HEMCO_Config.rc` to be applied to the emission fluxes at runtime. WRF-GC calls HEMCO to compute meteorology-dependent emissions online using WRF meteorological variables WRF-simulated meteorology. These currently include emissions of dust (Zender et al., 2003), sea salt (Gong, 2003), biogenic precursors (Guenther et al., 2012), and the emissions of biogenic species (Guenther et al., 2012), soil NO_x (Hudman et al., 2012). Meteorology-dependent emission of lightning NO_x , sea salt (Gong, 2003), and dust (Zender et al., 2003). Lightning NO_x emissions is not yet included in this supported in WRF-GC version. The HEMCO module is part of the GEOS-Chem parent model and is updated together with it. v1.0 but will be added in a future version.

3.3.2 Sub-grid vertical transport of chemical species

Sub-grid vertical transport of chemical species in WRF-GC, including convective transport and boundary layer mixing, are calculated within by GEOS-Chem. Convective mass fluxes are using WRF meteorology. GEOS-Chem uses the convective mass flux variable to drive convective transport (Allen et al., 1996; Wu et al., 2007). This variable is calculated in WRF using the cumulus parameterizationscheme selected by the user, but the convective mass fluxes are user's choice of cumulus parameterization, but its value is not stored in the WRF meteorological variable array. We re-diagnosed the convective mass fluxes in the The WRF-GC state conversion module using the WRF cumulus parameterization scheme selected by the user. This methodology is the same as that in the WRF-Chem model. The re-diagnoses convective mass fluxes using the user's choice of parameterization in WRF and then pass the values to GEOS-Chem. The WRF-GC state conversion module cur-

415 rently supports ~~the calculation of convective mass fluxes from convective mass flux calculations~~ using the New Tiedtke
scheme (Tiedtke, 1989; Zhang et al., 2011; Zhang and Wang, 2017) and the Zhang-McFarlane scheme (Zhang and McFar-
lane, 1995) ~~in WRF~~ (Table 1), because these two cumulus parameterization schemes are more physically-compatible with the
convective transport ~~scheme algorithm currently~~ in GEOS-Chem. ~~The diagnosed convective mass fluxes are then passed to~~
420 ~~GEOS-Chem to calculate convective transport (Allen et al., 1996; Wu et al., 2007)~~ In addition, the users should consider the
horizontal resolution of the model when choosing which cumulus parameterization to use. The New Tiedtke scheme and the
Zhang-McFarlane schemes are generally recommended for use in simulations at horizontal resolutions larger than 10 km
(Arakawa and Jung, 2011; Skamarock et al., 2008). At horizontal resolutions between 2 to 10 km, the so-called "convective
grey zone" (Jeworrek et al., 2019), the use of the Grell-Freitas scheme is recommended for the WRF model (Grell and Freitas,
2014), as it allows subsidence to spread to neighboring columns; this option will be implemented in a future WRF-GC version.
425 At horizontal resolutions finer than 2 km, it is assumed that convections are resolved and cumulus parameterizations should not
be used (Grell and Freitas, 2014; Jeworrek et al., 2019). The scale-dependence of cumulus parameterizations and their impacts
on convective mixing of chemical species is an active area of research, which we will explore in the future using WRF-GC.

~~Boundary layer~~ Boundary layer mixing is calculated in GEOS-Chem using a non-local scheme ~~implemented by~~
~~Lin and McElroy (2010)~~ (Holtzlag and Boville, 1993; Lin and McElroy, 2010). The boundary layer height, thermodynamic
430 variables, and the vertical level and pressure information are ~~passed from WRF calculated by WRF~~ and passed to GEOS-
Chem through the state conversion module. Again, this methodology is the same as that in the WRF-Chem model.

3.3.3 Dry deposition and wet scavenging of chemical species

Dry deposition is calculated in GEOS-Chem using a resistance-in-series scheme (Wesely, 1989; Wang et al., 1998). ~~We mapped~~
~~the land cover information in WRF to~~ The land cover data for the simulated domain is read by and used in WRF, but for now
435 WRF-GC only supports the use of the U.S. Geological Survey (USGS) classification. The land cover information is passed
to GEOS-Chem, where it is mapped to the land cover ~~types of Olson et al. (2001) for use in GEOS-Chem.~~ classifications
of Olson et al. (2001) to assign values of surface roughness and canopy resistance (Wang et al., 1998). The dry deposition
velocities are calculated locally using WRF-simulated surface air momentum, sensible heat fluxes, temperature, and solar
radiation.

440 To calculate the wet scavenging of chemical species ~~in WRF-GC, we diagnosed the~~, the WRF-GC Coupler diagnoses
the WRF-simulated precipitation variables using the microphysical ~~schemes~~ scheme and cumulus parameterization ~~schemes~~
scheme selected by the user (Table 1). The precipitation variables passed to GEOS-Chem include large-scale/convective precip-
itation production rates, large-scale/convective precipitation evaporation rates, and the downward fluxes of large-scale and con-
vective ice/liquid precipitation. The microphysical schemes currently supported in WRF-GC include the Morrison 2-moment
445 scheme (Morrison et al., 2009), the CAM5.1 scheme (Neale et al., 2012), the WSM6 scheme (Hong and Lim, 2006), and
the Thompson scheme (Thompson et al., 2008). ~~The cumulus parameterization schemes currently supported by the WRF-GC~~
~~model include the New Tiedtke scheme (Tiedtke, 1989; Zhang et al., 2011; Zhang and Wang, 2017) and the Zhang-McFarlane~~
~~scheme (Zhang and McFarlane, 1995).~~

4 Application: surface PM_{2.5} over China during January 22 to 27, 2015

450 We simulated surface PM_{2.5} concentrations over China during a severe haze event in January 2015 using both the WRF-GC model (~~WRF version v1.0~~ (WRF v3.9.1.1 ~~;~~ and GEOS-Chem v12.2.1) and the GEOS-Chem Classic model (v12.2.1) in its nested-grid configuration ~~for China~~. We compared the ~~simulated~~ results from the two models against each other, as well as against surface measurements, ~~to assess the performance of the~~. ~~Both the WRF-GC model. Both WRF-GC and the GEOS-Chem Classic nested-China simulations were conducted from January 18 to 27, 2015; the first four days initialized the~~
455 ~~model~~models. Results from January 22 to 27, 2015 were analyzed. ~~Our goal was to compare the performance of the two models in simulating Chinese surface PM_{2.5} under their normal mode of operation. To this end, the two simulations were configured as similarly as possible, but there are important innate differences between the two models, as described below.~~

4.1 Setup of the WRF-GC model and the GEOS-Chem model

Figure 2(a) shows the domain of the GEOS-Chem Classic ~~nested-grid simulation. The GEOS-Chem Classic nested-grid simulation was nested-China simulation, which was~~ driven by the GEOS-FP ~~dataset from NASA-GMAO assimilated meteorological dataset~~ at its native horizontal resolution of ~~0.25° × 0.3125°~~ 0.25° latitude × 0.3125° longitude. The vertical resolution of the GEOS-FP dataset was reduced from its native 72 levels to 47 levels by lumping levels in the stratosphere. ~~The resulting~~This treatment is standard in GEOS-Chem Classic simulations. The 47 vertical layers extended from the surface to 0.01 hPa, with 7 levels in the bottom 1 km. ~~The top-edge of the bottom layer was at approximately 120 m over Eastern China.~~
465 Meteorological variables were updated every three hours (every hour for surface variables). ~~Initial~~IC/BC boundary conditions of chemical species ~~concentration~~ concentrations were taken from the outputs of a global GEOS-Chem Classic simulation and updated at the boundaries of the ~~nested-grid nested-China~~ domain every 3 hours. ~~The dynamic time step and the external chemistry time step were 5 minutes and 10 minutes, respectively.~~

Figure 2(b) shows the ~~domain of our~~WRF-GC simulation domain, with a horizontal resolution of 27 km × 27 km. We
470 chose this domain and horizontal resolution ~~for our WRF-GC simulation~~ to be comparable to those of the GEOS-Chem Classic nested-grid simulation. There were 50 vertical levels in our WRF-GC simulation, which extended from the surface up to 10 hPa with 7 levels below 1 km. ~~Meteorological boundary conditions were from the~~The top-edge of the bottom layer was at approximately 60 m over Eastern China. The WRF model does not have the option of using the GEOS-FP dataset for meteorological IC/BC. ~~Instead, we used the~~ NCEP FNL dataset (doi:10.5065/D6M043C6) at 1° × 1° resolution ~~;~~interpolated
475 ~~to WRF vertical levels and updated every 6 hours. Initial~~as IC/BC boundary conditions of chemical species concentrations were identical to those used in the GEOS-Chem Classic nested-grid simulation but for WRF-GC; the FNL dataset was interpolated to WRF vertical levels and updated every 6 hours. In addition, we nudged the WRF-simulated meteorological fields with surface (every 3 hours) and upper air (every 6 hours) observations of temperature, specific humidity, and winds from the NCEP ADP Global Surface/Upper Air Observational Weather Database (doi:10.5065/39C5-Z211). ~~This mimicked the effect~~
480 ~~of meteorological data assimilation and allowed the WRF-simulated meteorology to stay close to the observed states of the atmosphere. IC/BC of chemical species concentrations were identical to those used in the GEOS-Chem Classic nested-China~~

simulation but interpolated to WRF vertical levels and updated every 6 hours. The dynamic time step and the external chemistry time step were 2 minutes and 10 minutes, respectively. Other physical options used in our WRF-GC simulation are summarized in Table 2.

485 Our WRF-GC and GEOS-Chem Classic simulations used the exact same **GEOS-Chem** chemical mechanism for gases and aerosols, including a total of 241 chemical species. Emissions in the two simulations were both calculated by ~~the HEMCO module in GEOS-Chem and were completely HEMCO and were~~ identical for anthropogenic and biomass burning sources. Monthly mean anthropogenic emissions from China were from the Multi-resolution Emission Inventory for China (MEIC, Li et al. (2014)) at $0.25^\circ \times 0.25^\circ$ horizontal resolution. The MEIC inventory was ~~developed~~ updated for the year 2015 and
490 included emissions from power generation, industry, transportation, and residential activities. ~~Agricultural ammonia emission was Sector-specific weekly and diurnal variation from the MEIC inventory were applied (Li et al., 2017a). Agricultural emissions of ammonia were~~ from Huang et al. (2012). Anthropogenic emissions from the rest of the Asia were from Li et al. (2017b), developed for the year 2010. Monthly mean biomass burning emissions were taken from Global Fire Emissions Database version 4 (GFED4) (Randerson et al., 2018). Emissions of biogenic species (Guenther et al., 2012), soil NO_x (Hudman et al.,
495 2012), sea salt (Gong, 2003), and dust (Zender et al., 2003) in the two simulations were ~~calculated online by HEMCO using meteorology-sensitive parameterizations and thus slightly different~~ coupled to model meteorology in HEMCO and thus different between the two models. $\text{PM}_{2.5}$ mass concentrations were diagnosed for both simulations as the sum of masses of sulfate, nitrate, ammonium, ~~black carbon, primary and secondary organic carbon, EC, primary organic aerosol (assumed to be 2.1 times the primary organic carbon mass), SOA,~~ fine dust (100% of dust between 0 and $0.7 \mu\text{m}$ and 38% of dust between 0.7 and
500 $1.4 \mu\text{m}$), and accumulation-mode sea salt, taking into consideration the hygroscopic growth for each species at 35% relative humidity.

4.2 Validation of the WRF-GC simulation against surface $\text{PM}_{2.5}$ measurements and comparison with the GEOS-Chem Classic simulation

Figure 2 compares the 6-day average surface $\text{PM}_{2.5}$ concentrations ~~(during January 22 00:00 UTC to January 28 00:00 UTC to~~
505 ~~27, 2015) simulated by as in the~~ WRF-GC and ~~the~~ GEOS-Chem Classic ~~nested-China simulations~~, respectively. Also shown are the $\text{PM}_{2.5}$ concentrations measured at 578 surface sites, managed by the Ministry of Ecology and Environment of China (www.cnemc.cn). We ~~selected these removed~~ invalid hourly surface $\text{PM}_{2.5}$ observations following the protocol in Jiang et al. (2020). The 578 sites were selected by (1) removing surface sites with less than 80% valid hourly measurements during our simulation period, and (2) sampling the site closest to the model grid center, if that model grid contained multiple surface sites. Both
510 models ~~were able to reproduce~~ reproduced the general spatial distributions of the observed $\text{PM}_{2.5}$ concentrations, including the ~~higher-high~~ concentrations over Eastern China ~~relative to Western China~~, as well as the hotspots over the North China Plain, Central China, and the Sichuan Basin. However, both models overestimated the $\text{PM}_{2.5}$ concentrations over Eastern China. The mean 6-day $\text{PM}_{2.5}$ concentrations averaged for the 578 sites as simulated by WRF-GC and by GEOS-Chem Classic ~~nested-China~~
515 averaged for the 578 sites was $98 \pm 43 \mu\text{g m}^{-3}$.

Figure 3 shows the scatter plots of the simulated and observed daily average PM_{2.5} concentrations over Eastern China (eastward of 103°E, 507 sites) during January 22 to 27, 2015. We focused ~~here~~ on Eastern China, because the spatiotemporal variability of PM_{2.5} concentrations ~~is~~ ~~was~~ higher over this region. Again, both models overestimated the daily PM_{2.5} concentrations over Eastern China, ~~with WRF-GC performing better than GEOS-Chem Classic~~. The daily PM_{2.5} concentrations simulated by WRF-GC were 29% higher than the observations (quantified by the reduced major-axis regression slope between the simulated and observed daily PM_{2.5} concentration), with a correlation coefficient of $r = 0.68$. The daily PM_{2.5} concentrations ~~simulated by~~ ~~in~~ the GEOS-Chem Classic ~~nested-China simulation~~ were 55% higher than the observations, with a correlation coefficient of $r = 0.72$.

~~Our preliminary comparison above shows that the~~ Figure 4 shows the Taylor diagrams of the hourly PM_{2.5} concentrations simulated by the two models at 48 major eastern Chinese cities, including 13 cities in the Beijing-Tianjin-Hebei (BTH) area, 22 cities in the Yangtze River Delta (YRD) area, and 13 other major cities. The Taylor diagram (Taylor, 2001) evaluates the simulated time series of PM_{2.5} against the observations, using the Pearson correlation coefficients, the ratio between the simulated and observed standard deviations ($\frac{\sigma_{sim}}{\sigma_{obs}}$), and the normalized root-mean-square differences (RMSDs) as metrics. Proximity to the point "1" on the X-axis in Figure 4 indicates that the simulation accurately reproduced both the mean concentration and the temporal variability of the observations. For most cities in the BTH area and for most of the other 13 major cities, the hourly PM_{2.5} concentrations simulated by WRF-GC showed smaller RMSDs and higher correlation coefficients against observations, compared to those in the GEOS-Chem Classic nested-china simulation. In the YRD area, the performances of the two models were similar.

Our analyses above show that the hourly and daily surface PM_{2.5} concentrations simulated by the WRF-GC model were in better agreement with ~~the surface~~ observations than those simulated by the GEOS-Chem Classic ~~nested-grid model~~, ~~nested-China model~~ over Eastern China during January 22 to 27, 2015. We found that this was partially because the WRF-GC model ~~better represented pollution meteorology at high resolution relative to~~, nudged with surface and upper-air meteorological observations, better represented the pollution meteorology, compared to the GEOS-FP dataset that was used to drive the GEOS-Chem Classic nested-China simulation. Figure S1 shows the average surface air temperature, relative humidity, and 10-m wind speed as simulated by the WRF-GC model and as provided by the GEOS-FP dataset against the observations during January 22 and 27, 2015 at 367 sites over China. The surface air temperature simulated by WRF-GC and those in the GEOS-FP dataset were both in good agreement with the observations over China. However, the relative humidity and wind speeds simulated by WRF-GC were more consistent with the observations, compared to those in the GEOS-FP dataset. Figure S2 assesses the hourly surface air temperature, relative humidity, and near-surface winds simulated by the WRF-GC model and those in the GEOS-FP assimilated meteorological dataset, against hourly surface measurements over China during January 22-27, 2015. For the 34 sites with publicly-available hourly measurements, the meteorological fields simulated by the WRF-GC were generally more consistent with the measurements.

Figure 5 shows the ~~average mean~~ planetary boundary layer ~~heights~~ height (PBLH) at 08:00 local time (00:00 UTC) and 20:00 local time (12:00 UTC) during January 22 to 27, 2015, ~~as simulated by~~ ~~in~~ the GEOS-Chem Classic ~~nested-grid model~~, ~~nested-China~~ and the WRF-GC ~~model~~ simulations, respectively, and compares them with the rawinsonde observations ~~over China~~ dur-

ing this period (Guo et al., 2016). The PBLH in the GEOS-Chem Classic model was taken from the GEOS-FP dataset generally underestimated the PBLH over the low-altitude areas of Eastern China. This led to significant overestimation of the simulated, whereas the boundary layer height was simulated by WRF in WRF-GC. Compared to the observations, the PBLH in the GEOS-FP dataset were generally biased-low over Eastern China and biased-high over over the mountainous areas in Southwestern China and Western China. This likely was a major reason for the severe overestimation of surface PM_{2.5} concentrations in the GEOS-Chem Classic nested-China simulation over Eastern China, given the well-established negative correlation between PBLH and PM_{2.5} concentration (Li et al., 2017c; Lou et al., 2019). In addition, GEOS-FP severely overestimated PBLH over the mountainous areas in Southwestern China. In comparison, the WRF-GC model correctly represented the PBLH over most regions in China, which was critical to its more accurate simulation of surface PM_{2.5} concentrations.

5 Computational performance and scalability of WRF-GC

5.1 Computational performance of the WRF-GC model

We evaluated the computational performance of a WRF-GC simulation and compared it with that of the GEOS-Chem Classic nested-grid simulation of a similar configuration. We performed the WRF-GC and GEOS-Chem Classic simulations over nested-grid simulations for the exact same domain (as shown in Figure 2(a)), with the exact same projection and grid sizes horizontal resolution (0.25° latitude × 0.3125° longitude resolution, 225 × 161 grid boxes) as well as the atmospheric columns). The GEOS-Chem Classic nested-grid simulation had 47 vertical levels, and the WRF-GC simulation comparably had 50 levels. Both simulations used the same emissions and chemical configurations. Both simulations ran for 48 hours and used with a total of 241 chemical species and 10-minute external chemical time steps with scheduled output for every 1 hour. The WRF-GC model calculated online meteorology with a 120-second time step, while the calculated meteorology online with a 2-minute dynamic time step. The GEOS-Chem Classic model read in nested-grid simulation calculated transport (5-minute time step) driven by archived GEOS-FP meteorological data. In addition, read from an Ethernet-connected hard disk array. WRF-GC used MPI parallelization, while GEOS-Chem Classic used OpenMP. Both simulations executed on a single node were conducted for 48 hours with scheduled output for every 1 hour. Both simulations were executed on the same single-node hardware with 32 Intel Broadwell physical cores on a local and an Ethernet-connected file system hard disk array.

Figure 6 compares the timing results computational wall times for the WRF-GC and the GEOS-Chem Classic nested-grid simulations. The overall total wall time for the WRF-GC simulation was 5127 seconds, which was only 31% of the wall time for the GEOS-Chem Classic nested-grid simulation (16391 seconds). We found that the difference in computational performance efficiency was mainly due to the much faster dynamic and transport calculations in the WRF-GC model relative to the transport calculation in the GEOS-Chem Classic nested-grid model. In WRF-GC, calculates meteorology online entirely in node memory, which eliminates the need to read archived meteorological data. In comparison, the wall time taken up by the entire WRF (including transport, physics, I/O, and model initiation) was 2462.5 seconds. In the GEOS-Chem Classic reads meteorological data from disks, which poses a bottleneck. Finally, the MPI parallelization used by WRF-GC is more efficient than the OpenMP used by nested-grid simulation, 50% (8192 seconds) of the total wall time was

used for the transport of tracers, including large-scale advection (6355.7 seconds), convective transport (694.2 seconds), and boundary-layer mixing (1142.5 seconds). As a CTM, the GEOS-Chem Classic, such that the GEOS-Chem modules actually run faster in Classic read archived meteorological data for the entire domain at 3-model-hour intervals from hard drives using a single computational core, which becomes increasingly burdensome for simulations with more grid boxes. In comparison, WRF-GC than they do in calculated meteorology online in node memory and updated the model boundary conditions from hard drives every 6 model-hours. Finally, the OpenMP-parallelization in GEOS-Chem Classic. This is because OpenMP parallelization in GEOS-Chem is was only at the loop level, while. In contrast, WRF-GC performs domain decomposition used MPI-parallelization to decompose domain at the model level, thus parallelizing all code within the GEOS-Chem module. As a result, the same chemistry routines actually ran faster in WRF-GC than they did in GEOS-Chem Classic. In WRF-GC, the chemistry routines (deposition, emissions computation, convection, boundary-layer mixing, and chemistry) took up 2462.5 seconds in total; the same routines took up 5263.5 in GEOS-Chem Classic. The WRF-GC Coupler consumed negligible wall time (39 seconds) in this test simulation.

A side-by-side wall time comparison between WRF-GC and WRF-Chem is difficult to do, because (1) the chemical routines in the two models are very different, and (2) the WRF-Chem has many possible configurations for chemistry. Nevertheless, we conducted one test simulation with WRF-Chem using a typical chemistry option (CBMZ-MOSAIC gas-phase chemistry, 4-bin aerosol microphysics and chemistry, and aqueous reactions; chem_opt = 9 in registry.chem) with a total of 133 chemical species. This WRF-Chem simulation was configured for the same domain at the same horizontal and vertical resolutions and used the same physical and dynamical options as those in the WRF-GC simulation described above. The total wall time for the WRF-Chem simulation was 9985.8 seconds, which was almost twice as long as the wall time of WRF-GC (5127 seconds). Chemical routines in this WRF-Chem test simulation took up 61% of the total wall time (6134.3 seconds), despite it having much fewer chemical species than the WRF-GC (241 chemical species). This may be partially due to the computationally intensive bin-resolved aerosol microphysics calculation in the WRF-Chem simulation.

5.2 Scalability of the WRF-GC model

We analyzed the scalability of the WRF-GC model using timing tests of a 48-hour simulation over East and Southeast Asia. The domain size was 225×161 grid boxes ($27 \text{ km} \times 27 \text{ km}$ resolution). The WRF-GC simulation used the standard GEOS-Chem troposphere-stratosphere-oxidant-aerosol-chemical-mechanism. The time steps were 120 seconds for WRF and 10 minute for GEOS-Chem chemistry (external time step), with scheduled output every hour. The WRF-GC simulation, including its input/output processes was parallelized across computational cores. The WRF-GC model using the 48-hour simulation described in Section 5.1. The model was compiled using the Intel C and Fortran Compilers (v16.0.3) and the mvapich2 (v2.3) MPI library. The computing environment (Tianhe-1A) had 28 Intel Broadwell physical cores with 125 GB of RAM per node. Input and output used a networked Lustre high-performance file system.

Figure 7 shows the scalability of the WRF-GC simulation in terms of the total WRF-GC wall time, as well as the wall times of its three components: (1) the WRF model (including input/output), (2) the GEOS-Chem model, and (3) the WRF-GC Coupler. For the domain of this test simulation, the total wall time and the WRF wall time both scaled well up to 136

cores. This ~~is~~ because the simulation domain ~~becomes~~ too fragmented above 136 cores, such that ~~MPI communication times dominate the MPI communication time~~ took up much of the run time, resulting in performance degradation. Chemical calculations in the GEOS-Chem model ~~are perfectly scalable~~ were perfectly scalable up to the largest number of cores tested (250 cores), consistent with previous GCHP performance analyses (Eastham et al., 2018). Figure 7 also shows that the WRF-GC Coupler ~~seals~~ scaled nearly perfectly and ~~consumes~~ consumed less than 1% of the total WRF-GC wall time ~~up to 250 cores~~. At above 200 cores, ~~there is~~ there was a slight degradation of the scalability due to cross-core communications at the sub-domain boundaries. However, ~~since the WRF-GC Coupler is so light-weight, the~~ the degradation had negligible impact on the total WRF-GC wall time ~~is completely negligible~~ as the WRF-GC Coupler was computationally efficient.

WRF-GC also scales to massively parallel architectures and can be deployed on the cloud, because both the WRF and GEOS-Chem model are already operational on the cloud with ~~the necessary~~ their input data readily available (Hacker et al., 2017; Zhuang et al., 2019). We conducted a ~~preliminary test using test simulation running~~ WRF-GC on the Amazon Web Services (AWS) cloud with ~~32 nodes and 1152~~ up to 128 nodes and 4608 cores. The simulation domain was over the continental ~~United States-U.S.~~ at 5 km \times 5 km resolution ~~with (950 \times 650 grid boxes, with 10-second atmospheric columns),~~ with 10-second dynamical time step and ~~5-minute~~ 5-minute chemical time step. ~~We found that in~~ The scalability test results are shown in Figure S3. In this massively parallel environment, ~~the chemical wall time normalized by number of grid cells and per core was 85% of the 252-core simulation. This indicates good scalability of the chemistry component in~~ WRF-GC ~~scaled well up to 1728 cores, with the chemical module scaling well up to 2304 cores.~~ The WRF-GC Coupler took less than 0.2% of the total computational time in this simulation ~~and scaled perfectly up to 4608 cores. The deployability of WRF-GC on the cloud will enhance WRF-GC's accessibility to new users by saving them the investment in hardware purchases and the effort in downloading and hosting large input datasets locally.~~

6 Conclusions

We developed the WRF-GC model, which is an online coupling of the WRF meteorological model and the GEOS-Chem chemical model, to simulate regional atmospheric chemistry at high resolution, with high computational efficiency, and underpinned by the latest scientific understanding of atmospheric processes. By design, the WRF-GC model is structured to work with ~~unmodified~~ native copies of the parent models and involves no hard-wired code to either parent model. This allows the WRF-GC model to integrate future updates of ~~both models with immediacy and ease, such that WRF-GC can stay state-of-the-science~~ either parent model with relative ease.

WRF-GC provides current users of WRF-Chem and other regional models with access to GEOS-Chem, which is state-of-the-science, well-documented, traceable, benchmarked, actively developed by a large international community, and centrally managed. ~~GEOS-Chem users also benefit from the coupling to the open-source, community-supported WRF meteorological model.~~ At the same time, WRF-GC enables GEOS-Chem users to perform high resolution regional chemistry simulations in both forecast and hindcast mode at any location and time of interest, with high performance.

650 Our ~~preliminary test shows~~ first application showed that the WRF-GC model ~~is able to better represent~~ was able to reproduce the spatiotemporal variation of surface PM_{2.5} concentrations over China in ~~winter than the~~ January 2015, with smaller biases compared to the results of the GEOS-Chem Classic ~~nested-grid model. This is nested-China simulation.~~ This was partially because the WRF-GC model better represented the ~~pollution meteorology, including the variability of the planetary boundary layer heights,~~ over the region. In addition, the WRF-GC simulation was 3 times faster than a comparable GEOS-Chem Classic
655 ~~nested-grid~~ simulation.

WRF-GC ~~also scales nearly perfectly demonstrated~~ good scalability to massively parallel architectures, ~~with near-perfect scalability of its chemistry component.~~ This enables the WRF-GC model to be used on multiple-node systems ~~and on supercomputing clusters, which was or high-performance cloud computing platforms, which is~~ not possible with the GEOS-Chem Classic. The GCHP model also scales to massively parallel architectures (Zhuang et al., 2020), but GCHP can
660 only operate as a global model. ~~Furthermore, the~~ The deployability of WRF-GC ~~model can be deployed~~ on the cloud ~~, which will greatly increase will enhance~~ WRF-GC's accessibility to new users.

The WRF-GC coupling structure, including the GEOS-Chem column interface and the state conversion module, are extensible and can be adapted to models other than WRF. This opens up possibilities of coupling GEOS-Chem to other weather and Earth System models in an online, modular manner. Using ~~unmodified native, out-of-the-box~~ copies of parent models in
665 coupled models reduces maintenance ~~, and~~ avoids branching of the parent model code ~~, and~~. It also enables the community to ~~quickly and easily contribute more easily transfer~~ developments in the ~~coupled model back to the parent models~~ parent models to the coupled model, and vice versa.

The WRF-GC model is free and open-source to all users. The one-way coupled version of WRF-GC (v1.0) is now publicly available at wrf.geos-chem.org. A two-way coupled version with ~~chemistry feedback to meteorology~~ chemical feedbacks from
670 GEOS-Chem to WRF is under development and will be presented in a ~~future paper.~~ forthcoming paper. Further development of WRF-GC will aim to enable nested-domain simulations, support size-dependent aerosol microphysical calculations, as well as further improve the physical compatibility with WRF. We envision WRF-GC to become a powerful tool for research, forecast, and regulatory applications of regional atmospheric chemistry and air quality.

Code availability.

675 WRF-GC is free and open-source and can be obtained at <http://wrf.geos-chem.org>. The version of WRF-GC (v1.0) described in this paper ~~supports coupled~~ WRF v3.9.1.1 ~~and with~~ GEOS-Chem v12.2.1 and is permanently archived at <https://github.com/jimmielin/wrf-gc-pt1-paper-code> (doi:10.5281/zenodo.3550330). The two parent models, WRF and GEOS-Chem, are also open-source and can be obtained from their developers at <https://www.mmm.ucar.edu/weather-research-and-forecasting-model> and <http://www.geos-chem.org>, respectively.

Acronym	Description
ARW	Advanced Research WRF (dynamical core)
BC	Boundary condition
CCN	Cloud condensation nuclei
CMAQ	Community Multiscale Air Quality Modeling System
CTM	Chemical transport model
EC	Elemental carbon
ESMF	Earth System Modeling Framework
GCC	GEOS-Chem Classic
GCHP	GEOS-Chem High Performance
GCM	General circulation model
GDAS	Global Data Assimilation System
GEOS	Goddard Earth Observing System
GEOS-FP	GEOS Forward Processing
GMAO	NASA Global Modeling and Assimilation Office
HEMCO	Harvard-NASA Emissions Component
IC	Initial condition
KPP	Kinetic PreProcessor
MAPL	Model Analysis and Prediction Layer
MERRA-2	Modern-Era Retrospective analysis for Research and Applications, Version 2
MMM	Mesoscale and Microscale Meteorology Laboratory, NCAR
MPI	Message Passing Interface
NCAR	National Center of Atmospheric Research
NCEP	National Centers for Environmental Prediction
NWP	Numerical weather prediction
PBLH	Planetary Boundary Layer Height
POA-POC	Primary organic aerosol-carbon
SOA	Secondary organic aerosol
WRF	Weather Research and Forecasting Model
WRF-Chem	Weather Research and Forecasting model coupled with Chemistry
UCX	Unified Chemistry Extension
VBS	Volatility Basis Set

Author contributions.

685 TMF envisioned and oversaw the project. HL designed the WRF-GC Coupler. HL, XF, and HT developed the WRF-GC code, with assistance from YM and LJZ. XF, HL, and TMF performed the simulations and wrote the manuscript. HL performed the scalability and **performance** analysis. RMY, MPS, EWL, JZ, DJJ, XL, SDE, and CAK assisted in the adaptation of the GEOS-Chem model and the HEMCO module to WRF-GC. QZ provided the MEIC emissions inventory for China. XL, LZ, and LS prepared the MEIC emissions for GEOS-Chem. JG provided the boundary layer height observations. All authors contributed to the manuscript.

Competing interests. The authors declare no competing interests.

690 *Acknowledgements.* This project was supported by the National Natural Sciences Foundation of China (41975158). GEOS-FP data was provided by the Global Modeling and Assimilation Office (GMAO) at NASA Goddard Space Flight Center. We gratefully acknowledge the developers of WRF for making the model free and in the public domain.

References

- Alexander, B., Park, R. J., Jacob, D. J., Li, Q., Yantosca, R. M., Savarino, J., Lee, C., and Thiemens, M.: Sulfate formation in sea-salt aerosols: Constraints from oxygen isotopes, *J. Geophys. Res. Atmos.*, 110, <https://doi.org/10.1029/2004JD005659>, 2005.
- 695 Allen, D. J., Rood, R. B., Thompson, A. M., and Hudson, R. D.: Three-dimensional radon 222 calculations using assimilated meteorological data and a convective mixing algorithm, *J. Geophys. Res. Atmos.*, 101, 6871–6881, <https://doi.org/10.1029/95JD03408>, 1996.
- Amos, H. M., Jacob, D. J., Holmes, C. D., Fisher, J. A., Wang, Q., Yantosca, R. M., Corbitt, E. S., Galarneau, E., Rutter, A. P., Gustin, M. S., Steffen, A., Schauer, J. J., Graydon, J. A., Louis, V. L. S., Talbot, R. W., Edgerton, E. S., Zhang, Y., and Sunderland, E. M.: Gas-particle partitioning of atmospheric Hg (II) and its effect on global mercury deposition, *Atmos. Chem. Phys.*, 12, 591–603, <https://doi.org/10.5194/acp-12-591-2012>, 2012.
- 700 Arakawa, A. and Jung, J. H.: Multiscale modeling of the moist-convective atmosphere - A review, *Atmos. Res.*, 102, 263–285, <https://doi.org/10.1016/j.atmosres.2011.08.009>, 2011.
- Baklanov, A., Schlutzen, K., Suppan, P., Baldasano, J., Brunner, D., Aksoyoglu, S., Carmichael, G., Douros, J., Flemming, J., Forkel, R., Galmarini, S., Gauss, M., Grell, G., Hirtl, M., Joffre, S., Jorba, O., Kaas, E., Kaasik, M., Kallos, G., Kong, X., Korsholm, U., Kurganskiy, A., Kushta, J., Lohmann, U., Mahura, A., Manders-Groot, A., Maurizi, A., Moussiopoulos, N., Rao, S. T., Savage, N., Seigneur, C., Sokhi, R. S., Solazzo, E., Solomos, S., Sorensen, B., Tsegas, G., Vignati, E., Vogel, B., and Zhang, Y.: Online coupled regional meteorology chemistry models in Europe: current status and prospects, *Atmos. Chem. Phys.*, 14, 317–398, <https://doi.org/10.5194/acp-14-317-2014>, 2014.
- 705 Bey, I., Jacob, D. J., Yantosca, R. M., Logan, J. A., Field, B. D., Fiore, A. M., Li, Q., Liu, H. Y., Mickley, L. J., and Schultz, M. G.: Global modeling of tropospheric chemistry with assimilated meteorology: Model description and evaluation, *J. Geophys. Res. Atmos.*, 106, 23 073–23 095, <https://doi.org/10.1029/2001JD000807>, 2001.
- Byun, D. and Schere, K. L.: Review of the governing equations, computational algorithms, and other components of the Models-3 Community Multiscale Air Quality (CMAQ) modeling system, *Appl. Mech. Rev.*, 59, 51–77, <https://doi.org/10.1115/1.2128636>, 2006.
- Cao, H., Fu, T.-M., Zhang, L., Henze, D. K., Miller, C. C., Lerot, C., Abad, G. G., De Smedt, I., Zhang, Q., van Roozendaal, M., Hendrick, F., Chance, K., Li, J., Zheng, J., and Zhao, Y.: Adjoint inversion of Chinese non-methane volatile organic compound emissions using space-based observations of formaldehyde and glyoxal, *Atmos. Chem. Phys.*, 18, 15 017–15 046, <https://doi.org/10.5194/acp-18-15017-2018>, 2018.
- 715 Chapman, E. G., Gustafson, Jr., W. I., Easter, R. C., Barnard, J. C., Ghan, S. J., Pekour, M. S., and Fast, J. D.: Coupling aerosol-cloud-radiative processes in the WRF-Chem model: Investigating the radiative impact of elevated point sources, *Atmos. Chem. Phys.*, 9, 945–964, <https://doi.org/10.5194/acp-9-945-2009>, 2009.
- 720 Chen, D., Wang, Y., McElroy, M. B., He, K., Yantosca, R. M., and Le Sager, P.: Regional CO pollution and export in China simulated by the high-resolution nested-grid GEOS-Chem model, *Atmos. Chem. Phys.*, 9, 3825–3839, <https://doi.org/10.5194/acp-9-3825-2009>, 2009.
- Chen, F. and Dudhia, J.: Coupling an advanced land surface-hydrology model with the Penn State-NCAR MM5 modeling system. Part I: Model implementation and sensitivity, *Mon. Weather Rev.*, 129, 569–585, [https://doi.org/10.1175/1520-0493\(2001\)129<0569:CAALSH>2.0.CO;2](https://doi.org/10.1175/1520-0493(2001)129<0569:CAALSH>2.0.CO;2), 2001a.
- 725 Chen, F. and Dudhia, J.: Coupling an advanced land surface-hydrology model with the Penn State-NCAR MM5 modeling system. Part II: Preliminary model validation, *Mon. Weather Rev.*, 129, 587–604, [https://doi.org/10.1175/1520-0493\(2001\)129<0587:CAALSH>2.0.CO;2](https://doi.org/10.1175/1520-0493(2001)129<0587:CAALSH>2.0.CO;2), 2001b.

- Damian, V., Sandu, A., Damian, M., Potra, F., and Carmichael, G. R.: The kinetic preprocessor KPP—a software environment for solving
730 chemical kinetics, *Comput. Chem. Eng.*, 26, 1567–1579, [https://doi.org/10.1016/S0098-1354\(02\)00128-X](https://doi.org/10.1016/S0098-1354(02)00128-X), 2002.
- Ding, A. J., Fu, C. B., Yang, X. Q., Sun, J. N., Petaja, T. and Kerminen, V. M., Wang, T., Xie, Y., Herrmann, E., Zheng, L. F., Nie, W.,
Liu, Q., Wei, X. L., and Kulmala, M.: Intense atmospheric pollution modifies weather: a case of mixed biomass burning with fossil fuel
combustion pollution in eastern China, *Atmos. Chem. Phys.*, 13, 10 545–10 554, <https://doi.org/10.5194/acp-13-10545-2013>, 2013.
- Eastham, S. D., Weisenstein, D. K., and Barrett, S. R.: Development and evaluation of the unified tropospheric–stratospheric
735 chemistry extension (UCX) for the global chemistry-transport model GEOS-Chem, *Atmos. Environ.*, 89, 52–63,
<https://doi.org/10.1016/j.atmosenv.2014.02.001>, 2014.
- Eastham, S. D., Long, M. S., Keller, C. A., Lundgren, E., Yantosca, R. M., Zhuang, J., Li, C., Lee, C. J., Yannetti, M., Auer, B. M., Clune,
T. L., Kouatchou, J., Putman, W. M., Thompson, M. A., Trayanov, A. L., Molod, A. M., Martin, R. V., and Jacob, D. J.: GEOS-Chem High
Performance (GCHP v11-02c): a next-generation implementation of the GEOS-Chem chemical transport model for massively parallel
740 applications, *Geosci. Model. Dev.*, 11, 2941–2953, <https://doi.org/10.5194/gmd-11-2941-2018>, 2018.
- Fairlie, T. D., Jacob, D. J., and Park, R. J.: The impact of transpacific transport of mineral dust in the United States, *Atmos. Environ.*, 41,
1251–1266, <https://doi.org/10.1016/j.atmosenv.2006.09.048>, 2007.
- Fast, J. D., Gustafson Jr., W. I., Easter, R. C., Zaveri, R. A., Barnard, J. C., Chapman, E. G., Grell, G. A., and Peckham, S. E.: Evolution of
ozone, particulates, and aerosol direct radiative forcing in the vicinity of Houston using a fully coupled meteorology-chemistry-aerosol
745 model, *J. Geophys. Res. Atmos.*, 111, <https://doi.org/10.1029/2005JD006721>, 2006.
- Fisher, J. A., Murray, L. T., Jones, D. B. A., and Deutscher, N. M.: Improved method for linear carbon monoxide simulation
and source attribution in atmospheric chemistry models illustrated using GEOS-Chem v9, *Geosci. Model. Dev.*, 10, 4129–4144,
<https://doi.org/10.5194/gmd-10-4129-2017>, 2017.
- Fountoukis, C. and Nenes, A.: ISORROPIA II: a computationally efficient thermodynamic equilibrium model for K^+ - Ca^{2+} - Mg^{2+} - NH_4^+ -
750 Na^+ - SO_4^{2-} - NO_3^- - Cl^- - H_2O aerosols, *Atmos. Chem. Phys.*, 7, 4639–4659, <https://doi.org/10.5194/acp-7-4639-2007>, 2007.
- Friedman, C. L., Zhang, Y., and Selin, N. E.: Climate change and emissions impacts on atmospheric PAH transport to the Arctic, *Environ.
Sci. Technol.*, 48, 429–437, <https://doi.org/10.1021/es403098w>, 2013.
- Fu, T.-M., Jacob, D. J., Wittrock, F., Burrows, J. P., Vrekoussis, M., and Henze, D. K.: Global budgets of atmospheric glyoxal and methylgly-
oxal, and implications for formation of secondary organic aerosols, *J. Geophys. Res. Atmos.*, 113, <https://doi.org/10.1029/2007JD009505>,
755 2008.
- Fu, T.-M., Jacob, D. J., and Heald, C. L.: Aqueous-phase reactive uptake of dicarbonyls as a source of organic aerosol over eastern North
America, *Atmos. Environ.*, 43, 1814–1822, <https://doi.org/10.1016/j.atmosenv.2008.12.029>, 2009.
- Gong, S. L.: A parameterization of sea-salt aerosol source function for sub-and super-micron particles, *Global Biogeochem. Cy.*, 17,
<https://doi.org/10.1029/2003GB002079>, 2003.
- 760 Grell, G. A. and Freitas, S. R.: A scale and aerosol aware stochastic convective parameterization for weather and air quality modeling, *Atmos.
Chem. Phys.*, 14, 5233–5250, <https://doi.org/10.5194/acp-14-5233-2014>, 2014.
- Grell, G. A., Peckham, S. E., Schmitz, R., McKeen, S. A., Frost, G., Skamarock, W. C., and Eder, B.: Fully coupled “online” chemistry
within the WRF model, *Atmos. Environ.*, 39, 6957–6975, <https://doi.org/10.1016/j.atmosenv.2005.04.027>, 2005.
- Guenther, A. B., Jiang, X., Heald, C. L., Sakulyanontvittaya, T., Duhl, T., Emmons, L. K., and Wang, X.: The Model of Emissions of Gases
765 and Aerosols from Nature version 2.1 (MEGAN2.1): an extended and upYear framework for modeling biogenic emissions, *Geosci.
Model. Dev.*, 5, 1471–1492, <https://doi.org/10.5194/gmd-5-1471-2012>, 2012.

- Guo, J., Miao, Y., Zhang, Y., Liu, H., Li, Z., Zhang, W., He, J., Lou, M., Yan, Y., Bian, L., and Zhai, P.: The climatology of planetary boundary layer height in China derived from radiosonde and reanalysis data, *Atmos. Chem. Phys.*, 16, 13 309–13 319, <https://doi.org/10.5194/acp-16-13309-2016>, 2016.
- 770 Gustafson, Jr., W. I., Chapman, E. G., Ghan, S. J., Easter, R. C., and Fast, J. D.: Impact on modeled cloud characteristics due to simplified treatment of uniform cloud condensation nuclei during NEAQS 2004, *Geophys. Res. Lett.*, 34, <https://doi.org/10.1029/2007GL030021>, 2007.
- Hacker, J. P., Exby, J., Gill, D., Jimenez, I., Maltzahn, C., See, T., Mullendore, G., and Fossell, K.: A containerized mesoscale model and analysis toolkit to accelerate classroom learning, collaborative research, and uncertainty quantification, *B. Am. Meteorol. Soc.*, 98, 1129–
775 1138, <https://doi.org/10.1175/BAMS-D-15-00255.1>, 2017.
- Hoesly, R. M., Smith, S. J., Feng, L., Klimont, Z., Janssens-Maenhout, G., Pitkanen, T., Seibert, J. J., Vu, L., Andres, R. J., Bolt, R. M., Bond, T. C., Dawidowski, L., Kholod, N., Kurokawa, J.-I., Li, M., Liu, L., Lu, Z., Moura, M. C. P., O'Rourke, P. R., and Zhang, Q.: Historical (1750–2014) anthropogenic emissions of reactive gases and aerosols from the Community Emissions Data System (CEDS), *Geosci. Model. Dev.*, 11, 369–408, <https://doi.org/10.5194/gmd-11-369-2018>, 2018.
- 780 Holtzlag, A. and Boville, B.: Local Versus Nonlocal Boundary-Layer Diffusion in a Global Climate Model, *J. Climate*, 6, 1825–1842, [https://doi.org/10.1175/1520-0442\(1993\)006<1825:LVNBLD>2.0.CO;2](https://doi.org/10.1175/1520-0442(1993)006<1825:LVNBLD>2.0.CO;2), 1993.
- Hong, S.-Y. and Lim, J.-O. J.: The WRF single-moment 6-class microphysics scheme (WSM6), *J. Korean Meteor. Soc.*, 42, 129–151, 2006.
- Horowitz, H. M., Jacob, D. J., Zhang, Y., Dibble, T. S., Slemr, F., Amos, H. M., Schmidt, J. A., Corbitt, E. S., Marais, E. A., and Sunderland, E. M.: A new mechanism for atmospheric mercury redox chemistry: implications for the global mercury budget, *Atmos. Chem. Phys.*, 17,
785 6353–6371, <https://doi.org/10.5194/acp-17-6353-2017>, 2017.
- Hu, L., Keller, C. A., Long, M. S., Sherwen, T., Auer, B., Da Silva, A., Nielsen, J. E., Pawson, S., Thompson, M. A., Trayanov, A. L., Travis, K. R., Grange, S. K., Evans, M. J., and Jacob, D. J.: Global simulation of tropospheric chemistry at 12.5 km resolution: performance and evaluation of the GEOS-Chem chemical module (v10-1) within the NASA GEOS Earth system model (GEOS-5 ESM), *Geosci. Model. Dev.*, 11, 4603–4620, <https://doi.org/10.5194/gmd-11-4603-2018>, 2018.
- 790 Huang, X., Song, Y., Li, M., Li, J., Huo, Q., Cai, X., Zhu, T., Hu, M., and Zhang, H.: A high-resolution ammonia emission inventory in China, *Global Biogeochem. Cy.*, 26, <https://doi.org/10.1029/2011GB004161>, 2012.
- Hudman, R. C., Moore, N. E., Mebust, A. K., Martin, R. V., Russell, A. R., Valin, L. C., and Cohen, R. C.: Steps towards a mechanistic model of global soil nitric oxide emissions: implementation and space based-constraints, *Atmos. Chem. Phys.*, 12, 7779–7795, <https://doi.org/10.5194/acp-12-7779-2012>, 2012.
- 795 Iacono, M. J., Delamere, J. S., Mlawer, E. J., Shephard, M. W., Clough, S. A., and Collins, W. D.: Radiative forcing by long-lived greenhouse gases: Calculations with the AER radiative transfer models, *J. Geophys. Res. Atmos.*, 113, <https://doi.org/10.1029/2008JD009944>, 2008.
- Jaeglé, L., Quinn, P. K., Bates, T. S., Alexander, B., and Lin, J.-T.: Global distribution of sea salt aerosols: new constraints from in situ and remote sensing observations, *Atmos. Chem. Phys.*, 11, 3137–3157, <https://doi.org/10.5194/acp-11-3137-2011>, 2011.
- Jeworrek, J., West, G., and Stull, R.: Evaluation of Cumulus and Microphysics Parameterizations in WRF across the Convective Gray Zone,
800 *Weather. Forecast.*, 34, 1097–1115, <https://doi.org/10.1175/WAF-D-18-0178.1>, 2019.
- Jiang, Z., Jolleys, M. D., Fu, T.-M., Palmer, P. I., Ma, Y. P., Tian, H., Li, J., and Yang, X.: Spatiotemporal and probability variations of surface PM_{2.5} over China between 2013 and 2019 and the associated changes in health risks: An integrative observation and model analysis, *Sci. Total. Environ.*, 723, 137 896, <https://doi.org/10.1016/j.scitotenv.2020.137896>, 2020.

- Jimenez, P. A., Dudhia, J., Gonzalez-Rouco, J. F., Navarro, J., Montavez, J. P., and Garcia-Bustamante, E.: A Revised Scheme for the WRF
805 Surface Layer Formulation, *Mon. Weather Rev.*, 140, 898–918, <https://doi.org/10.1175/MWR-D-11-00056.1>, 2012.
- Keller, C. A., Long, M. S., Yantosca, R. M., Da Silva, A. M., Pawson, S., and Jacob, D. J.: HEMCO v1.0: a versatile, ESMF-compliant
component for calculating emissions in atmospheric models, *Geosci. Model Dev.*, 7, 1409–1417, <https://doi.org/10.5194/gmd-7-1409-2014>, 2014.
- Kim, P. S., Jacob, D. J., Fisher, J. A., Travis, K., Yu, K., Zhu, L., Yantosca, R. M., Sulprizio, M. P., Jimenez, J. L., Campuzano-Jost, P.,
810 Froyd, K. D., Liao, J., Hair, J. W., Fenn, M. A., Butler, C. F., Wagner, N. L., Gordon, T. D., Welti, A., Wennberg, P. O., Crouse, J. D.,
St. Clair, J. M., Teng, A. P., Millet, D. B., Schwarz, J. P., Markovic, M. Z., and Perring, A. E.: Sources, seasonality, and trends of southeast
US aerosol: an integrated analysis of surface, aircraft, and satellite observations with the GEOS-Chem chemical transport model, *Atmos.
Chem. Phys.*, 15, 10411–10433, <https://doi.org/10.5194/acp-15-10411-2015>, 2015.
- Kodros, J. and Pierce, J.: Important global and regional differences in aerosol cloud-albedo effect estimates between simulations with and
815 without prognostic aerosol microphysics, *J. Geophys. Res. Atmos.*, 122, 4003–4018, <https://doi.org/10.1002/2016JD025886>, 2017.
- Li, M., Zhang, Q., Streets, D. G., He, K. B., Cheng, Y. F., Emmons, L. K., Huo, H., Kang, S. C., Lu, Z., Shao, M., Su, H., Yu, X., and Zhang,
Y.: Mapping Asian anthropogenic emissions of non-methane volatile organic compounds to multiple chemical mechanisms, *Atmos. Chem.
Phys.*, 14, 5617–5638, <https://doi.org/10.5194/acp-14-5617-2014>, 2014.
- Li, M., Liu, H., Geng, G., Hong, C., Liu, F., Song, Y., Tong, D., Zheng, B., Cui, H., Man, H., Zhang, Q., and He, K.: Anthropogenic emission
820 inventories in China: a review, *Natl. Sci. Rev.*, 4, 834–866, <https://doi.org/10.1093/nsr/nwx150>, 2017a.
- Li, M., Zhang, Q., Kurokawa, J.-i., Woo, J.-H., He, K., Lu, Z., Ohara, T., Song, Y., Streets, D. G., Carmichael, G. R., Cheng, Y., Hong,
C., Huo, H., Jiang, X., Kang, S., Liu, F., Su, H., and Zheng, B.: MIX: a mosaic Asian anthropogenic emission inventory under the
international collaboration framework of the MICS-Asia and HTAP, *Atmos. Chem. Phys.*, 17, 935–963, <https://doi.org/10.5194/acp-17-935-2017>, 2017b.
- 825 Li, Z., Niu, F., Fan, J., Liu, Y., Rosenfeld, D., and Ding, Y.: Long-term impacts of aerosols on the vertical development of clouds and
precipitation, *Nat. Geosci.*, 4, 888–894, <https://doi.org/10.1038/NGEO1313>, 2011.
- Li, Z., Guo, J., Ding, A., Liao, H., Liu, J., Sun, Y., Wang, T., Xue, H., Zhang, H., and Zhu, B.: Aerosol and boundary-layer interactions and
impact on air quality, *Natl. Sci. Rev.*, 4, 810–833, <https://doi.org/10.1093/nsr/nwx117>, 2017c.
- Lin, J.-T. and McElroy, M. B.: Impacts of boundary layer mixing on pollutant vertical profiles in the lower troposphere: Implications to
830 satellite remote sensing, *Atmos. Environ.*, 44, 1726–1739, 2010.
- Liu, H., Jacob, D. J., Bey, I., and Yantosca, R. M.: Constraints from ²¹⁰Pb and ⁷Be on wet deposition and transport in a global
three-dimensional chemical tracer model driven by assimilated meteorological fields, *J. Geophys. Res. Atmos.*, 106, 12 109–12 128,
<https://doi.org/10.1029/2000JD900839>, 2001.
- Liu, Y., Bourgeois, A., Warner, T., Swerdlin, S., and Hacker, J.: Implementation of Observation-Nudging Based FDDA into WRF for Sup-
835 porting ATEC Test Operations, 2005 WRF user workshop, Boulder, CO, pp. 1–4, 2005.
- Liu, Y., Bourgeois, A., Warner, T., Swerdlin, S., and Yu, W.: An update on "observation nudging"-based FDDA for WRF-ARW: Verification
using OSSE and performance of real-time forecasts, 2006 WRF user workshop, Boulder, CO, pp. 1–6, 2006.
- Long, M. S., Yantosca, R., Nielsen, J. E., Keller, C. A., da Silva, A., Sulprizio, M. P., Pawson, S., and Jacob, D. J.: Development of a
grid-independent GEOS-Chem chemical transport model (v9-02) as an atmospheric chemistry module for Earth system models, *Geosci.
840 Model Dev.*, 8, 595–602, <https://doi.org/10.5194/gmd-8-595-2015>, 2015.

- Lou, M., Guo, J., Wang, L., Xu, H., Chen, D., Miao, Y., Lv, Y., Li, Y., Guo, X., Ma, S., et al.: On the relationship between aerosol and boundary layer height in summer in China under different thermodynamic conditions, *Earth Space Sci.*, 6, 887–901, <https://doi.org/10.1029/2019EA000620>, 2019.
- 845 Lu, X., Zhang, L., Wu, T., Long, M. S., Wang, J., Jacob, D. J., Zhang, F., Zhang, J., Eastham, S. D., Hu, L., Zhu, L., Liu, X., and Wei, M.: Development of the global atmospheric general circulation-chemistry model BCC-GEOS-Chem v1.0: model description and evaluation, *Geosci. Model Dev. Discuss.*, 2019, 1–39, <https://doi.org/10.5194/gmd-2019-240>, 2019.
- Maasakkers, J. D., Jacob, D. J., Sulprizio, M. P., Scarpelli, T. R., Nesser, H., Sheng, J.-X., Zhang, Y., Hersher, M., Bloom, A. A., Bowman, K. W., Worden, J. R., Janssens-Maenhout, G., and Parker, R. J.: Global distribution of methane emissions, emission trends, and OH concentrations and trends inferred from an inversion of GOSAT satellite data for 2010–2015, *Atmos. Chem. Phys.*, 19, 7859–7881, 850 <https://doi.org/10.5194/acp-19-7859-2019>, 2019.
- Marais, E. A., Jacob, D. J., Jimenez, J. L., Campuzano-Jost, P., Day, D. A., Hu, W., Krechmer, J., Zhu, L., Kim, P. S., Miller, C. C., Fisher, J. A., Travis, K., Yu, K., Hanisco, T. F., Wolfe, G. M., Arkinson, H. L., Pye, H. O. T., Froyd, K. D., Liao, J., and McNeill, V. F.: Aqueous-phase mechanism for secondary organic aerosol formation from isoprene: application to the southeast United States and co-benefit of SO₂ emission controls, *Atmos. Chem. Phys.*, 16, 1603–1618, <https://doi.org/10.5194/acp-16-1603-2016>, 2016.
- 855 McLinden, C., Olsen, S., Hannegan, B., Wild, O., Prather, M., and Sundet, J.: Stratospheric ozone in 3-D models: A simple chemistry and the cross-tropopause flux, *J. Geophys. Res. Atmos.*, 105, 14 653–14 665, <https://doi.org/10.1029/2000JD900124>, 2000.
- Michalakes, J., Dudhia, J., Gill, D., Klemp, J., and Skamarock, W.: Design of a next-generation regional weather research and forecast model., *Towards Teracomputing: The Use of Parallel Processors in Meteorology*, 1999.
- Morrison, H., Thompson, G., and Tatarskii, V.: Impact of Cloud Microphysics on the Development of Trailing Stratiform Precipitation in a Simulated Squall Line: Comparison of One- and Two-Moment Schemes, *Mon. Weather Rev.*, 137, 991–1007, 860 <https://doi.org/10.1175/2008MWR2556.1>, 2009.
- Nakanishi, M. and Niino, H.: An improved mellor-yamada level-3 model: Its numerical stability and application to a regional prediction of advection fog, *Bound.-Lay. Meteorol.*, 119, 397–407, <https://doi.org/10.1007/s10546-005-9030-8>, 2006.
- Nassar, R., Jones, D. B. A., Suntharalingam, P., Chen, J. M., Andres, R. J., Wecht, K. J., Yantosca, R. M., Kulawik, S. S., Bowman, K. W., 865 Worden, J. R., Machida, T., and Matsueda, H.: Modeling global atmospheric CO₂ with improved emission inventories and CO₂ production from the oxidation of other carbon species, *Geosci. Model. Dev.*, 3, 689, <https://doi.org/10.5194/gmd-3-689-2010>, 2010.
- Neale, R. B. et al.: NCAR Tech. Note NCAR/TN-486+STR: Description of the NCAR Community Atmosphere Model (CAM 5.0), 2012.
- Olson, D. M., Dinerstein, E., Wikramanayake, E. D., Burgess, N. D., Powell, G. V. N., Underwood, E. C., D'amico, J. A., Itoua, I., Strand, H. E., Morrison, J. C., Loucks, C. J., Allnutt, T. F., Ricketts, T. H., Kura, Y., Lamoreux, J. F., Wettengel, W. W., Hedao, P., and Kassem, 870 K. R.: Terrestrial Ecoregions of the World: A New Map of Life on Earth: A new global map of terrestrial ecoregions provides an innovative tool for conserving biodiversity, *BioScience*, 51, 933–938, [https://doi.org/10.1641/0006-3568\(2001\)051\[0933:TEOTWA\]2.0.CO;2](https://doi.org/10.1641/0006-3568(2001)051[0933:TEOTWA]2.0.CO;2), 2001.
- Park, R. J., Jacob, D. J., Field, B. D., Yantosca, R. M., and Chin, M.: Natural and transboundary pollution influences on sulfate-nitrate-ammonium aerosols in the United States: Implications for policy, *J. Geophys. Res. Atmos.*, 109, <https://doi.org/10.1029/2003JD004473>, 2004.
- 875 Philip, S., Martin, R. V., Pierce, J. R., Jimenez, J. L., Zhang, Q., Canagaratna, M. R., Spracklen, D. V., Nowlan, C. R., Lamsal, L. N., Cooper, M. J., and Krotkov, N. A.: Spatially and seasonally resolved estimate of the ratio of organic mass to organic carbon, *Atmos. Environ.*, 87, 34–40, <https://doi.org/10.1016/j.atmosenv.2013.11.065>, 2014.

- 880 Pye, H. O. T., Liao, H., Wu, S., Mickley, L. J., Jacob, D. J., Henze, D. K., and Seinfeld, J. H.: Effect of changes in climate and emissions on future sulfate-nitrate-ammonium aerosol levels in the United States, *J. Geophys. Res. Atmos.*, 114, <https://doi.org/10.1029/2008JD010701>, 2009.
- Pye, H. O. T., Chan, A. W. H., Barkley, M. P., and Seinfeld, J. H.: Global modeling of organic aerosol: the importance of reactive nitrogen (NO_x and NO_3), *Atmos. Chem. Phys.*, 10, 11 261–11 276, <https://doi.org/10.5194/acp-10-11261-2010>, 2010.
- Randerson, J., G.R., v. d. W., L., G., G.J., C., and P.S., K.: Global Fire Emissions Database, Version 4, (GFEDv4). ORNL DAAC, Oak Ridge, Tennessee, USA., <https://doi.org/10.3334/ORNLDAAC/1293>, 2018.
- 885 Robinson, A. L., Donahue, N. M., Shrivastava, M. K., Weitkamp, E. A., Sage, A. M., Grieshop, A. P., Lane, T. E., Pierce, J. R., and Pandis, S. N.: Rethinking organic aerosols: Semivolatile emissions and photochemical aging, *Science*, 315, 1259–1262, <https://doi.org/10.1126/science.1133061>, 2007.
- Sandu, A. and Sander, R.: Technical note: Simulating chemical systems in Fortran90 and Matlab with the Kinetic PreProcessor KPP-2.1, *Atmos. Chem. Phys.*, 6, 187–195, <https://doi.org/10.5194/acp-6-187-2006>, 2006.
- 890 Sandu, A., Verwer, J., Blom, J., Spee, E., Carmichael, G., and Potra, F.: Benchmarking stiff ode solvers for atmospheric chemistry problems II: Rosenbrock solvers, *Atmos. Environ.*, 31, 3459–3472, [https://doi.org/10.1016/S1352-2310\(97\)83212-8](https://doi.org/10.1016/S1352-2310(97)83212-8), 1997.
- Skamarock, W. C., Klemp, J. B., Dudhia, J., Gill, D. O., Liu, Z., Berner, J., and Huang, X.: NCAR Tech. Note NCAR/TN-556+STR: A Description of the Advanced Research WRF Model Version 4, <https://doi.org/10.5065/1dfh-6p97>, 2019.
- Skamarock, W. C. et al.: NCAR Tech. Note NCAR/TN-475+STR: A Description of the Advanced Research WRF Version 3, <https://doi.org/10.5065/D68S4MVH>, 2008.
- 895 Soerensen, A. L., Sunderland, E. M., Holmes, C. D., Jacob, D. J., Yantosca, R. M., Skov, H., Christensen, J. H., Strode, S. A., and Mason, R. P.: An improved global model for air-sea exchange of mercury: High concentrations over the North Atlantic, *Environ. Sci. Technol.*, 44, 8574–8580, <https://doi.org/10.1021/es102032g>, 2010.
- Stauffer, D. R. and Seaman, N. L.: Use of Four-Dimensional Data Assimilation in a Limited-Area Mesoscale Model. Part I: Experiments with
900 Synoptic-Scale Data, *Mon. Weather. Rev.*, 118, 1250–1277, [https://doi.org/10.1175/1520-0493\(1990\)118<1250:UOFDDA>2.0.CO;2](https://doi.org/10.1175/1520-0493(1990)118<1250:UOFDDA>2.0.CO;2), 1990.
- Stauffer, D. R. and Seaman, N. L.: Multiscale Four-Dimensional Data Assimilation, *J. Appl. Meteorol.*, 33, 416–434, [https://doi.org/10.1175/1520-0450\(1994\)033<0416:MFDDA>2.0.CO;2](https://doi.org/10.1175/1520-0450(1994)033<0416:MFDDA>2.0.CO;2), 1994.
- Suarez, M., Trayanov, A., Hill, C., Schopf, P., and Vikhliav, Y.: MAPL: a high-level programming paradigm to support more rapid and
905 robust encoding of hierarchical trees of interacting high-performance components, in: Proceedings of the 2007 symposium on Component and framework technology in high-performance and scientific computing, pp. 11–20, ACM, <https://doi.org/10.1145/1297385.1297388>, 2007.
- Taylor, K.: Summarizing multiple aspects of model performance in a single diagram., *J. Geophys. Res. Atmos.*, 106, 7183–7192, <https://doi.org/10.1029/2000JD900719>, 2001.
- 910 Thompson, G., Field, P. R., Rasmussen, R. M., and Hall, W. D.: Explicit Forecasts of Winter Precipitation Using an Improved Bulk Microphysics Scheme. Part II: Implementation of a New Snow Parameterization, *Mon. Weather Rev.*, 136, 5095–5115, <https://doi.org/10.1175/2008MWR2387.1>, 2008.
- Tiedtke, M.: A comprehensive mass flux scheme for cumulus parameterization in large-scale models, *Mon. Weather. Rev.*, 117, 1779–1800, [https://doi.org/10.1175/1520-0493\(1989\)117<1779:ACMFSF>2.0.CO;2](https://doi.org/10.1175/1520-0493(1989)117<1779:ACMFSF>2.0.CO;2), 1989.
- 915 U.S. Environmental Protection Agency: 2011 National Emissions Inventory, version 1 Technical Support Document, 2014.

- Wang, J., Wang, S., Jiang, J., Ding, A., Zheng, M., Zhao, B., Wong, D. C., Zhou, W., Zheng, G., Wang, L., Pleim, J. E., and Hao, J.: Impact of aerosol-meteorology interactions on fine particle pollution during China's severe haze episode in January 2013, *Environ. Res. Lett.*, 9, <https://doi.org/10.1088/1748-9326/9/9/094002>, 2014a.
- 920 Wang, Q., Jacob, D. J., Spackman, J. R., Perring, A. E., Schwarz, J. P., Moteki, N., Marais, E. A., Ge, C., Wang, J., and Barrett, S. R. H.: Global budget and radiative forcing of black carbon aerosol: Constraints from pole-to-pole (HIPPO) observations across the Pacific, *J. Geophys. Res. Atmos.*, 119, 195–206, <https://doi.org/10.1002/2013JD020824>, 2014b.
- Wang, Y., Jacob, D. J., and Logan, J. A.: Global simulation of tropospheric O₃-NO_x-hydrocarbon chemistry: 1. Model formulation, *J. Geophys. Res. Atmos.*, 103, 10 713–10 725, <https://doi.org/10.1029/98JD00158>, 1998.
- Wang, Y. X., McElroy, M. B., Jacob, D. J., and Yantosca, R. M.: A nested grid formulation for chemical transport over Asia: Applications to CO, *J. Geophys. Res. Atmos.*, 109, <https://doi.org/10.1029/2004JD005237>, 2004.
- 925 Wesely, M. L.: Parameterization of surface resistances to gaseous dry deposition in regional-scale numerical models, *Atmos. Environ.*, 23, 1293–1304, [https://doi.org/10.1016/0004-6981\(89\)90153-4](https://doi.org/10.1016/0004-6981(89)90153-4), 1989.
- Wong, D. C., Pleim, J., Mathur, R., Binkowski, F., Otte, T., Gilliam, R., Pouliot, G., Xiu, A., Young, J. O., and Kang, D.: WRF-CMAQ two-way coupled system with aerosol feedback: software development and preliminary results, *Geosci. Model. Dev.*, 5, 299–312, <https://doi.org/10.5194/gmd-5-299-2012>, 2012.
- 930 Wu, S., Mickley, L. J., Jacob, D. J., Logan, J. A., Yantosca, R. M., and Rind, D.: Why are there large differences between models in global budgets of tropospheric ozone?, *J. Geophys. Res. Atmos.*, 112, <https://doi.org/10.1029/2006JD007801>, 2007.
- Yu, F. and Luo, G.: Simulation of particle size distribution with a global aerosol model: contribution of nucleation to aerosol and CCN number concentrations, *Atmos. Chem. Phys.*, 9, 7691–7710, <https://doi.org/10.5194/acp-9-7691-2009>, 2009.
- 935 Yu, K., Keller, C. A., Jacob, D. J., Molod, A. M., Eastham, S. D., and Long, M. S.: Errors and improvements in the use of archived meteorological data for chemical transport modeling: an analysis using GEOS-Chem v11-01 driven by GEOS-5 meteorology, *Geosci. Model Dev.*, 11, 305–319, <https://doi.org/10.5194/gmd-11-305-2018>, 2018.
- Yu, S., Mathur, R., Pleim, J., Wong, D., Gilliam, R., Alapaty, K., Zhao, C., and Liu, X.: Aerosol indirect effect on the grid-scale clouds in the two-way coupled WRF-CMAQ: model description, development, evaluation and regional analysis, *Atmos. Chem. Phys.*, 14, 11 247–11 285, <https://doi.org/10.5194/acp-14-11247-2014>, 2014.
- 940 Zender, C. S., Bian, H., and Newman, D.: Mineral Dust Entrainment and Deposition (DEAD) model: Description and 1990s dust climatology, *J. Geophys. Res. Atmos.*, 108, <https://doi.org/10.1029/2002JD002775>, 2003.
- Zhang, C. and Wang, Y.: Projected future changes of tropical cyclone activity over the western North and South Pacific in a 20-km-Mesh regional climate model, *J. Climate*, 30, 5923–5941, <https://doi.org/10.1175/JCLI-D-16-0597.1>, 2017.
- 945 Zhang, C., Wang, Y., and Hamilton, K.: Improved representation of boundary layer clouds over the southeast Pacific in ARW-WRF using a modified Tiedtke cumulus parameterization scheme, *Mon. Weather Rev.*, 139, 3489–3513, <https://doi.org/10.1175/MWR-D-10-05091.1>, 2011.
- Zhang, G. J. and McFarlane, N. A.: Sensitivity of climate simulations to the parameterization of cumulus convection in the Canadian Climate Centre general circulation model, *Atmos. Ocean.*, 33, 407–446, <https://doi.org/10.1080/07055900.1995.9649539>, 1995.
- 950 Zhang, L., Gong, S., Padro, J., and Barrie, L.: A size-segregated particle dry deposition scheme for an atmospheric aerosol module, *Atmos. Environ.*, 35, 549–560, [https://doi.org/10.1016/S1352-2310\(00\)00326-5](https://doi.org/10.1016/S1352-2310(00)00326-5), 2001.

- Zhang, L., Liu, L., Zhao, Y., Gong, S., Zhang, X., Henze, D. K., Capps, S. L., Fu, T.-M., Zhang, Q., and Wang, Y.: Source attribution of particulate matter pollution over North China with the adjoint method, *Environ. Res. Lett.*, 10, <https://doi.org/10.1088/1748-9326/10/8/084011>, 2015.
- 955 Zhuang, J., Jacob, D. J., Gaya, J. F., Yantosca, R. M., Lundgren, E. W., Sulprizio, M. P., and Eastham, S. D.: Enabling immediate access to Earth science models through cloud computing: application to the GEOS-Chem model, *B. Am. Meteorol. Soc.*, <https://doi.org/10.1175/BAMS-D-18-0243.1>, 2019.
- Zhuang, J., Jacob, D. J., Lin, H., Lundgren, E. W., Yantosca, R. M., Gaya, J. F., Sulprizio, M. P., and Eastham, S. D.: Enabling high-performance cloud computing for Earth science modeling on over a thousand cores: application to the GEOS-Chem atmospheric chemistry
960 model, *J. Adv. Model. Earth. Sy.*, n/a, e2020MS002 064, <https://doi.org/10.1029/2020MS002064>, 2020.

WRF-GC Model (v1.0)

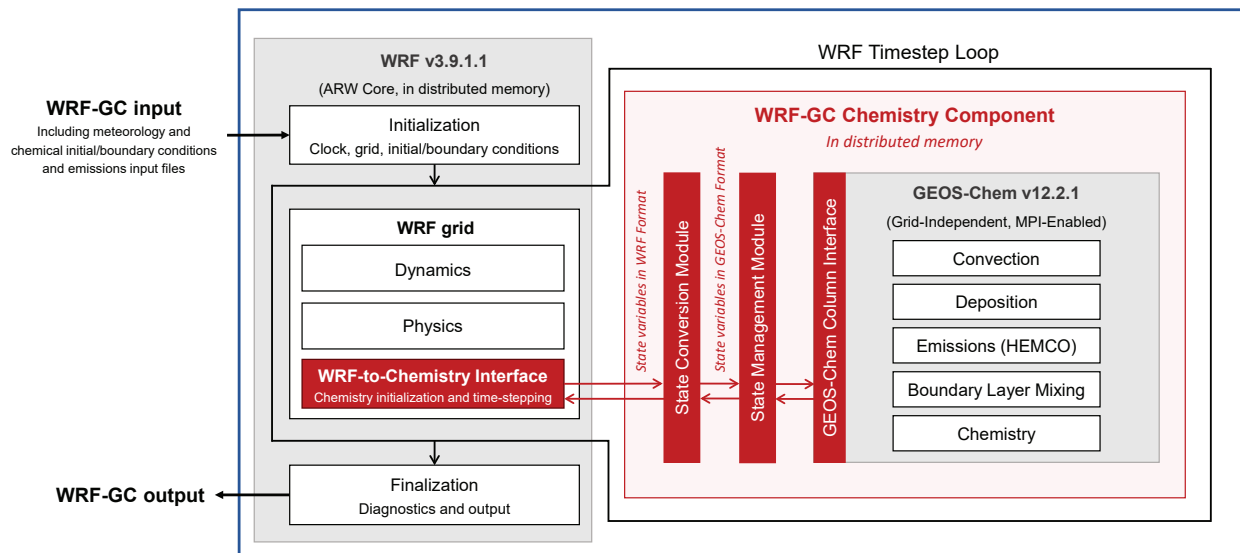


Figure 1. Architectural overview of the WRF-GC coupled-model (v1.0). The WRF-GC Coupler (all parts shown in red) includes interfaces to the two parent models, as well as the state conversion and state management modules. The parent models (shown in grey) are standard codes downloaded from their sources, without any modifications.

6-Day Time-averaged PM_{2.5} concentrations [$\mu\text{g m}^{-3}$]

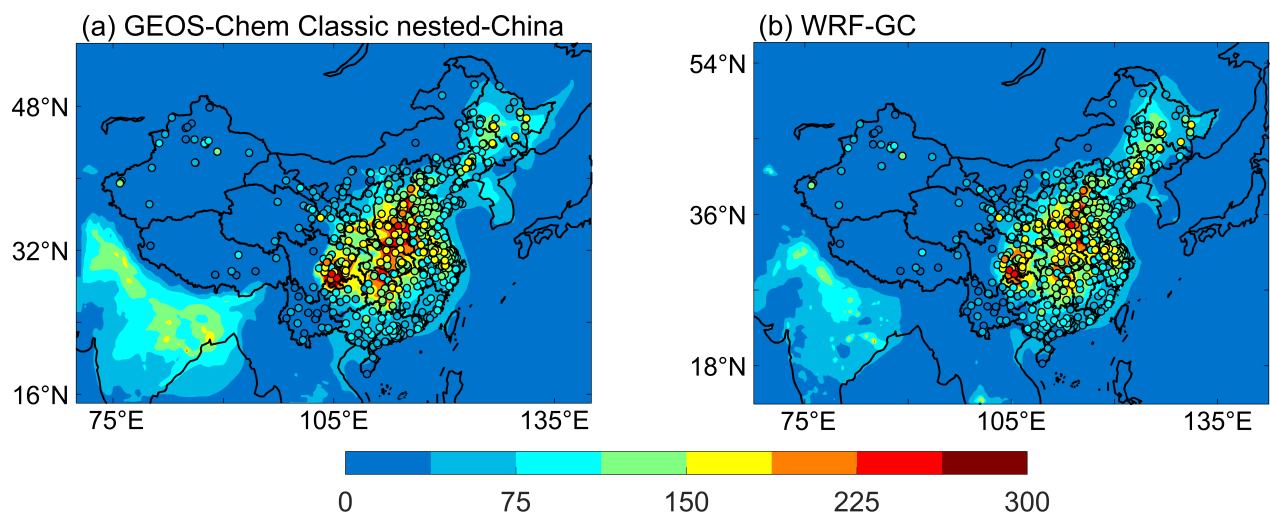


Figure 2. Comparison of the simulated (filled contours) 6-day average PM_{2.5} concentrations during Jan 22 to 27, 2015 from (a) the GEOS-Chem Classic nested-China simulation and (b) the WRF-GC nudged simulation. Also shown are the observed 6-day average PM_{2.5} concentrations during this period at 578 surface sites managed by the Ministry of Ecology and Environment of China.

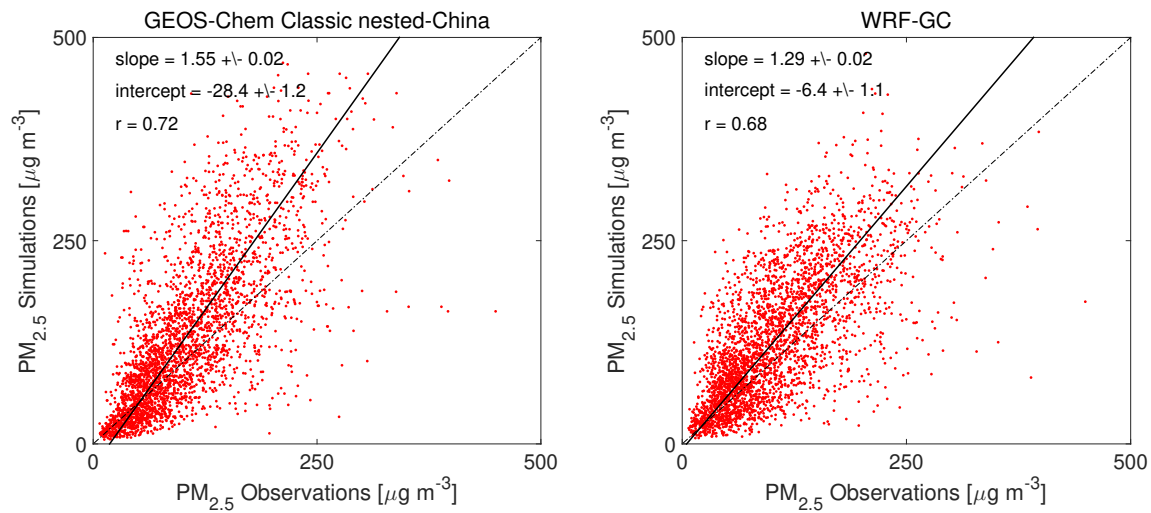


Figure 3. Scatter plots of observed and simulated daily mean PM_{2.5} during Jan-January 22 to 27, 2015 at 507 surface sites over Eastern China for (a) the ~~the~~ **GEOS-Chem** the **GEOS-Chem** Classic nested-China simulation and (b) the WRF-GC nudged simulation. The solid lines indicate the reduced major axis regression lines, with slopes, intercepts, and correlation coefficients (r) shown inset. The dotted lines indicate the 1:1 lines.

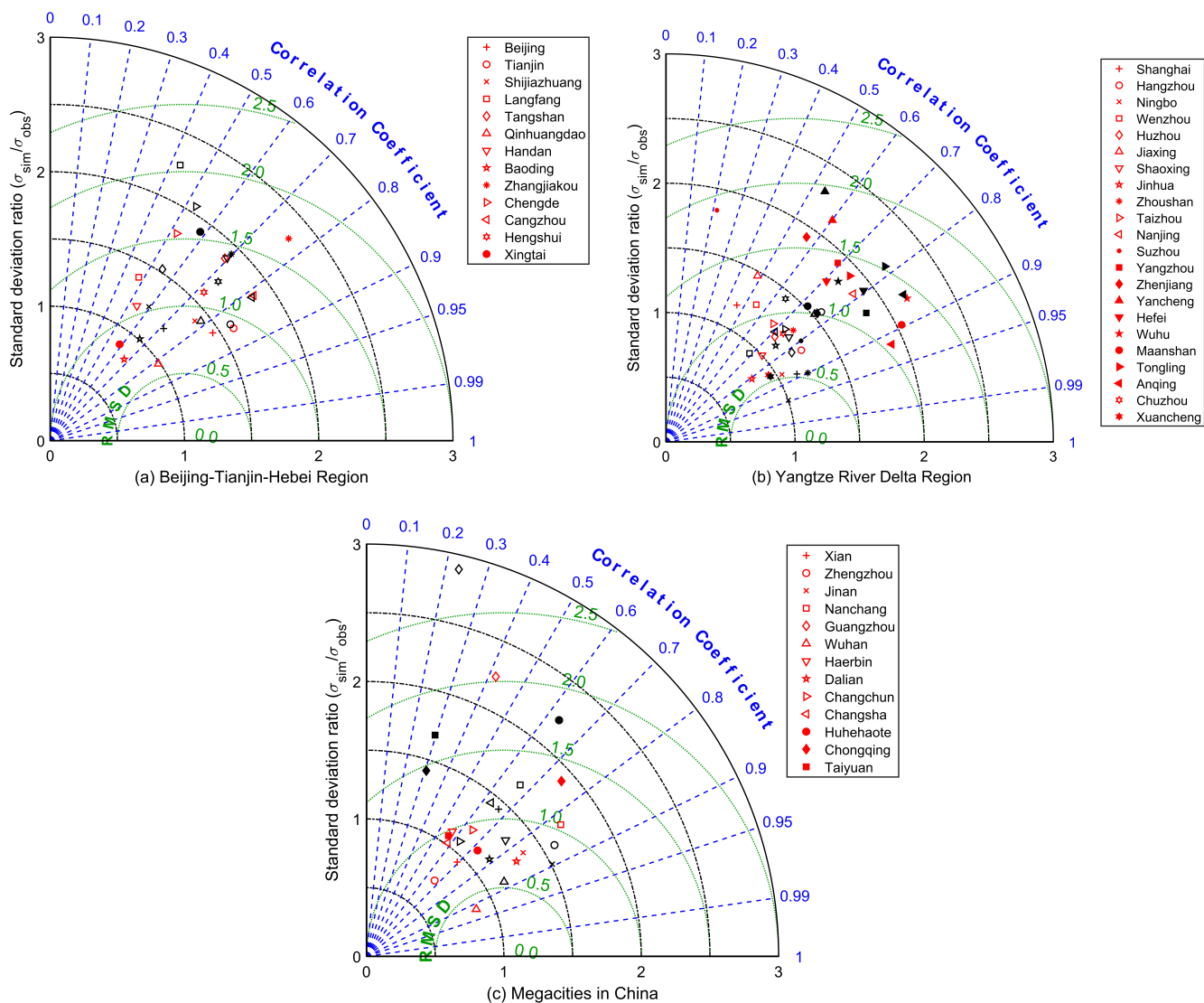


Figure 4. Taylor diagrams of hourly $PM_{2.5}$ concentrations during Jan 22 to 27, 2015 from the GEOS-Chem Classic nested-China simulation (black symbols) and the WRF-GC simulation (red symbols) for (a) 13 cities in the Beijing-Tianjin-Hebei area, (b) 22 cities in the Yangtze River Delta area, and (c) 13 other major Chinese cities. Green, black, and blue dashed lines indicate contours of the normalized centered root-mean-square differences (RMSD), the ratios of simulated versus observed standard deviation, and the Pearson correlation coefficients, respectively.

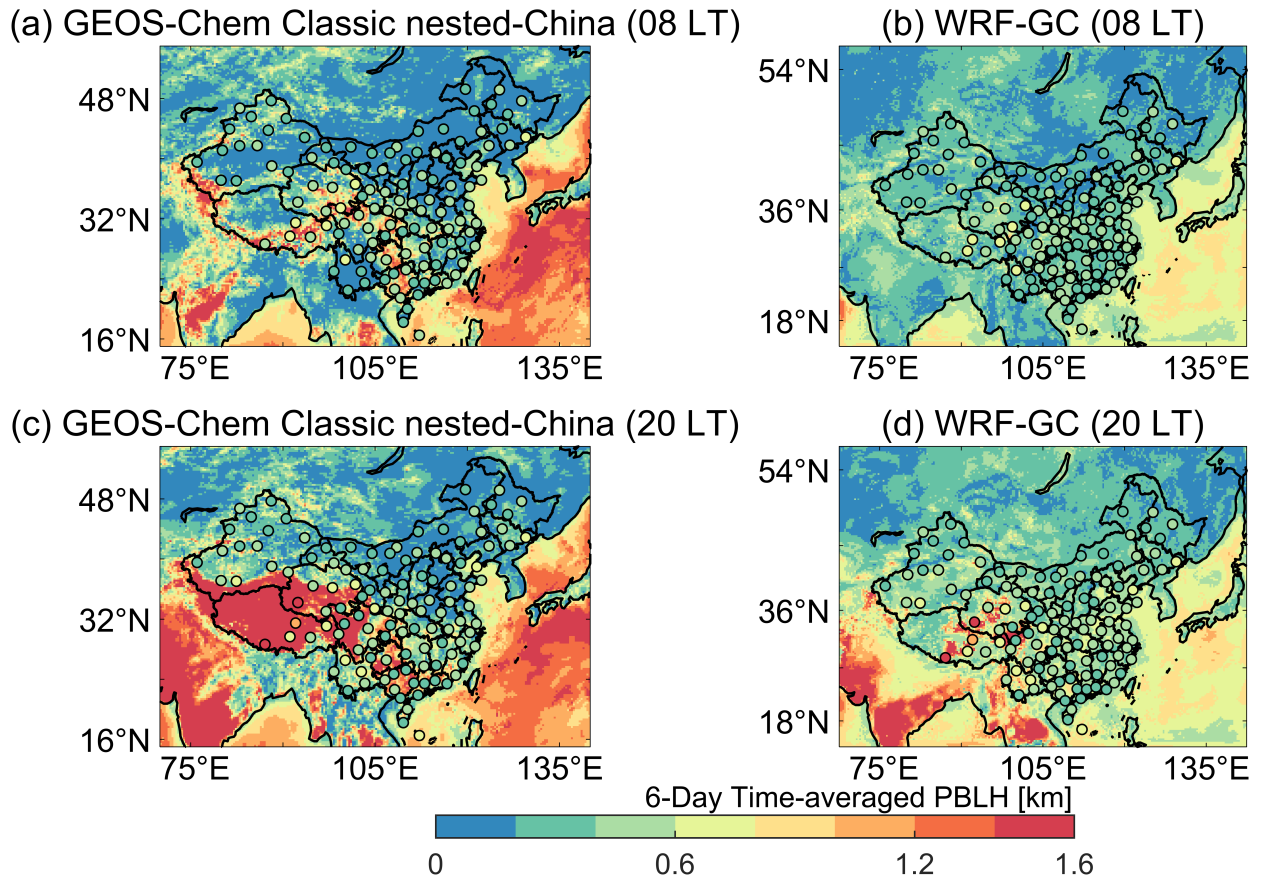


Figure 5. Comparison of the simulated (fill contours) and observed (fill symbols) planetary boundary layer heights (PBLH) at 08:00 local time (upper panel) and 20:00 local time (bottom panel) averaged between [Jan-January 22](#) and 27, 2015. (a,c) [GEOS-Chem Classic nested-China simulation \(read-PBLH from the GEOS-FP dataset\)](#), which was used to drive the GEOS-Chem Classic nested-China simulation, and (b,d) PBLH simulated by the WRF-GC [simulation model](#).

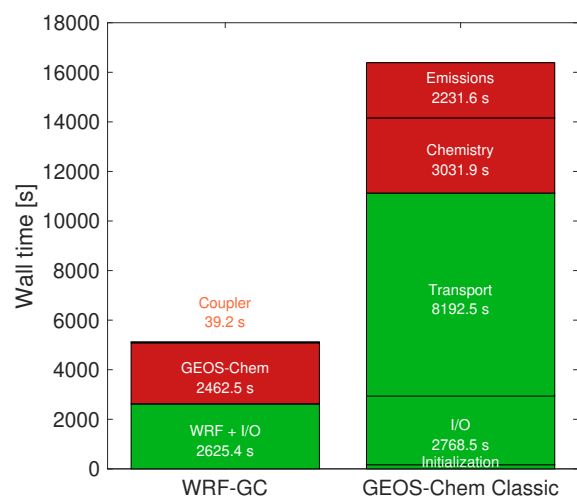


Figure 6. Comparison of wall time for the WRF-GC model (v1.0) and the GEOS-Chem Classic nested-grid model (version 12.2.1)

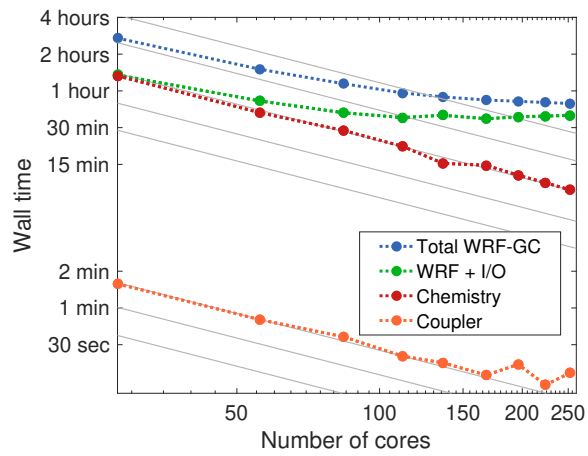


Figure 7. WRF-GC model scalability by processes. Gray lines indicate perfect scalability, i.e. halved computational time for each doubling of processor cores.

Table 1. Meteorological variables needed for GEOS-Chem.

No.	Variable(s) in GEOS-Chem [unit]	Description	Usage in GEOS-Chem	Passed or calculated from which variable(s) in WRF [unit]
Treatment in Coupler: passed from WRF without change				
1	ALBD [unitless]	Visible surface albedo	Dry deposition	ALBEDO [unitless]
2	CLDF [unitless]	3-D cloud fraction	Photolysis; chemistry	CLDFRA [unitless]
3	CLDFRC [unitless]	Column cloud fraction	Photolysis	CLDT [unitless]
4	EFLUX [W m^{-2}]	Latent heat flux	Diagnostics	LH [W m^{-2}]
5	FRSEAICE [unitless]	Fraction of sea ice	Hg simulation	FRSEAICE [unitless]
6	GWETROOT [unitless]	Root soil wetness	Diagnostics	SM100200 [$\text{m}^3 \text{m}^{-3}$]
7	GWETTOP [unitless]	Top soil moisture	CH ₄ simulation; dust mobilization	SM000010 [$\text{m}^3 \text{m}^{-3}$]
8	HFLUX [W m^{-2}]	Sensible heat flux	Dry deposition	HFX [W m^{-2}]
9	LAI [$\text{m}^2 \text{m}^{-2}$]	Leaf area index	Diagnostics	LAI [$\text{m}^2 \text{m}^{-2}$]
10	PBLH [m]	Planetary boundary layer height	PBL mixing	PBLH [m]
11	PFILSAN [$\text{kg m}^{-2} \text{s}^{-1}$]	Downward flux of large-scale + anvil ice precipitation	Wet scavenging	PRECR [$\text{kg m}^{-2} \text{s}^{-1}$]
12	QI [kg kg^{-1}]	Cloud ice water mixing ratio	Chemistry; aerosol micro-physics	QI [kg kg^{-1}]
13	QL [kg kg^{-1}]	Cloud liquid water mixing ratio	Chemistry; aerosol micro-physics	QC [kg kg^{-1}]
14	SNODP [m]	Snow deposition	Diagnostics	SNOWH [m]
15	SNOMAS [kg m^{-2}]	Snow mass	Dust mobilization; Hg simulation; dry deposition;	ACSNOW [kg m^{-2}]
16	SWGDN [W m^{-2}]	Surface incident radiation	Soil NO _x emissions; Hg simulation; dry deposition	SWDOWN [W m^{-2}]
17	TS [K]	Surface temperature	Many locations	T2 [K]
18	TSKIN [K]	Surface skin temperature	CH ₄ simulation; Hg simulation; sea salt emissions	TSK [K]
19	U [m s^{-1}]	East-west component of wind	Advection	U [m s^{-1}]
20	USTAR [m s^{-1}]	Friction velocity	Dry deposition	UST [m s^{-1}]
21	U10M [m s^{-1}]	East-west wind at 10m height	Dry deposition; dust mobilization; Hg simulation; sea salt emissions	U10 [m s^{-1}]
22	V [m s^{-1}]	North-south component of wind	Advection	V [m s^{-1}]

Table 1. Continued.

Treatment in Coupler: converted into GEOS-Chem units or diagnosed from WRF variables				
23	V10M [m s ⁻¹]	North-south wind at 10m height	Dry deposition; dust mobilization; Hg simulation; sea salt emissions	V10 [m s ⁻¹]
24	Z0 [m]	Surface roughness height	Dry deposition	ZNT [m]
25	AREA_m ² [m ²]	Grid box surface area	Many locations	DX/DY (X/Y horizontal resolution) [m]; MSFTX/MSFTY (Map scale factor on mass grid, x/y direction) [unitless]
26	CMFMC [kg m ⁻² s ⁻¹]	Cloud mass flux	Convective transport	MFUP_CUP [kg m ⁻² s ⁻¹]; CMFMC [kg m ⁻² s ⁻¹]; CMFMC [kg m ⁻² s ⁻¹]
27	DQRCU [kg kg ⁻¹ s ⁻¹]	Convective precipitation production rate	Wet scavenging (in convective updraft)	DQRCU [kg kg ⁻¹ s ⁻¹]
28	DQRLSAN [kg kg ⁻¹ s ⁻¹]	Large-scale precipitation production rate	Wet scavenging	RAINPROD [kg kg ⁻¹ s ⁻¹]; PRRAIN3D [kg kg ⁻¹ s ⁻¹];
29	DTRAIN [kg m ⁻² s ⁻¹]	Detrainment flux	Convective transport	DU3D [s ⁻¹]; DTRAIN [kg m ⁻² s ⁻¹]
30	FRLAKE [unitless]; FRLAND [unitless]; FRLANDIC [unitless]; FROCEAN [unitless]; FRSNO [unitless];	Fraction of land/ocean/surface snow/lake/land ice	Chemistry; Hg simulation; CH4 simulation; PBL mixing; emissions; diagnostics	LU_MASK (0-land, 1-water) [unitless]; LAKE-MASK [unitless]; SNOWH [m]
31	LANDTYPEFRAC [unitless]	Olson fraction per land type	Dry deposition	LU_INDEX (land use category) [unitless]
32	LWI [unitless]	Land-water-ice indices	Many locations	LU_MASK [unitless]
33	OMEGA [Pa s ⁻¹]	Updraft velocity	Diagnostics	W [m s ⁻¹]
34	OPTD [unitless]	Visible cloud optical depth	Photolysis; chemistry	TAUCLDI [unitless]; TAUCLDC [unitless]

Table 1. Continued.

35	PARDF [W m^{-2}]	Diffuse photosynthetically active radiation	Biogenic emissions	SWVISDIF (Diffuse photosynthetically active radiation) [W m^{-2}]; P (perturbation pressure) [Pa]; PB (base state pressure) [Pa]; COSZEN (cosine of solar zenith angle) [unitless]; SWDOWN [W m^{-2}]
36	PARDR [W m^{-2}]	Direct photosynthetically active radiation	Biogenic emissions	SWVISDIR (Direct photosynthetically active radiation) [W m^{-2}]; SWDOWN [W m^{-2}]; P [Pa]; PB [Pa]; COSZEN [unitless]
37	PEDGE [hPa]	Wet air pressure at level edges	Many locations	PSFC [Pa]; P_TOP [Pa]; C3F [unitless]; C4F [unitless]
38	PFICU [$\text{kg m}^{-2} \text{s}^{-1}$]	Downward flux of convective ice precipitation	Wet scavenging (in convective updraft)	PMFLXSNOW [$\text{kg m}^{-2} \text{s}^{-1}$]
39	PFLCU [$\text{kg m}^{-2} \text{s}^{-1}$]	Downward flux of convective liquid precipitation	Wet scavenging (in convective updraft)	PMFLXRAIN [$\text{kg m}^{-2} \text{s}^{-1}$]
40	PFLLSAN [$\text{kg m}^{-2} \text{s}^{-1}$]	Downward flux of large-scale + anvil liquid precipitation	Wet scavenging	PRECI [$\text{kg m}^{-2} \text{s}^{-1}$]; PRECS [$\text{kg m}^{-2} \text{s}^{-1}$]
41	PHIS [$\text{m}^2 \text{s}^{-2}$]	Surface geopotential height	Diagnostics	PHB (base state geopotential) [$\text{m}^2 \text{s}^{-2}$]; PH (perturbation geopotential) [$\text{m}^2 \text{s}^{-2}$]
42	PRECANV [$\text{kg m}^{-2} \text{s}^{-1}$]	Anvil precipitation	Diagnostics	SNOWNCV/ GRAUPELNCV/ HAILNCV (time-step non-convective snow and ice/graupel/hail) [mm]
43	PRECCON [$\text{kg m}^{-2} \text{s}^{-1}$]	Surface convective precipitation	Soil NO _x emissions; wet scavenging	PRATEC [mm s^{-1}]
44	PRECLSC [$\text{kg m}^{-2} \text{s}^{-1}$]	Non-anvil large-scale precipitation	Diagnostics	RAINNCV (time-step non-convective rain) [mm]

Table 1. Continued.

45	PRECTOT [kg m ⁻² s ⁻¹]	Surface total precipitation	Soil NO _x emissions; wet scavenging	RAINNCV/ SNOWNCV/ GRAUPELNCV/ HAILNCV [mm]; PRATEC [mm s ⁻¹]
46	PS1DRY [hPa]	Dry surface pressure at dt start	Advection; many other locations	PSFC [Pa]
47	REEVAPCN [kg kg ⁻¹ s ⁻¹]	Evaporation of convective precipitation	Wet scavenging (in convective updraft)	REEVAPCN [kg kg ⁻¹ s ⁻¹]
48	REEVAPLS [kg kg ⁻¹ s ⁻¹]	Evaporation of large-scale + anvil precipitation	Wet scavenging	EVAPPROD [kg kg ⁻¹ s ⁻¹]; NEVAPR3D [kg kg ⁻¹ s ⁻¹]
49	RH [%]	Relative humidity	Chemistry; wet scavenging; Aerosol thermal equilibrium; Aerosol microphysics	T (perturbation potential temperature) [K]; QV (water vapor mixing ratio) [kg kg ⁻¹]; P [Pa]; PB [Pa]
50	SPHU [g kg ⁻¹]	Specific humidity	Chemistry; wet scavenging; PBL mixing	QV [kg kg ⁻¹]
51	T [K]	Temperature	Many locations	T [K]; P [Pa]; PB [Pa]
52	TAUCLI [unitless]	Optical depth of ice clouds	Diagnostics	TAUCLDI (Optical depth of ice clouds) [unitless]; T [K]; P [Pa]; PB [Pa]; QI [kg kg ⁻¹]
53	TAUCLW [unitless]	Optical depth of water clouds	Diagnostics	TAUCLDC (Optical depth of water clouds) [unitless]; T [K]; P [Pa]; PB [Pa]; QC [kg kg ⁻¹]; QNDROP (droplet number mixing ratio) [# kg ⁻¹]
54	TO3 [DU]	Total overhead O ₃ column	Photolysis	O3 [ppmv]
55	TROPP [hPa]	Tropopause pressure	Tropopause height diagnosis	TROPO_P [Pa]
56	XLAI [unitless]	MODIS LAI per land type	Dry deposition	LAI [unitless]; LU_INDEX [unitless]

Table 2. WRF-GC physics configuration-

Physical Options	
Microphysics	Morrison 2-moment (Morrison et al., 2009)
Longwave radiation	RRTMG (Iacono et al., 2008)
Shortwave radiation	RRTMG (Iacono et al., 2008)
Surface layer	MM5 Monin-Obukhov (Jimenez et al., 2012)
Land surface	Noah (Chen and Dudhia, 2001a, b)
Planetary boundary layer	MYNN2 (Nakanishi and Niino, 2006)
Cumulus	New Tiedtke (Tiedtke, 1989; Zhang et al., 2011; Zhang and Wang, 2017)

Table 3. List of WRF configuration and physical options supported in WRF-GC v1.0

Namelist option	Description	Supported value
WRF Preprocessing System (WPS)		
max_dom	Maximum number of domains	1
map_proj	Map projection	lat-lon; mercator
geog_data_res	Static geographical data source	usgs_*
WRF dynamics		
hybrid_opt	Use hybrid sigma-pressure grid?	2 (Yes)
WRF physics		
bl_pbl_physics	Planetary boundary layer	All
cu_physics	Cumulus parameterization	7 (Zhang-McFarlane scheme), 16 (New Tiedtke scheme)
mp_physics	Microphysics option	6 (WRF single-moment 6-class scheme), 8 (New Thompson scheme), 10 (Morrison double-moment scheme)
ra_lw_physics	Longwave radiation	3 (CAM3 scheme), 4 (RRTMG), 5 (New Goddard scheme)
ra_sw_physics	Shortwave radiation	4 (RRTMG shortwave)
sf_sfclay_physics	Surface layer	All
sf_surface_physics	Land surface	All
sf_lake_physics	Lake physics	All
sf_urban_physics	Urban surface	All